UNIVERSIDADE DE LISBOA
FACULDADE DE CIÊNCIAS
DEPARTAMENTO DE BIOLOGIA VEGETAL

Complementary tools for aquaculture management: remote sensing and *in situ* approaches for Sines

Mara Ramos Gomes

Mestrado em Ciências do Mar

Dissertação orientada por:
Profª. Doutora Vanda Brotas e Doutora Carolina Sá

2020

Acknowledgements

The elaboration of this dissertation would not have been possible without the help of several people and institutions to whom I would like to express my gratitude.

I am thankful to my advisors, Prof. Vanda Brotas and Dr. Carolina Sá for their trust, guidance and valuable scientific advisory transmitted throughout this work. Thank you for always helping me even when times were busy and for being my inspirations.

I would like to thank the Marine and Environmental Science Centre where I developed the major part of this work, for all the facilities granted. Also, I would like to specially thank the Marine Botany Laboratory team.

Thanks to the Piscismod team, especially Marcos Mateus, Lígia Pinto and Alexandre Correia, for the support during this work, weather at the sea or on land. The sampling campaigns would not have been the same without your participation and good mood.

I would like to emphasize the help from the Seaculture team for supporting the sampling operations at the aquaculture site, providing boats and making us feel at home in the onshore facilities. A special thanks to Dr. Pedro Encarnação and Miguel Neto for making the sampling work possible.

Thanks to Dr. Steve Groom and Dr. Nick Selmes from the Plymouth Marine Laboratory, for the data provided and clarification of my doubts.

A special thanks to Andreia Tracana and Rui Cereja, for all the help with the laboratory work and sharing of experience, and for the patience throughout this work.

To Vera Veloso, I would like to express my deepest gratitude for providing data on phytoplankton community composition, for having helped to start the writing of this dissertation, and for the constant motivation to finish it.

I would also like to express my deepest gratitude to my colleagues Giulia Sent and Beatriz Biguino for the constant motivation and help in the sampling campaigns. This path would have been much more complicated without your support.

Finally, I express my most sincere gratitude to my dear friends: Patrícia, Pedro, Joana, and Alexandre for the daily support and constant encouragement; and to my sisters and parents without whom this would have not been possible.

This study was performed in the framework of PiscisMod - Roteiro para a sustentabilidade ambiental e otimização da eficiência energética em aquicultura de peixes, funded by the operational program MAR2020 (MAR-02.01.01-FEAMP-0049). This work has also been supported by Portwims Project – Portugal Twinning for Innovation and Excellence in Marine Science and Earth Observation, funded by the European Union Horizon 2020 research and innovation programme under grant agreement n. 810139.

Part of the work and dataset presented in this thesis will be included (forthcoming Frontiers in Marine Science Brief Research Report) in the publication: **Gomes, M.**, Correia, A., Pinto, L., Sá, C., Brotas, V., Mateus, M. (2020). Coastal water quality in an Atlantic sea bass farm site (Sines, Portugal): a first assessment. Brief Research Report, Front. Mar. Sci – Marine Fisheries, Aquaculture and Living Resources. doi: 10.3389/fmars.2020.509106.

Resumo

O estado crítico dos recursos marinhos tem vindo a impulsionar o rápido desenvolvimento da aquacultura. De facto, a nível mundial, a produção aquícola regista atualmente um crescimento mais rápido que qualquer outro setor da indústria alimentar. No entanto, o aumento de práticas intensivas de aquacultura tem gerado preocupações, principalmente devido aos potenciais impactos ambientais associados. A presente dissertação teve como foco uma produção intensiva de robalo (*Dicentrarchus labrax*, L. 1758) localizada no sudoeste da Costa Ibérica (Sines, Portugal). Na área de produção, a qualidade da água e os possíveis impactos da atividade no meio envolvente foram avaliados. Para tal, seis campanhas de amostragem, realizadas entre junho de 2018 e julho de 2019, foram realizadas para recolha de dados de parâmetros físicos, químicos e biológicos ao longo das jaulas onde se encontram os peixes. Foram analisados dados de temperatura, salinidade, parâmetros de claridade da água, matéria particulada em suspensão, oxigénio dissolvido, pH, nutrientes e biomassa e composição fitoplanctónica. Parte dos dados foram adquiridos a partir de sondas multiparamétricas (e.g. temperatura, salinidade, oxigénio dissolvido e pH); as concentrações de matéria particulada em suspensão, nutrientes e biomassa fitoplanctónica foram determinadas analiticamente em laboratório. Os parâmetros de claridade da água foram obtidos através de dados de radiometria e da profundidade de Secchi. Os resultados dos parâmetros de qualidade da água foram comparados com as gamas consideradas como aceitáveis e ótimas para a aquacultura de peixes em ambientes marinhos, de acordo com a literatura internacional. Atualmente, a literatura científica disponível ainda fornece uma orientação direta limitada para a avaliação da qualidade da água nas águas costeiras portuguesas. Os resultados apresentaram valores dentro das gamas aceitáveis definidas na literatura (exceto um valor isolado de fosfatos obtido em outubro de 2018). Para avaliar o impacto desta produção de peixe no meio recetor, as médias e extremos dos parâmetros de qualidade da água passíveis de serem diretamente influenciados pela aquacultura foram comparados com os dados disponíveis para a região de Sines, anteriores ao início da produção de robalo na região. Neste caso, foram obtidas concentrações mais elevadas de azoto inorgânico dissolvido em comparação com os valores de referência para Sines. No geral, a claridade da água, oxigénio dissolvido, nutrientes e biomassa fitoplanctónica não sugeriram impactos negativos das unidades de produção na qualidade da água local. Não obstante, são necessárias mais análises para diferenciar os potenciais impactos da elevada industrialização em Sines, dos impactos da aquacultura. Os resultados do presente trabalho apontam como causas para o baixo *stress* ambiental diversos fatores: o regime hidrodinâmico, o baixo tempo de residência da água no sistema, a estratégia de alimentação e a dimensão das unidades de produção.

As campanhas de amostragem *in situ* permitiram ainda verificar uma grande variabilidade dos parâmetros analisados na região, e a necessidade de utilizar métodos complementares para uma melhor caracterização espácio-temporal da área envolvente. Os produtos de deteção remota (DR) disponibilizam dados com grande resolução espácio-temporal, que podem complementar as abordagens amostragens *in situ* fornecendo informações relevantes os *end users*, neste caso, o aquacultor. Dados climatológicos da temperatura da água e da concentração de clorofila-*a* (indicador de biomassa fitoplanctônica) com os respetivos parâmetros estatísticos (desvio padrão e percentis 10 e 90) foram determinados para a região envolvente da aquacultura. Para verificar a coerência dos mesmos para a região, estes foram comparados com os dados *in situ* recolhidos durante as campanhas de amostragem. As médias semanais do percentil 90 (p90) da temperatura da superfície do mar (TSM) provaram ser adequados para alertar condições anómalas no local da aquacultura. Por outro lado, devido à alta variabilidade sazonal e interanual de clorofila-*a* (Chl-*a*) na região, a média do p90 mostrou ser mais fidedigna para a deteção de condições de alerta. O cálculo de anomalias diárias em comparação com dias anteriores (7 e 14 dias) também forneceu informações relevantes sobre a ocorrência de *blooms* na

região. Atualmente, a disponibilização de dados de satélite quase em tempo real em várias bases de dados públicas, possibilita facultar ferramentas valiosas de baixo custo ao aquacultor. Para além da região envolvente, a área onde se encontram instaladas as jaulas de peixe foi também caracterizada utilizando dados de DR (TSM, Chl-*a* e turbidez) e comparada com os dados obtidos *in situ*. Para fins de monitorização, medições discretas de temperatura e turbidez indicam ser suficientes para representar a área devido à baixa variabilidade espacial. A alta variabilidade de Chl-*a* na região revelam a necessidade de recolher dados em várias estações ao longo da produção, ou complementar dados *in situ* mais escassos com produtos de DR de maior resolução.

A adequabilidade de diversos produtos de DR considerados ao longo desta tese foi preliminarmente avaliada para a área da aquacultura em Sines. Para analisar a Chl-*a*, os novos sensores de alta resolução espacial da Agência Espacial Europeia, desenvolvidos no âmbito do Programa Copernicus da Comissão Europeia, como o *Ocean and Land Color Instrument* (OLCI) e o *Multispectral Instrument* (MSI) a bordo dos satélites Sentinel-3 e Sentinel-2, mostrou contribuições importantes para as áreas adjacentes ao litoral. Missões com dados históricos de Chl-*a*, como o *Medium Resolution Imaging Spectrometer* (MERIS) a bordo do Envisat e o produto que engloba múltiplos sensores da *Ocean Colour Climate Change Initiative* (OC-CCI), possibilitam uma melhor compreensão de variações intra-anuais. O produto de TSM do *Group of High Resolution Sea Surface Temperature* (GHRSST) revelou captar consistentemente o sinal de temperatura em Sines. Dada a intensa industrialização da zona de Sines e, neste caso, a presença de uma descarga de água quente proveniente da central termoelétrica de Sines a sul da produção, o uso deste último produto requer atenção na interpretação dos dados. Tal facto destaca a necessidade de aquisição de conhecimentos sólidos sobre a região de estudo para posteriores aplicações de produtos de DR, de modo a minimizar possíveis erros nas análises. Por fim, é salientada a necessidade da utilização de produtos de alta resolução espacial e temporal para monitorar as áreas costeiras, bem como a complementaridade da deteção remota com a recolha de dados *in situ*.

Palavras-chave: Aquacultura marinha, zonas costeiras, qualidade da água, impacto ambiental, deteção remota, climatologias, variabilidade ambiental

Abstract

The critical status of marine resources has provided impetus for rapid growth in aquaculture, which has become the fastest growing sector of the food industry worldwide. However, the increase of intensive aquaculture practices has been raising global concern mostly due to the associated potential environmental impacts. The present dissertation focused on an intense aquaculture in the SW Iberian Coast (Sines, Portugal) dedicated to the production of European sea bass (*Dicentrarchus labrax*, L. 1758). Water quality and potential impacts were assessed in the production area. Physical, chemical and biological parameters were collected along the cages in the course of six field campaigns, carried out between June 2018 and July 2019. These were temperature, salinity, water clarity parameters, suspended particulate matter, dissolved oxygen, pH, nutrients, and phytoplankton biomass and composition. The obtained water quality parameters were compared with threshold values for marine fish production, according to international literature. The scientific literature currently provides limited direct guidance for water quality assessment in Portuguese coastal waters. Results showed values within the acceptable for marine fish production (except an isolated value of phosphates obtained in October 2018). To assess the impact of this fish production in the receiving medium, the averages and extremes of water quality parameters that might be directly influenced by aquaculture were further compared with available data for Sines region, previous to the sea bass production in the area. A higher dissolved inorganic nitrogen signal was found in the collected data, compared to background nutrient levels for Sines. Overall, water clarity, dissolved oxygen, nutrients and phytoplankton biomass did not suggest any detrimental impacts of the production units on local water quality, although more research is needed. The findings point to the hydrodynamic regime, low water residence time in the system, feeding strategy and the dimension of production units as the reason for the lack of stress on the receiving waters.

Typically, coastal aquaculture faces with high water quality variability. Given the capabilities of satellite remote sensing (RS) products to provide high spatio-temporal data, they have the potential to be used as complementary tools to support the activity, providing important knowledge for end users. Climatological water temperature and phytoplankton biomass (indexed as chlorophyll-*a* concentration) data with respective statistics were provided for the aquaculture region and compared with the *in situ* data collected to verify consistency. Sea surface temperature (SST) weekly 90^{th} percentiles (p90) proved to be suitable to alert anomalous conditions in the aquaculture site. On the other hand, due to high chlorophyll-*a* (Chl-*a*) seasonal and interannual variability in the region, the mean p90 proved to be more reliable for the detection of alert conditions. The computation of daily anomalies compared to previous days (7-days and 14-days) also provided valuable information on the occurrence of blooms in the region. Currently, near real time satellite data can be accessed freely, providing users with valuable tools in a cost-effect way. The aquaculture site was also characterized using RS retrieved variables (SST, Chl-*a* and turbidity) and compared with the ground truth. For monitoring purposes, single discrete measures of SST and turbidity were found to be most likely sufficient to represent the area due to low spatial variability. High Chl-*a* variability in the region emphasized the need to collect several datapoints along the production or to complement scarcer *in situ* data with higher resolution RS products.

In this thesis, several remote sensing products were considered, and their suitability for the aquaculture area in Sines was preliminarily assessed. To study the variability of Chl-*a*, novel high spatio-temporal resolution RS sensors, such as the Ocean and Land Colour Instrument on Sentinel-3 (OLCI-S3) and the Multispectral Instrument on Sentinel-2 (MSI-S2), showed important contributions when focusing areas adjacent to the coast. Missions with available historical Chl-*a* data such as the Medium Resolution Imaging Spectrometer on-board Envisat, and the multi-sensor product from Ocean Colour Climate Change Initiative (OC-CCI), further enable understanding interannual features. The SST product from the Group of High Resolution Sea Surface Temperature (GHRSST) revealed to

consistently capture the temperature signal in Sines area. For the aquaculture surroundings, given the high industrialization of the region and, in this case, the presence of a hot water discharge from a thermoelectric powerplant south of the production, the use of this product requires caution to not misinterpret data contamination. This highlights the need to have knowledge of the study region in order to minimize possible error inducers in analyzes with satellite products. The necessity of high spatial and temporal resolution products to monitor coastal areas is therefore underlined, as well as the complementarity of remote sensing and *in situ* approaches.

Keywords: Marine aquaculture, coastal waters, water quality, environmental impact, remote sensing, climatologies, environmental variability

Index

Tables Index

Figures Index

List of acronyms

ADEC	Alaska Department of Environmental Conservation
AMSR	Advanced Microwave Scanning Radiometer
ANZECC	Australian and New Zealand Environmental and Conservation Council
APA	Portuguese Environmental Agency
APD	Absolute Percentage Difference
APS	Porto f Sines Administration
ARMCANZ	Agriculture and Research Management Council of Australia and New Zealand
AVHRR	Advanced Very-High Resolution Radiometer
CCI	Climate Change Initiative
CFP	Common Fisheries Policy
Chl-*a*	Chlorophyll-*a*
CI	Colour Index
CTD	Conductivity Temperature Depth
DGAV	General Directorate of Food and Veterinary
DGRM	General Directorate of Natural Resources, Safety and Maritime Services
DIN	Dissolved inorganic nitrogen
DL	Detection limit
DO	Dissolved oxygen
EC	European Commission
ECV	Essential Climate Variables
ENM	Portuguese National Sea Strategy
EO	Earth Observation
EOS	Earth Observing System
ESA	European Space Agency
EU	European Union
FAO	Food and Agriculture Organization of the United States
FTP	File Transfer Protocol
GHRSST	Group for High Resolution Sea Surface Temperature
HABs	Harmful Algal Blooms
HPLC	High Performance Liquid Chromatography
IMTA	Integrated Multi-trophic Aquaculture
IOCCG	International Ocean Colour Coordination Group
IPMA	Portuguese Institute for Sea and Atmosphere
JAXA	Japan Aerospace Exploration Agency
JM	Jerónimo Martins
JPL	Jet Propulsion Laboratory
MEaSUREs	Making Earth Science Data Record for Use in Research Environment
MERIS	Medium Resolution Imaging Spectrometer
MODIS	Moderate Resolution Imaging Spectroradiometer
MSI	Multispectral Instrument
MUR	Multi-scale Ultra-high Resolution
N	Nitrites and nitrates
NASA	National Aeronautics and Space Administration

NEODAAS	NERC Earth Observation Data Acquisition and Analysis Service
NERC	Natural Environment Research Council
NetCDF	Network Common Data Form
NOAA	National Ocean and Atmospheric Administration
NTU	Nephelometric Turbidity Unit
OATA	Ornamental Aquatic Trade Association
OC	Ocean Colour
OCI	Ocean Colour Index
OLCI	Ocean and Land Colour Instrument
OPeNDAP	Open-source Project for a Network Data Access Protocol
P	Phosphates
p10	Percentile 10
p90	Percentile 90
PEAP	Strategic Plan for Portuguese Aquaculture
Phaeos	Phaeopigments
PML	Plymouth Marine Laboratory
QL	Quantification limit
ROI	Region of interest
RPD	Relative Percentage Deviation
RS	Remote sensing
S	Salinity
S2	Sentinel-2
S3	Sentinel-3
SD	Secchi Depth
SeaDAS	SeaWiFS Data Analysis System
SeaWiFS	Sea-viewing Wide Field-of-view Sensor
Si	Silicates
SNAP	Sentinel Application Platform
SPM	Suspended Particulate Matter
SST	Sea Surface Temperature
T	Temperature
Turb	Turbidity

1. Introduction

Our vast dynamical oceans are an integral part of our society and economy, supplying living and non-living resources which provide a range of important goods and services. Undoubtedly, oceans are a major source of food worldwide serving as the primary source of protein of more than three billion people (United Nations, 2020). However, many of the world fisheries are rapidly declining due to consistently depletion of the fish stock at a rate higher than the capability of the system to replenish it. As a consequence, in 2014 31.4% of the assessed fish stocks had been already fished at a biologically unsustainable level (i.e., overfished), 58.1% were fully fished and only 10.5% were underfished (Food and Agriculture Organization of the United Nations (FAO), 2018), meaning that nearly 90% of global fish stocks are either fully fished or overfished.

In response to the limited potential to increase wild fishery catches, rising demand for seafood (driven by both population growth and increased per capita consumption (Godfray et al., 2010), and improved technology, alternative sustainable food supplies such as fish and shellfish farming (i.e. aquaculture), have been rapidly developing. Aquaculture is currently the fastest growing food sector in the world (Garcia and Rosenberg, 2010; FAO, 2014), and the coastal and oceanic areas are seen as one of the most likely areas for large-scale expansion (Aguilar-Manjarrez et al., 2013). Aquaculture provides opportunities to reduce the dependence on capture fisheries, to meet increased demand for year-round stable supplies of quality seafood, and to alleviate the economic impact of wild stock decline on coastal communities (through the creation of new jobs and businesses). Nonetheless, these benefits must be balanced with a commitment to marine stewardship, to endorse a modern marine aquaculture industry that is both profitable and environmentally friendly (e.g., Sugiura et al., 2006; Navarrete-Mier et al., 2012).

1.1. Marine aquaculture in Portugal

The average yearly consume of seafood in Europe is 25.1 kg per capita, which is almost 4 kg more than in the rest of the world (European Comission (EC), 2018). This consumption, however, varies greatly between countries, ranging from 4.8 kg to 55.9 kg per person per year in Hungary and in Portugal, respectively. Besides being the highest seafood consumer in Europe, Portugal has one of the highest consumes in the world (after Iceland and Japan), yet aquaculture and fisheries only represent 0.71 % and 3.59 % in volume (EC, 2015) of total European production, respectively. The above facts suggest a high dependency of this country on importations, almost two third of the consumed seafood is imported (Almeida et al., 2015); as well as an undeveloped and small productive sector.

Until the 1970s, Portuguese aquaculture production was dominated by species of low commercial value (e.g., rainbow trout). In the following decades, greater importance was given to the production of bivalves and the development of both freshwater and marine species (Strategic Plan for Portuguese Aquaculture (PEAP), 2016). According to the 2017 statistics, production in brackish and marine waters was the most important, accounting for about 94.4% of total production (12 549 tonnes), in which fish production accounted for 37.5% (4 706 tonnes). Along with the increasing importance of marine aquaculture, an increasing trend in intensive production regimes is observed in the country, where the main cultivated species are Turbot, Seabream, Sea bass and Sole (Portuguese Environment Agency (APA), 2019). However, national aquaculture production accounted for only 7.6% of fish onloaded in

port in 2017 (APA, 2019), and growth rates of this sector are considered to be limited by technical and/or natural conditions, available spaces for cultivation and accessibility of financing.

Despite still being an undeveloped sector, the high potential of marine aquaculture in Portugal is acknowledged. Nowadays, aquaculture is considered to be one of the value chains of the sea economy, and the Portuguese National Sea Strategy (ENM, 2013-2020) stresses that conditions must be created to attract national and international investments in this sector. Also, the PEAP (2014-2020) clearly identifies the need for development of national fish aquaculture production, to enhance its contribution to the fish supply market.

Marine aquaculture in Portugal is particularly attractive due to the extensive maritime territory and general favourable water quality conditions along the coast (Relvas et al., 2007; PEAP, 2016). However, the strong hydrological conditions along the western coast make it less suitable than the calmer south coast, where the pioneer marine aquaculture infrastructures are located (Algarve coast). Hence, 89% of the farms are located in the Algarve (with 46% of its coastal area used), while the Central and Northern regions of Portugal only account for 6% (22% used area) and 0.1% (0.1% used area) of the farms, respectively (Table 1.1). Generally, marine culture areas are located in sheltered areas such as bays, lagoons and estuaries, and to a less extent, in offshore regions (Ramalho and Dinis, 2011). At the end of 2017, there were 1532 establishments licenced for aquaculture in marine, fresh and brackish waters; floating structures (i.e. cages), accounted only for 2.3% of the total licenced establishments (APA, 2019).

Table 1.1 - Prevailing Portuguese regions and correspondent production, percentage of used surface and of farms. Source: Portuguese National Institute of Statistics (INE, 2010), in Ramalho and Dinis (2011).

Region	*Production (tons and %)*	*Used surface (%)*	*Farms (%)*
North	976 (12%)	0.1%	0.1%
Centre	1305 (16%)	22%	6%
Lisbon Region	599 (8%)	25%	4%
Alentejo	321 (4%)	6%	1%
Algarve	4331 (54%)	46%	89%

As a member of the European Union (EU), fisheries management in Portugal, under the responsibility of the General Directorate of Natural Resources, Safety and Maritime Services (DGRM), is governed mainly by the EU Common Fisheries Policy (CFP). Table 1.2 shows the Portuguese regulations and legislation controlling marine aquaculture and monitoring programmes. Regarding water quality, prior to the creation of new aquaculture production zones, the Portuguese Institute for Sea and Atmosphere (IPMA), as a public body responsible for monitoring water quality, assesses the characteristics of those areas. As part of the National Bivalve Mollusc Monitoring Program, IPMA monitors water quality and evaluates the environmental conditions. However, Portugal does not regulate carrying capacities for ecosystems, nor has an established environmental monitoring program for marine finfish aquaculture.

Defined measures to boost the sector and promote effective, efficient and sustainable development of aquaculture industry in Portugal encompass the following:

- Good environmental and climatic conditions in culture areas;
- Spatial planning and clear identification of available areas (both offshore and in lagoons);
- Skilled human resources;

- Strengthen technological capacity;
- Access national research facilities;
- Support industry with scientific research;
- Promote faster licensing and implementation processes.

Table 1.2 – Portuguese regulations and legislation controlling marine aquaculture and monitoring programmes. Source: Holmer et al., 2008 (adapted from Fernandes et al., 2000). DGAV – General Directorate of Food and Veterinary.

	Shellfish (clams, oysters, cockles)	*Finfish (sea bass, seabream, turbot)*
Carrying capacity	-	-
Environmental standards	Water quality (maximum admissible values of pH, temperature, water coloration, suspended solids, salinity, dissolved oxygen, biotoxins, microbes)	Water quality (maximum admissible values of pH, temperature, water coloration, suspended solids, salinity, dissolved oxygen, biotoxins, microbes)
Food standards	In accordance with EU regulations	In accordance with EU regulations
Medicine and Pesticide licences	Permission required from DGAV	Permission required from DGAV
Environmental monitoring	Mollusc water quality monitoring of metals, harmful phytoplankton and microbiological analyses by IPMA	-
Food monitoring	Compliance with food quality standards	Compliance with food quality standards

Scientific knowledge is a key aspect for the expansion of marine aquaculture in Portugal. Thereupon, several national and international studies, particularly under the framework of EU-funded projects, have been contributing to the evaluation of environmental suitability for new aquaculture units (e.g., AQUIMAR Project under Mar2020 program); evaluation of water quality and impact assessment of aquaculture farms (e.g., Piscismod Project under Mar2020 program), development of integrated systems as a possibility to reduce environmental risk (e.g., Matos et al., 2006), studies on species diversification, application of new technologies such as remote sensing support management decisions (e.g., AQUA-USERS Project, EU-FP7 project), among others. Also, advanced technological solutions required to implement marine cage aquaculture in highly energetic environments have been gradually emerging as an effect of cooperation between private and public sector and aided by scientific research (e.g., Kaiser et al., 2010).

1.2. Thesis motivation, objectives and structure

The main aim of this thesis is to provide elements that can support a marine sea bass cage production in Sines, Portugal, considering the end user (i.e., aquacultor) requirements. These focus on increasing the profitability of economic investment by decreasing the costs involved in production; as well as the reduction of environmental impacts. The aforementioned aim is materialized through three specific objectives:

- Characterize the aquaculture site using satellite data: long-term, seasonal and monthly patterns;
- Assess water quality and environmental impacts of aquaculture: *in situ* data;
- Combine *in situ* and satellite data to support aquaculture management.

The first is to characterize the Sines region, where aquaculture is located, through the establishment of the mean annual, seasonal and monthly abiotic (i.e., sea surface temperature) and biotic (i.e., phytoplankton biomass) conditions, as well as extreme occurrences of these parameters, using long-term remote sensing data. In addition to knowledge of species biology, understanding local dynamics and environmental conditions of the aquaculture site allows producers to manage the activity more efficiently by:

- Introducing new fish in the cages in the ideal time of the year;
- Harvesting fish at ideal times;
- Adjusting feed quantities administered;
- Predicting fish grow rates;
- Preventing the loss of fish stock due to anomalous conditions.

Therefore, this knowledge can contribute to the profitability of production.

The second objective is to evaluate water quality in the aquaculture vicinity, addressing spatial and seasonal variability in *in situ* physical, chemical and biological parameters and indicators, and make a first assessment of the direct effects of marine aquaculture in the receiving medium. Moreover, secondary impacts on primary production, including the formation of harmful algal blooms will also be considered. Currently, there are little scientific guidelines for best environmental practices in relation to control and monitoring of aquaculture. Hence, this section should contribute to set a roadmap for monitoring environmental quality in aquaculture suitable regions. Finally, *in situ* and remote sensing approaches will be combined to provide complementary tools to support aquaculture activities. In particular, these tools may further guide decision making, provide useful information for alert conditions and also contribute to the understanding of remote sensing products reliability for Sines region.

The thesis is organized in 6 sections, including the present introductory section. Section 2 considers the literature overview of water quality and impact assessment in marine fish aquaculture, as well as the use of Earth Observation tools to support this activity. The used data (*in situ* and remote sensing) and methods applied are detailed in section 3. Results are presented in section 4 and discussed in section 5. Concluding remarks, as well as future work are addressed in section 6.

2. Literature overview

2.1. Marine aquaculture water quality and impact assessment

There is significant diversity in marine aquaculture (i.e., mariculture) species, with nearly 200 species currently being farmed (FAO, 2015) and many more under development. Yet, all types of mariculture fall into three broad categories: fed (e.g., fish, most crustaceans), unfed (e.g., filter-feeding bivalves, some grazers, and detritivores), and autotrophic species (kelp and other algae). Each one of these interacts with the environment in fundamentally different ways (see Gentry et al., 2017). The present work focuses on marine finfish cultures, both the impacts of the environment on the production (e.g., external inputs to the farm) and the effects of the farm on its surrounding ecosystem.

2.1.1. Effects of the environment on aquaculture production

The overall state and characteristics of the marine ecosystem impacts the quality of the produced seafood. Physical, biogeochemical, biological and geographical features can have direct effects on the growth of aquaculture species (e.g., Ferreira et al., 2007), so that the farm location plays a critical role in determining its productivity, environmental impact, and interactions with other ecosystem services (Gentry et al., 2017). For example, characteristics such as shallow depths and slow currents are likely to be risk factors for aquaculture operations (Jansen et al., 2016). Although optimal conditions depend on the cultured species, reference values/ranges for acceptable and optimal water quality parameters are provided in Table 2.1 for marine finfish species in general and, in case of available information, for the European sea bass as it is the species farmed in the region of interest (ROI) of this thesis. The critical physical, chemical and biological parameters to be considered include water temperature, salinity, suspended solids, turbidity, pH, dissolved oxygen, nutrient concentrations, and phytoplankton biomass. Water quality standards can be ambiguous since they may depend on regional features, and they also vary depending on the implementing countries. On Table 2.1 water quality reference values (acceptable and optimal) are shown, based on international literature.

Physical parameters

Temperature and salinity

The sea bass is an eurythermic and euryhaline marine fish that thrives in coastal waters of the Northeast Atlantic Ocean and the Mediterranean Sea. It undertakes seasonal migrations to estuaries and lagoons (which are characterized by fluctuations in environmental conditions). In fact, sea bass ability to cope with these unstable habitats is undeniable and has been widely studied (e.g., Dülger et al., 2012; Masroor et al., 2018; Yilmaz et al., 2019). Temperature (T) is one of the most important abiotic factors affecting survival and growth of marine organisms (Lutterschmidt and Hutchison, 1997), therefore knowledge of critical and ideal values is of practical interest for aquaculture. Extreme temperatures can induce stress in the animal, and the metabolic activities of fish are affected, which ultimately affects the growth and health of the fish. It is generally accepted that sea bass is tolerant to a wide range of temperature (5 – 28 °C) and salinity (S) extremes (5 – 50 ‰) (Claridge and Potter, 1983; FAO, 2020). Regarding the optimal temperature, according to Barnabé (1991), juvenile sea bass grow fast between

22 – 25 °C. Yet, Russel et al. (1996) and reported that the growth of this species in British waters was higher at 18 °C. Therefore, it is suggested that different strains of the same species from various geographical regions might respond differently to environmental factors (Imsland et al., 2003). In pond aquaculture of sea bass, Dülger et al. (2012) found that for optimal growth temperature should be kept at 25 °C. Concerning salinity, Ercan et al. (2015) found an optimum positive effect on the growth of sea bass at 18 ‰ salinity concentration.

Water clarity parameters

Turbidity and Secchi depth

Turbidity (Turb) is an optical property of water that can indicate the degree of clearness of sea water affected by the existence of dissolved matters and suspended particles. The quantity and quality of the turbidity causing matter at any particular moment is largely determined by water movement (i.e., tides and currents). Like suspended particulate matter (SPM), increased turbidity may result in lower light penetration affecting phytoplankton production (Anderson et al., 2005). However, for marine fish that derive a majority of their nutrition from feed inputs, light for phytoplankton growth is not imperative and therefore turbidity can be higher than when organisms that depend upon phytoplankton for feed are cultured. According to the Alaska Department of Environmental Conservation (ADEC, 2016), values of turbidity at marine finfish aquaculture cages should not exceed 25 nephelometric turbidity units (NTU). Secchi disk visibility can also be taken as a measure of transparency of the water in marine life cage culture. Optimum transparency expressed as Secchi depth (SD) for marine culture should be higher than 5 m as a yearly mean (Prema, 2013).

Suspended particulate matter

SPM in the water, i.e. particles larger than 0.45 μm in size (American Public Health Association, 1998), can, among others, originate from bottom resuspension, soil erosion, decaying plant and animals, industry wastes, urban run-off, wastewater effluents, uneaten aquaculture feeds and faecal matter. High concentrations of SPM can have several negative effects, such as:

- Decreasing the amount of light that can penetrate the water, thereby slowing photosynthetic processes which in turn can lower the production of dissolved oxygen;
- Increase the absorption of heat from sunlight, thus increasing the temperature which can also result to lower the oxygen level;
- Prevent the development of egg and larvae.

Furthermore, it can also indicate higher concentrations of bacteria, nutrients and pollutants in the water. For marine finfish aquaculture, SPM concentration in the water should be below 10 mg L^{-1}, according to the Australian and New Zealand Environmental and Conservation Council and the Agriculture and Resource Management Council of Australia and New Zealand (ANZECC and ARMCANZ, 2000).

Chemical parameters

pH

Marine species tolerate a narrower range of hydrogen ion concentration (pH) than freshwater species, thus the optimum pH is usually between 7.5 and 8.5 (Boyd, 1998; Santhosh and Singh, 2007) although a range between 6.5 and 9.0 is also acceptable (Wurts and Durborow, 1992; ANZECC and ARMCANZ, 2000; Bhatnagar et al., 2004). Below pH 6.5 some species experience slow growth (Lloyd,

1992). At lower pH, the ability of organisms to maintain its salt balance is affected (Lloyd, 1992) and reproduction ceases. At approximately pH 4.0 or below and pH 11 or above, most species die (Lawson, 1995). The pH values vary directly or indirectly with other water parameters like salinity and temperature, which also influences the dissolved oxygen and ammonia levels (e.g., Kroupova et al., 2005).

Oxygen

In a water body, oxygen is available in a dissolved state. Dissolved oxygen (DO) is considered as one of the most important aspects of aquaculture: it is needed by fish to respire and perform metabolic activities (Philminaq Project, 2013). Thus, low levels of DO are often linked to fish kill incidents. On the other hand, optimum levels can result in good growth and high production yields. DO levels are mainly influenced by other environmental factors, such as temperature and salinity: concentrations decrease with increase in temperature and salinity. In general, saturation level of at least 5 mg L^{-1} is required (ANZECC and ARMCANZ, 2000) for marine finfish production. According to Huguenin and Colt (1989) and the Ornamental Aquatic Trade Association (OATA, 2008), ideal DO in the water should be higher than 6 mg L^{-1}.

Nutrients

Nutrients can enter the system through rainfall, *in situ* fixation (e.g., nitrogen fixation by cyanobacteria), river runoff, upwelling of nutrient rich waters and diffusion from sediments. In the water column, soluble nutrients can alter the species composition and density of phytoplankton, increasing the risk of toxic algal blooms. Aquaculture is also known to increase the nutrient load of an ecosystem and, therefore, this issue will be addressed in the next section (*Effects of aquaculture production on the environment*). Nevertheless, background nutrient levels and the trophic status of the ecosystem can be crucial to understand the suitability of a site. Tolerance levels for marine finfish species are shown in Table 2.1.

Ammonium (NH_4^+) is the initial product of the decomposition of nitrogenous organic wastes (e.g., originated from uneaten feds and excretion of fishes) and respiration. High concentrations of ammonium cause an increase in pH and ammonia concentration in the fish which in turn can damage the gills, affect osmoregulation, reduce the oxygen-carrying capacity of blood and increase the oxygen demand of tissues (Lawson, 1995). Generally, ammonium levels below 55 μmol L^{-1} are considered safe (ANZECC and ARMCANZ, 2000), although there is no consensus yet on the permissible levels. According to Prema (2013), level of ammonium in the water should preferably be less than 6 μmol L^{-1}.

Nitrite (NO_2^-) is a by-product of oxidized ammonia, an intermediary in the conversion of ammonia (NH_3) or NH_4^+ into nitrate (NO_3^-). This process is completed through nitrification, which is a rapid reaction, thus high nitrite concentrations are not commonly found in natural waters. However, if high levels do occur , it can lead to the oxidation of iron in fish haemoglobin, which causes hypoxia in fish (Lawson, 1995). The toxicity of nitrite is dependent on chemical factors (e.g., pH, DO and ammonia, among others), but overall is was found that it is more toxic in freshwater than brackish and marine waters (Boyd, 1990). Thus, more stringent nitrite standards are imposed in freshwater aquaculture operations. According to the OATA (2008), acceptable concentrations of nitrites for marine finfish production should be < 3 μmol L^{-1}.

NO_3^- is formed through the nitrification process, i.e. oxidation of NO_2^- into NO_3^- by the action of aerobic bacteria. Nitrate not taken up directly by aquatic plants is denitrified in anaerobic sediments. Generally, nitrate is stable over a wide range of environmental conditions. Compared with other inorganic nitrogen compounds, it is also the least toxic. However, high levels can affect osmoregulation, oxygen transport, eutrophication and algal blooms (Lawson, 1995). According to Stone and Thomforde

(2003) nitrate is relatively nontoxic to fish and may cause no health hazard except at exceedingly high levels (above 1452 μmol L^{-1}). OATA (2008) and ANZECC and ARMCANZ (2000) recommend that nitrate levels in marine systems never exceed 1613 μmol L^{-1}.

Almost all the phosphorous present in water is in the form of phosphate (PO_4^{3-}). Among the common sources of phosphorous in coastal waters are wastewater, industrial discharges and riverine runoff (containing fertilizers and insecticides). It is a limiting nutrient needed for the growth of phytoplankton and aquatic plants. However, excess concentrations can result in algal blooms. According to Stone and Thomforde (2003), the phosphate level of 0.63 μmol L^{-1} or lower is desirable for marine fish culture.

Lastly, although silicates (SiO_2) may play a major role in the growth of phytoplankton (e.g., being a limiting nutrient for the growth of diatoms), no literature was found on the relation/impact of the concentration of silicon in the water column on fish growth and survival.

Biological parameters

Environmental biological parameters such as phytoplankton biomass and species composition can have direct impact on water quality and therefore also in aquaculture production. For example, phytoplankton biomass concentration is a relevant biological variable for the detection of the eutrophic conditions. Suspension-feeding aquaculture species (e.g. bivalves, shrimp) derive nutrition from natural particles, the most nutritious being phytoplankton (International Ocean-Colour Coordinating Group (IOCCG), 2009). Their growth is thus limited by phytoplankton depletion, making knowledge about their food source crucial for the production. When food is provided to the cultured organisms, as is the case with fish, the prime concerns with phytoplankton are related to potential risks to the aquaculture activity due to high phytoplankton biomass concentrations (e.g. blooms as generators of hypoxia conditions, presence of toxic species that may damage the fish gills, increase of suspended particulate matter). Nevertheless, phytoplankton can have a positive effect on the quality of water by maintaining the oxygen and carbon dioxide balance, and by assimilating large amounts of nitrogen and phosphorus (Boyd, 1998). Phytoplankton biomass is known to increase in response to nutrient loads from fish farms (e.g., Dalsgaard and Krause-Jensen, 2006). Hence, this topic will also be addressed in the next section (*Effects of aquaculture production on the environment*).

The chlorophyll-*a* (Chl-*a*) is ubiquitous to phytoplankton and is therefore used as a biomass proxy. In marine environments, biotic and abiotic environmental factors have important effects on phytoplankton succession and abundance. The typical Chl-*a* concentrations for coastal waters vary regionally and so there is no general acceptable value for marine finfish aquaculture. For the Portuguese coast, phytoplankton biomass distribution is highly related to the stratification of the water column, nutrient availability and the intensity and persistence of upwelling conditions (Moita, 2001). Typical values for the Portuguese coast range between from 0.01 to 10.15 mg m^{-3} (Sá, 2013).

Table 2.1 - Acceptable and optimal water quality parameters for marine finfish aquaculture. * For the European sea bass.

Parameter	*Acceptable*	*Reference*	*Optimal*	*Reference*
T (° C)	5 – 28 *	Claridge and Potter (1983); FAO (2020)	18 – 25 *	Barnabé (1991); Russel et al. (1996); Dulger et al. (2012)
S (‰)	5 – 50 *	Claridge and Potter (1983); FAO (2020)	18 *	Ercan et al. (2015)

Table 2.1 – Continued.

Turb (NTU)	< 25	ADEC (2016)		
SD (m)	> 5	Prema (2013)		
SPM (mg L^{-1})	< 10	ANZEECC and ARMCANZ (2000)		
pH	6.5 – 9.0	Wurts and Durborow (1992); ANZECC and ARMCANZ (2000); Bhatnagar et al. (2004)	7.5 – 8.5	Boyd (1988); Santhosh and Singh (2007)
DO (mg L^{-1})	> 5.0	ANZEECC and ARMCANZ (2000)	> 6.0	Huguenin and Colt (1989); OATA (2008)
NH_4^+ (µmol L^{-1})	< 55	ANZEECC and ARMCANZ (2000)	< 5.54	Prema (2013)
NO_2^- (µmol L^{-1})	< 3	OATA (2008)		
NO_3^- (µmol L^{-1})	< 1613	ANZEECC and ARMCANZ (2000); OATA (2008)		
PO_4^{3-} (µmol L^{-1})	< 0.63	Stone and Thomforde (2003)		
SiO_2 (µmol L^{-1})	Not defined	-		
Chl-a (mg m^{-3})	0.01 – 10.15	Sá (2013)		

2.1.2. Effects of aquaculture production on the environment

The perceived and potential environmental effects of marine finfish cage aquaculture on water quality are a primary concern for developing an ecologically responsible industry. Aquaculture itself has a vital interest in a healthy environment to provide quality products. By introducing a high density of additional life into the ocean, mariculture affects the surrounding environment in diverse complex ways (e.g., Gentry et al., 2017). In some cases, this can lead to desirable outcomes; for example, farming of filter feeders such as shellfish can improve water quality, and in fact shellfish are often integrated into finfish production in integrated multi-trophic aquaculture (IMTA) systems, also known as polyculture. However, aquaculture can also have adverse effects inducing environmental risk. The magnitude of these negative effects is influenced not only by the characteristics of the receiving medium, but also by operational characteristics (e.g., species farmed, stocking density, feeding strategy, preventive veterinary care).

Several reviews have broadly addressed the topic of the impacts of marine finfish aquaculture across a variety of cultures and environments (Wu, 1995; Black, 2001; Goldburg, Elliott and Naylor, 2001; Goldburg and Naylor, 2005; Harrison et al., 2005; Holmer, 2010; Grigorakis and Rigos, 2011; Price and Morris, 2015; Gentry et al., 2017). In most fish-producing jurisdictions, cage-based aquaculture impact studies focus on the deposition of organic wastes and the associated effects to benthic fauna and sediment biogeochemical processes (e.g., Karakassis et al., 1999; Kutti et al., 2007;

Holmer et al., 2008; Valdemarsen et al., 2012). Pelagic dispersion of organic particles and inorganic nutrients at fish culture operations is less well understood (e.g., Sara, 2007).

Figure 2.1 shows the key inputs and outputs to fish farms that can potentially lead to undesirable effects in fish mariculture. As addressed in the previous topic (*Effects of the environment on aquaculture production*), environmental conditions inevitably affect the fish farm production and cannot be controlled, again, making site selection an important factor to consider before farm implementation. Intensive fish farming requires external inputs, such as feed and chemicals (e.g., antibiotics) which can lead to nutrient and chemical pollution (e.g., Cao et al., 2007). Fish feed is partly transformed into fish biomass and partly released as suspended organic solids or dissolved matter, increasing the amount of carbon, nitrogen and phosphorous in the water. Besides from surplus food, suspended and dissolved matter can also originate from faeces and excretions via gills and kidneys (Tovar et al., 2000). It should be noted that decomposition of organic matter is the main cause of oxygen demand in an aquaculture systems (Philminaq Project, 2013) making food wastage and feed quality potential inductors of oxygen depletion. Thus, uneaten fish feed can trigger several negative outcomes (e.g., Ferreira et al., 2007; Price and Morris, 2015; Gentry et al., 2017), making the adjustment of the given food according to fish needs of utmost importance.

That said, it is noteworthy that the release of dissolved and particulate nutrients (as well as changes in nutrient stoichiometry) by intensive mariculture is well documented (e.g., Bouwman et al., 2013 and references therein). This consequence of intensive fish production may further promote the growth of algal blooms, including harmful algal blooms (HABs). Phytoplankton are known to increase in response to nutrient loads from fish farms. HABs can kill or intoxicate the mariculture product with severe economic losses and can increase risks to human health. This relationship between increasing prevalence of HABs and aquaculture operations are also increasingly reported (e.g., Furuya et al., 2010).

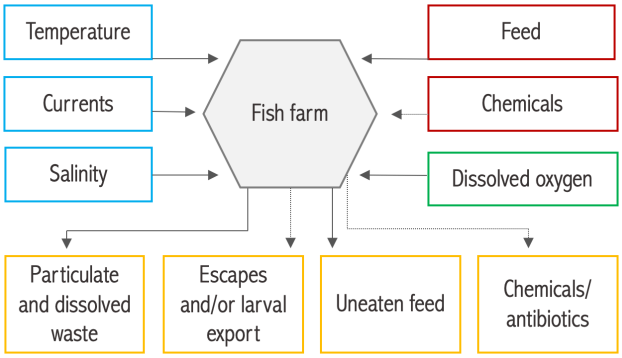

Figure 2.1 - Key inputs and outputs associated with fish aquaculture. Blue indicates other environmental conditions that affect the farm; red indicates external inputs into the farm; green indicates environmental inputs; and orange indicates outputs from the farm into the environment. Dashed lines indicate inputs and outputs that are only sometimes present. Source: Gentry et al., 2017.

Lastly, if not properly managed, aquaculture may also lead to habitat destruction (e.g., Ottinger et al., 2016; Gentry et al., 2017), introduction of diseases from escapees that might facilitate disease transmission (e.g., Lafferty et al., 2015) and genetic interaction with wild species (e.g., Holmer, 2010; Ertör and Ortega-Cerdà, 2015). Therefore, all these aspects have to be taken into consideration when managing an aquaculture facility. When good practices are used, it is possible to farm fish in a way that has little impact, limiting the aforementioned possible negative impacts on the environment.

2.2. Earth observation in support of marine aquaculture

Earth observation (EO) is based on the use of remote sensing (RS) technologies to obtain important information on variables about the physical, environmental and biological state of regions of interest. Satellite RS data has been successfully applied to aquaculture management by providing essential variables for this industry (e.g., sea surface temperature, salinity, turbidity, chlorophyll-*a* concentration and hydrodynamic parameters) with high temporal and spatial coverages. More than 20 years ago, Egna (1994) reviewed applications of remote sensing for monitoring water quality in tropical inland fisheries and aquaculture. Later, several reviews were made on the state of remote sensing applications for sustainable aquaculture at global and regional levels (e.g. Quansah et al., 2007; IOCCG, 2008; Dean and Salim, 2013). Ottinger et al. (2016) present an up-to-date holistic overview of satellite remote sensing studies, addressing the application to aquaculture including site selection, site detection and monitoring of related impacts on the environment. Current applications of RS to aquaculture include:

- Insight on local dynamics;
- Water quality monitoring;
- Site selection;
- HABs detection.

Satellite data application to fisheries is also of great importance and has already long been use. For example Santos and Fiúza (1992) related the distribution and availability of the European sardine with ocean features, namely with sea surface temperature (SST). They found that these fish concentrate in moderately cool upwelled waters on the inner shelf off western Portugal. Based on that knowledge, they further provided fisherman with near real-time advisory products optimizing the efficiency of fishing operations. Nonetheless, this section will focus on recent applications of RS tools to marine aquaculture, especially on providing relevant information to the activity when the infrastructure already exists (i.e., knowledge on local dynamics, water quality, and algal blooms).

2.2.1. Understanding local dynamics

Abiotic and biotic parameters of particular relevance to aquaculture may be inherently highly variable over space and time, adding to the complexity of site suitability and production optimization. The capacity of RS to reliably map aquaculture relevant parameters, providing spatially-explicit time-series of water quality indicators, has been demonstrated (e.g., Brotas et al., 2014). Surely, it offers a unique way to quantitatively incorporate such spatio-temporal nuance into modelling, planning, and decision-making. The recent acceleration in sensor and algorithm advances in coastal and nearshore marine environments adds to the potential of remote sensing data and tools in support of sustainable aquaculture. Furthermore, to identify the typical seasonal cycle of a region is a first step to detect anomalies and potential occurrence of anomalous conditions, constituting an early warning for aquacultures, or to detect productive areas essential for aquaculture site selection.

2.2.2. Water quality monitoring using remote sensing data

As previously mentioned, water quality is a critical factor when culturing aquatic organisms. IOCCG (2018) shows the bulk of water quality parameters directly measurable from space, emphasizing the need to couple them with field-based observations for operational applications. Those include the following:

- Water clarity parameters;

- Sea surface temperature;
- Suspended and dissolved matter concentrations;
- Chlorophyll-*a* concentration;
- Algal blooms detection (through specific marker pigments or other unique spectral features, and through rapid biomass increase).

Concerning fed aquaculture, the prime considerations relate to the dispersal of unconsumed feed, to transient water masses of temperature and phytoplankton biomass outside the tolerance range of the cultured species, and to the incidence of harmful algal blooms (Platt et al., 2015). For instance, in the densely fish aquaculture-explored region of Bolinao, Philippines, David et al. (2014) introduced an operational system for early detection of warm water masses from SST imagery (from the National Oceanic and Atmospheric Administration (NOAA) Coral Reef Watch hotspot products), using the Advanced Very-High Resolution Radiometer (AVHRR). This is a threatened region by the passage of transient anomalous warm water masses which caused massive cultured fish losses in the past. When the risk was considered high, daily monitoring of dissolved oxygen was carried out. If falling oxygen levels foretold an imminent fish kill, the fish were harvested early to reduce economic losses. In these cases, the understanding of local dynamics itself can also be determined using RS data.

The dispersal and assimilation of aquaculture waste subsidies in natural systems is an important factor to take into consideration when assessing its environmental impact. Aquaculture waste dispersal is a function of local residence time depending on tides and currents (or estuarine circulation) of the water at the site under consideration. Hence, these parameters can be assessed using satellite derived parameters (e.g. currents) as a complementary tool for hydrodynamic modelling.

2.2.3. Harmful algal bloom detection

The incidence of harmful algae in fixed aquaculture equipment may cause massive finfish suffocation and mortality through clogging the gill tissues, or concentration of toxins by filter-feeding shellfish causing amnesia of paralysis when ingested. Hence, harmful algal blooms (HABs) are considered a major environmental problem and threat to the aquaculture industry. On that account, the detection of HABs is essential for aquaculture operations.

If the bloom is high in biomass, it can certainly be detected as perturbations of the chlorophyll field in ocean colour imagery (Platt et al., 2015). In this case, remotely-sensed maps of Chl-*a* and SST can help quick detection (e.g. Stumpf et al., 2003), and understanding the formation of algal blooms (e.g. Tang et al., 2006). But it is only in exceptional cases that the increased chlorophyll can be diagnosed as an elevated abundance of a particular species. In this context, many studies focused on trying to determine whether or not the phytoplankton are harmful (e.g. Sathyendranath *et al.*, 1997; Yin *et al.*, 1999). Despite of all the efforts, in order for this to be possible, the harmful algae need to have spectral optical characteristics (i.e. *Trichodesmium* and *Gymnodinium*) that could be used to distinguish them from other types of phytoplankton (IOCCG, 2009).

In the absence of such traits, the primary usefulness of remote sensing is as a tool for systematic and sustained observations of algal dynamics in the vicinity of aquaculture sites and as a triggering factor for more detailed *in situ* observation (IOCCG, 2009). Once the presence of a potential harmful bloom is detected, ocean-colour imagery is highly useful as a means to track the spatial extent, movement and eventual dissipation of the bloom (Platt et al., 2015). Long term satellite time series can be an essential tool to identify the typical seasonal cycle of a region. This knowledge is necessary to detect anomalies of phytoplankton biomass and potential occurrence of an anomalous algal bloom, constituting an early warning for aquacultures, or to detect productive areas for aquaculture site selection (Sá et al., 2014). Moreover, biophysical modelling is also useful to simulate the spatial and

temporal response of harmful phytoplankton to environmental forcing factors (Anderson et al., 2005a), especially when combined with satellite remote sensing data (Davidson et al., 2014; Anderson et al., 2016; Ruiz-Villarreal et al., 2016). These approaches have been successful in providing real-time predictions that have been incorporated into national forecasting systems for public health and aquaculture protection (Berdalet et al., 2017).

3. Data and Methods

3.1. Study site

Sines is a city located on the west littoral margin of the Portuguese coast, about 150 km south of Lisbon (Figure 3.1), bathed by the Atlantic Ocean along the coastline. The city is characterized by its urban core (about 15.000 habitants), industry and port structure, with high growth prospects, mainly due to its strategic location and logistics conditions – in which the Port of Sines plays an important role (Port of Sines Administration (APS), 2020). The Port of Sines is the most important deep-water port in Portugal (28 m deep), which is the main entryway of primary energy (crude, coal and natural gas) and containerized cargo in the country. The port offers ideal geophysical characteristics to receive any type of vessels and, due to its specialized terminals (liquid bulk, petrochemical, multipurpose, natural gas and container terminals), it is able to handle the different types of cargoes (APS, 2020). Sines plays a major role in terms of energy production and storage due to two large production centres of oil and gas industry (Wronna et al., 2015), the Galp refinery and the Repsol petrochemical industrial complex, both connected via pipelines to the oil-bearing and petrochemical terminal of the port.

The aquaculture in Sines, operated by Seaculture (Jerónimo Martins Agro-business), is located in the inner region of the container terminal jetty which is protected from the strong hydrodynamics of the Atlantic coast (Figure 3.1 and Figure 3.2). It is the only aquaculture in the Iberian Peninsula that is established inside a port. Dedicated to the production of European sea bass (*Dicentrarchus labrax* L., 1758), Seaculture installed the first aquaculture facilities in 2016, starting production in that year (Jerónimo Martins (JM), 2017). The production of a commercial size sea bass, weighting between 350 and 400 g, takes up to 22 months until it can be catched. According to this, the first harvest happened in December 2017 (JM, 2018). Nowadays, the sea bass culture is composed by 16 fish cages situated in a row parallel to the dominant current direction, each holding around 150 000 specimens at different stages of growth, allowing a yearly production of up to 500 metric tons of fish. It is an intensive system, with feed delivered from land to the cages through a pressurized pipe system. A continuous adjustment of the amount of feed delivered to fish is made, based on a constant monitoring of fish behaviour using underwater cameras, and environmental conditions (i.e. temperature and oxygen concentration) using sensors installed in the cages.

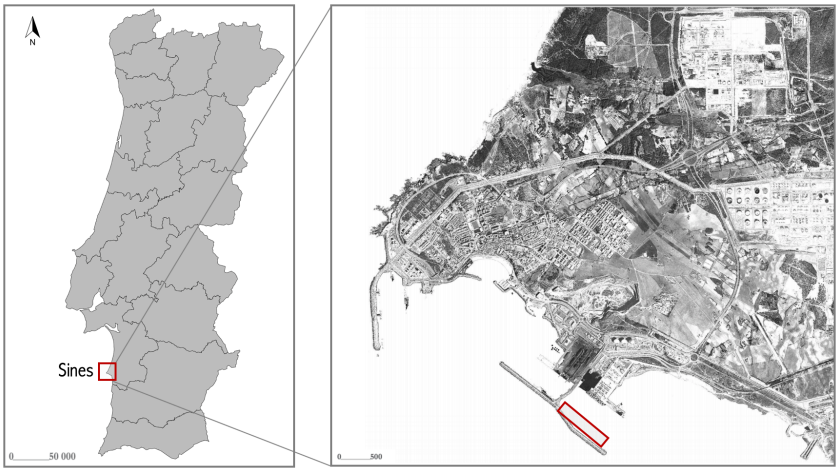

Figure 3.1 – ROI location in Portugal (left) and ortophotomap of Sines (right). Red rectangle indicates the area allocated for aquaculture production inside the container terminal of Port of Sines. Image: Dias (2018).

In Sines, coastal hydrodynamics, particularly in what concerns superficial currents and waves, is conditioned by dominant wind patterns (Salgueiro et al., 2015b). Wind is also responsible for the vertical movements caused by upwelling phenomena in this area (Barton, 2001). Coastal upwelling is frequent during the spring and summer months, triggered by dominant northerly winds, pumping colder subsurface waters to the upper layers along coast (Relvas et al., 2007; Kämpf and Chapman, 2016). During a typical year, 80% of wind observations exhibit north wind dominance leading to strong upwelling along the coast (Salgueiro et al., 2015b)., with the strongest upwelling centres located further south of Cape Sines and the Port of Sines (Alt-Epping et al., 2007). Outside the upwelling region, the presence of a poleward flow is a well-established characteristic along the Portuguese west coast (Relvas et al., 2009). However, tide may also change local-scale circulation, generating tidal currents that overlap wind induced currents (Trindade et al., 2016). Coastal topography and bathymetry also play an important role in shaping coastal circulation at a local scale. Water circulation in the vicinity of the study site is strongly conditioned by the breakwater, presenting lower velocities when compared with outside area (Correia et al., 2019). Tidal currents are the dominant forcing inside the port (mean depth of 24 m), promoting constant water renewal of the system.

3.2. *In situ* data: physical, chemical and biological parameters

In situ physical, chemical and biological data were collected in the scope of Piscismod Project – a roadmap for environmental sustainability and energy efficiency optimization in fish aquaculture, funded under the framework of Mar2020.

3.2.1. Sampling

Physical, chemical and biological water quality parameters and indicators were collected in the aquaculture cages vicinity at four different stations (Figure 3.2, Table A.1) to cover the spatial variability of the region. One station north of the fish cages (Station 1, 14 m deep), other station between two cages in the middle of the production area (Station 2, 21 m deep), one station in the southern extremity of the cages (Station 3, 25 m deep) and the last station south of the cages transect (Station 4, 30 m deep). All samples were collected within a timeframe of approximately 3 h. *In situ* data were collected during six field campaigns in 2018-06-29 (summer), 2018-10-25 (autumn), 2019-03-12 (spring), 2019-04-30 (spring), 2019-05-23 (spring) and 2019-07-29 (summer) to cover one seasonal cycle. Winter was not sampled because of meteorological conditions.

During the campaigns the sampling stations were adjusted, therefore in the first and second campaigns (June and October 2018) only stations 1 and, 3 were sampled. From the third on (March, April, May and July 2019) stations 1, 2, 3 and 4 were sampled. The sampling hours, meteorological conditions and tides of each field campaign are shown in Table 3.1. The sampling plan was based on *a priori* knowledge of the hydrodynamic conditions, which were known to be mostly wind driven. In addition, sampling was planned to match satellite overpasses, namely Sentinel 2 and Sentinel 3 from the European Space Agency (ESA) (see satellite overpass in Table 3.1). Stations 4, located in the extremity of the jetty that is present along the production area, is reference station with oceanic characteristics.

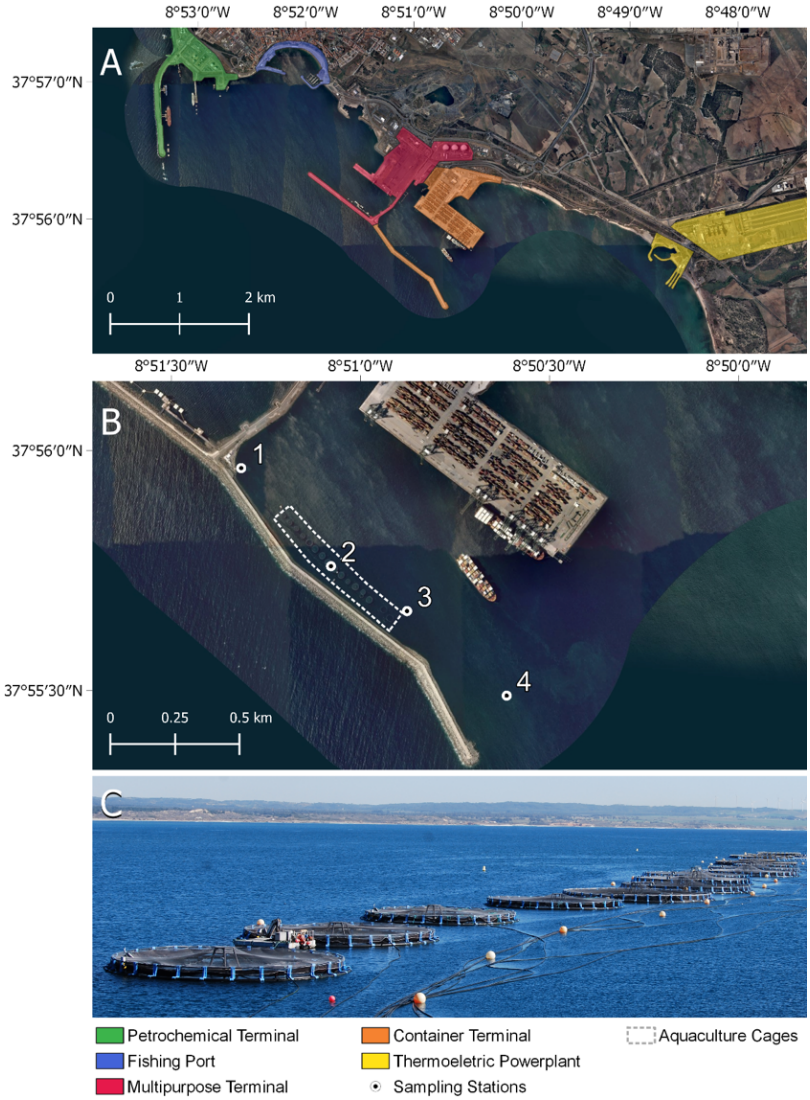

Figure 3.2 – The study site: (A) overview of Sines coast, highlighting the main infrastructures of the Port of Sines; (B) aquaculture and sampling stations location inside the container terminal; (C) production cages (viewpoint from the ground facilities, near station 1). Source: Gomes et al., (2020).

In total 13 water quality parameters and indicators were obtained: temperature, salinity, pH, dissolved oxygen, suspended particulate matter, turbidity, nutrients (ammonia, nitrites, nitrates, phosphates and silicates), light in the water column (light extinction coefficient, euphotic depth and Secchi depth), and phytoplankton biomass and community composition (through pigment analysis and microscopy). T, S, pH and DO were directly measured with both probes that performed continuous Conductivity Temperature Depth (CTD) and discrete (multiparametric probe) depth profiles. Radiometry profiles (discrete depths) and the SD were obtained using a radiometer and a Secchi disk, respectively. SPM, Turb, nutrients and pigments were analysed in the laboratory after collection of surface (0.5 m) and bottom (12 m for station 1, 20 m for station 2, 22 m for station 3 and 18 m for station 4) water samples in each station using a van Dorn water sampler. The bottom water collections were carried out at 2 m, 1 m and 3 m from the bottom for stations 1, 2 and 3, respectively. At station 4, given the strong current due to the oceanic exposure of the station (i.e., less protection of the jetty), it was only possible collect water 12 m from the bottom. Laboratory analysis occurred within 3 h after water collection in the Marine Botany Laboratory of the Marine and Environmental Science Centre in Lisbon. For qualitative microscopic analysis of phytoplankton, water samples of 125 mL were collected

with a 20 µm phytoplankton net that was used vertically along the water column (from 10 m depth until surface). Samples were immediately preserved with Lugol Iodine (12 mL) in dark flasks. For this purpose, samples were collected in station 1 in all campaigns. Next, the methods used to obtain the water quality parameters will be described. In Table 3.2 these methods are summarized.

Table 3.1 - Physical, chemical and biological parameters collected in each campaign and sampling stations. Short names of each parameters are indicated. Satellite overpass according to the Earth Observation Swath and Orbit Visualization tool (ESOV NG) from ESA. S2 – Sentinel 2; S3 – Sentinel 3. Tides according to the Portuguese Hydrographic Institute (IH, 2018). Meteorology from World Weather Online.

Campaign		*29/06/2018*				*25/10/2018*				*12/03/2019*				*30/04/2019*				*23/05/2019*				*29/07/2019*			
Sampling stations		1	2	3	4	1	2	3	4	1	2	3	4	1	2	3	4	1	2	3	4	1	2	3	4
Parameters	*T*	x		x		x		x		x	x	x	x	x	x	x	x	x	x	x	x				
	S	x		x		x		x		x	x	x	x	x	x	x	x	x	x	x	x				
	pH	x		x		x		x						x	x	x	x								
	DO	x		x		x		x		x	x	x	x	x	x	x	x								
	SPM			x		x		x		x	x	x	x	x	x	x	x	x	x	x	x	x	x	x	x
	Turbidity					x		x		x	x	x	x	x	x	x	x	x	x	x	x	x	x	x	x
	Nutrients	x		x		x		x		x	x	x	x	x	x	x	x	x	x	x	x	x	x	x	x
	SD	x		x		x		x		x	x	x	x	x	x	x	x	x	x	x	x	x	x	x	x
	Radiometry	x		x		x		x		x		x		x		x		x		x		x		x	
	Pigments	x		x		x		x		x	x	x	x	x	x	x	x	x	x	x	x	x	x	x	x
Microscopy		x				x				x				x				x				x			
Sampling time		11:00 – 13:50 h				11:45 – 13:00 h				11:20 – 13:35 h				11:45 – 14:20 h				10:10 – 11:30 h				11:45 – 12:45 h			
Meteorology		Air T: 20 °C Wind: 3 km/h Wind direction: NNW Clouds: 23% Precip.: 0 mm				Air T: 22 °C Wind: 4 km/h Wind direction: NNE Clouds: 8% Precip.: 0 mm				Air T: 16 °C Wind: 13 km/h Wind direction: NNW Clouds: 0% Precip.: 0 mm				Air T: 18 °C Wind: 15 km/h Wind direction: NW Clouds: 15% Precip.: 0 mm				Air T: 20 °C Wind: 23 km/h Wind direction: NW Clouds: 0% Precip.: 0 mm				Air T: 21 °C Wind: 27 km/h Wind direction: NW Clouds: 3% Precip.: 0 mm			
Low tide *High tide*		08:58 h (0.9 m) 15:16 h (3.2 m)				08:32 h (0.6 m) 14:44 h (3.4 m)				11:44 h (1.1 m) 18:03 (2.9 m)				05:48 h (1.2 m) 12:02 h (2.7 m)				11:06 h (1.1 m) 17:29 h (3.0 m)				05:54 h (1.1 m) 12:11 h (3.0 m)			
Tide		Flood tide				Flood tide				Low tide, flood tide				High tide, ebb tide				Ebb tide, low tide				Flood tide, high tide			
Satellite overpass		12:30 h (S-2A)				11:39 h (S-3A)				11:01 h (S-3A)				12:30 h (S-2B)				11:13h (S-3B)				12:30h (S-2B) 11:57h (S-3A)			

Table 3.2 - Summary of methods used to obtain the different water quality parameters and indicators.

Parameter	*Method*	*Reference*	*Instrument*
T	Resistance	-	CTD
S	Conductivity	-	CTD
pH	Potentiometry	-	Multiparametric probe
DO	Voltamperometry	-	Multiparametric probe
SPM	Filtration and weight	-	-
Turb	Nephelometry	-	Turbidity meter
Ammonium	Spectrophotometry (Indophenol blue)	Koroleff (1969)	Spectrophotometer
Nitrite	Spectrophotometry (Ammonium chloride and hydroxide/ Sulphanilamide/Hydrochloric acid/ N-(1-Naphthyl)-ethylenediamine dihydrochloride)	Bendschneider and Robinson (1952)	Colorimetric analyser
Nitrate	Spectrophotometry (reduction in Cd column and nitrite method)	Grasshof (1977)	Colorimetric analyser
Phosphate	Spectrophotometry (Ammonium molybdate/sulphuric acid/ tin chloride/ hydrazine sulphate)	Murphy and Riley (1962)	Colorimetric analyser
Silicate	Spectrophotometry (Ammonium molybdate/oxalic acid/tin chloride/hydrazine sulphate)	Fanning and Pilson (1973)	Colorimetric analyser
Light in the water column	Radiometry	-	Radiometer
Phytoplankton pigments	High Performance Liquid Chromatography	Zapata et al. (2000)	-
Phytoplankton community composition	Inverted light and optical microscopy	-	Inverted and light microscopes

3.2.2. Physical and chemical parameters

In situ temperature and salinity vertical profiles were measured using a CTD probe (model NXIC, from FSI). The CTD recorded one data point every second, data were then filtered, binning every 20 data points. Only data collected during the descent of the equipment in the water column were considered.

Dissolved oxygen and pH measurements were performed using a multiparametric probe (model EXO2, from YSI) with a DO meter (YSI optical dissolved oxygen sensor) and a pH meter (YSI pH/redox sensor). Both DO concentration and saturation in the water were measured. The probe collected discrete data at the subsurface and at depth intervals of 2.5 m. Whenever conditions allowed, more datapoints were collected along the water column.

3.2.3. Water clarity parameters and suspended particulate matter

Water turbidity in the surface and bottom of each sampling station was measured in the laboratory using a compact infrared turbidity meter (Lovibond TB 210 IR). For each water sample, triplicate measurements were performed. Transparency of water was measured onsite with a 30 cm diameter White Secchi disk. The penetration of light in the water column was determined using a radiometer (LI-COR Spherical SPQA 4108) that performed discrete measurements along the water column. The light attenuation coefficient (k_d) was calculated from the radiometric data using the Beer-Lambert Law equation:

$$E_z = E_0 e^{-k_d(z-z_0)}$$

E_z is the irradiance measurement at z depth, E_0 is the irradiance when the sensor is just under the water surface, k_d is the light attenuation coefficient and z is the depth. The K_d and Z_{eu} (1% of the surface light) were then calculated using logarithmization and linear regression.

Suspended particulate matter was determined by filtration of surface and bottom triplicate water samples onto Whatman GF/F filters (nominal pore size 0.7 μm and 4.7 cm diameter), previously submitted to 450 °C for 4 h and weighted following Van der Linde (Van Der Linde, 1998). The filtration was carried out with a filtration system coupled to a vacuum pump (used at a pressure of 200 mbar). After filtration, filtration cups and filters were rinsed with 20 mL and 10 mL of ultra-pure water, respectively. Then, the filters were stored at -20 °C in Petri dishes. Within one week, filters were dried for 2 h at 50 °C and weighted. This process was done twice, to guarantee correct filter dryness given by weight stability. The SPM concentration was then calculated through the weight difference (before and after filtering) and considering the filtered volume. For the determination of the organic and inorganic fractions, the filters were submitted to 450 °C for 4 h and weighted. Again, the organic and inorganic were obtained through weight differences. All the filters were weighted with a precision scale (Mettler AE160). For quality control of the SPM data, three blanks were used for each field campaign that followed the whole process described above.

3.2.4. Nutrients

To determine the inorganic nutrient concentrations, triplicate water samples were collected in each sampling station at surface and bottom waters. These were filtered through GF/C Whatman filters (nominal pore size 1.2 μm and 4.7 cm diameter) and immediately frozen at -20 °C for later colorimetric analysis with a Tecator FIAstar 5000 Analyser (except ammonium). Nitrite (NO_2^-), nitrate (NO_3^-), phosphates (PO_4^{3-}, hereafter referred to as P), and silicates (SiO_2, hereafter referred to as Si) were determined according to Bendschneider and Robison (Bendschneider and Robinson, 1952), Grasshoff (Grasshoff, 1977), Murphy and Riley (Murphy and Riley, 1962) and Fanning and Pilson (Fanning and Pilson, 1973), respectively. As nitrite levels in coastal waters are typically very low, the nitrite and nitrate sum were used (NO_3^- + NO_2^-, hereafter referred to as N). Ammonium (NH_4^+) concentrations were determined using manual colorimetric methods in filtered samples according to Koroleff (Koroleff, 1969), using a Shimadzu spectrophotometer (UV-2600). For the ammonium determination, the water samples were fixed immediately after collection and measurements were performed after 24h stored in the dark. Detection limits (DL) determined were 0.16 μmol L^{-1} for P, 0.20 μmol L^{-1} for NH_4^+, 0.36 μmol L^{-1} for N, 7.12 μmol L^{-1} for Si.

3.2.5. Phytoplankton pigments and community composition

For phytoplankton pigment analysis, surface and bottom water samples were taken during the six field campaigns using Van Dorn water sampling bottles. In total, 38 water samples for pigment analysis were taken (Table 3.3). Those were filtered onto Whatman 25 mm diameter GF/F filters (nominal pore size 0.7 μm) and stored at -80°C. The filtered volumes varied from 0.375 L to 1.00 L (Table 3.3). Pigment analysis was then performed using reversed phase High Performance Liquid Chromatography (HPLC). For this purpose, phytoplankton pigments were extracted with 3 mL of 95% cold-buffered methanol (2% ammonium acetate) enriched with a known concentration of trans-beta-apo-8'-carotenal (used as internal standard) for 1h at - 20 °C, in the dark. At half-time period of extraction, samples were sonicated for 5 minutes and after the extraction period centrifuged for 10 minutes (at 4000 rpm). All extracts were filtered (Fluoropore PTFE filter membranes, 0.2 μm pore size), mixed with 0.4 mL of ultra-pure water and injected in the HPLC. The solvent gradient followed Zapata et al. (2000) with a flow rate of 1 mL min^{-1}, and an injection volume of 100 μL and 40 min elution programme. Pigment extracts were analysed using a Shimadzu HPLC comprising a Shimadzu (Prominence I LC-2030C 3D) with a Fluorescence Detector (Shimadzu RF-20A Prominence), with LabSolution Lite version 5.82 software. Chromatographic separation was carried using a monometric C8 column for reverse phase chromatography (Symmetry C8, 15 cm long, 4.6 mm in diameter, and 3.5 μm particle size).

The identification of the different pigments was based on retention time and peak shape, i.e. through fingerprint matching with known peak shape from the spectra library created by running pure standard of individual pigments. Subsequently, concentrations of pigments were computed from the peak areas using the calibration curve of each pigment.

The main phytoplankton groups were then determined using a simple approach considering the following marking pigments: fucoxanthin for diatoms, peridinin for dinoflagellates, chlorophyll *b* for chlorophyta (green algae), alloxanthin for cryptophyta, zeaxanthin for cyanobacteria, and 19'-Hexanoyloxyfucoxanthin for haptophyte (coccolithophores). The relative abundance of each group was then calculated normalizing each pigment by the sum of all diagnosing pigments (TPigments). The Chl-*a* degradation pigments, i.e. phaeopigments (Phaeos) considered represent the sum of Chlorophyllide, Pheophorbide *a* and Phaeophytin.

The samples preserved with Lugol's Iodine were analysed for determination of the phytoplankton community composition. In the laboratory, observations were made using an inverted light microscope Axiovert 200 (Zeiss), with an Axiovision camera attached. The cells were quantified in a 10 mL Utermöhl chamber. Cells larger than 10 μm were quantified in the whole chamber for a total magnification of 200x (corresponding to a final volume of 10 mL). Whenever it was necessary, the cells were manipulated after quantification to obtain more favorable observations for their identification. This manipulation generally involved changing the position of the cells by blowing using a drawn tip Pasteur micropipette. Difficult-to-identify dinoflagellate cells were isolated with the same Pasteur micropipette with extended tip and observed under a BX 50 optical microscope (Olympus) coupled with fluorescence.

Table 3.3 - Details of collected samples including depth, filtration volume, extraction volume and HPLC method used.

Campaign	*Date*	*Station*	*Depth (m)*	*Filtration volume (L)*
1	29/06/2018	1	0.5	*0.75*
		3	0.5	*1.00*
2	25/10/2018	1	0.5; 12	*0.80; 0.50*
		3	0.5; 22	*1.00; 0.375*
3	12/03/2019	1	0.5; 12	*0.65; 0.50*
		2	0.5; 20	*0.50; 0.50*
		3	0.5; 22	*1.00; 0.50*
		4	0.5; 25	*1.00; 1.00*
4	30/04/2019	1	0.5; 12	*1.00; 1.00*
		2	0.5; 20	*1.00; 1.00*
		3	0.5; 22	*1.00; 1.00*
		4	0.5; 25	*1.00; 1.00*
5	23/05/2019	1	0.5; 12	*1.00; 1.00*
		2	0.5; 20	*1.00; 1.00*
		3	0.5; 22	*1.00; 1.00*
		4	0.5; 25	*1.00; 1.00*
6	29/07/2019	1	0.5; 12	*1.00; 1.00*
		2	0.5; 20	*1.00; 1.00*
		3	0.5; 22	*1.00; 1.00*
		4	0.5; 25	*1.00; 1.00*
Total number of samples	***38***			

3.2.6. Statistical analysis of in situ data

Descriptive statistics were used to report acquired and determined data. For each parameter, the results are reported graphically exposing all data. Further the mean of each sampling station, as well as the mean of all sampling stations for each field campaign, are reported numerically. Standard deviation is reported for each mean. In addition, the extremes (i.e., absolute minimum and maximum) of each parameter are given for each field campaign.

3.3.Remote sensing data: biological and physical parameters

The satellite retrieved variables of interest for this thesis were SST, Turb, and Chl-*a*. The data analysis and illustrative outputs were made using Python software (www.python.org), version 3.6, through Anaconda Spyder scientific environment. Table 3.4 summarizes the main details of the used products, and the means of data access. In the next subsections, the used products and the performed analyses will be described.

Table 3.4 - RS products details: product, satellites and sensors, variable, processing level, applied algorithm, spatial and temporal resolution and means of data access.* Temporal coverage of these products is dependent on the orbit of the satellites.

Product	*Satellite(s) and sensor(s)*	*Variable (units)*	*Processing level*	*Applied algorithm*	*Spatial res.*	*Temporal res.*	*Data access*
GHRSST	Aqua – AMSR-E Aqua – MODIS NOAA-19 – AVHRR-3 Terra – MODIS CORIOLIS – WINDSAT GCOM-W1 – AMSR2	SST (°C)	L4	Not applicable	1 km	Daily (May 2002 – July 2019)	Downloaded via FTP from the GHRSST dataset
OC-CCI	Orbview-2 – SeaWiFS Aqua – MODIS Envisat – MERIS Suomi-NPP - VIIRS	Chl-*a* *(mg m^{-3})*	L3	OCI (OC4v6+CI), OC3 and OC5	4 km	Monthly (September 1997 – June 2018); 8-day composites (September 1997 – December 2019); Daily (April – July 2019)	Via OPeNDAP, from the PML RSG Web Services CCI Development Catalog/Ocean Colour CCI
-	Envisat - MERIS	Chl-*a* *(mg m^{-3})*	L3	OC5	300 m	Daily * (May 2002 – April 2012)	NetCDF dataset provided by the PML; from the Aqua-USERS Project archive
-	OLCI – Sentinel-3A and 3B	Chl-*a* *(mg m^{-3})*	L3	Polymer	300 m	Daily * (April 2019 – January 2020)	Via OPeNDAP provided by the PML, supplied by the NEODAAS
-	MSI – Sentinel-2A	Chl-*a* *(mg m^{-3})*	L3	Polymer + OC2	100 m	Daily * (April 2019- January 2020)	Via OPeNDAP, from the Copernicus Global Land Operations Service, provided by the PML
-	MSI – Sentinel-2A	Turb (NTU)	L3	Optical water type dependant blending of SPM	100 m	Daily * (April 2019- January 2020)	Via OPeNDAP, from the Copernicus Global Land Operations Service, produced by the PML and Brockmann Consult

3.3.1. Satellite sea surface temperature

The physical basis for measurements of SST from space is the detection, by a spaceborne microwave or infrared radiometer, of the thermal energy emitted by the ocean surface. The amplitude of these wavelengths varies with the temperature of the ocean and therefore can be used to measure it. The surface radiation is modified while passing through the atmosphere and therefore appropriate corrections must be converted to surface temperature, which requires knowledge or measurement of the surface emissivity and corrections for reflected solar and atmospheric radiation (Njoku, 1990). Infrared and microwave techniques provide these measurements and corrections in somewhat different ways, each with unique advantages and disadvantages (see e.g. Maurer, 2002). For example, infrared satellite sensors have better spatial resolution but are more susceptible to cloud contamination than microwave (PODAAC, 2019).

GHRSST

Daily level 4 (i.e., level 3 data combined with in situ SST observations from the NOAA iQuam project) SST from the Group for High Resolution Sea Surface Temperature (GHRSST) was used with 1 km spatial resolution (0.01° x 0.01°), for the period 2002-2019. The data was extracted via File Transfer Protocol (FTP) from the Jet Propulsion Laboratory (JPL) Multi-scale Ultra-high Resolution (MUR) Making Earth Science Data Records for Use in Research Environments (MEaSUREs) Project dataset (JPL MUR MEaSUREs Project, 2015). The version 4 of the abovementioned dataset was used, which is based on the observation of several instruments including the National Aeronautics and Space Administration (NASA) Advanced Microwave Scanning Radiometer - Earth Observing System (AMSR-EOS), the Japan Aerospace Exploration Agency (JAXA) Advanced Microwave Scanning Radiometer 2 on GCOM-W1, the Moderate Resolution Imaging Spectroradiometer (MODIS) on the NASA Aqua and Terra platforms, the United States Navy microwave WindSat radiometer, the AVHRR on several NOAA satellites, and *in situ* SST observations from the NOAA iQuam project.

3.3.2. Satellite chlorophyll-a concentration

Satellite-based ocean colour instruments measure the radiant flux emanating upward from water bodies that reach the top of the atmosphere. Estimates of water-leaving radiances are then retrieved through the application of atmospheric correction processing (e.g. Polymer). Typically, multispectral radiometers (i.e. ocean colour satellite sensors) sample a limited number of narrow wavebands, chosen to capture the main structure of the spectral shape of the incoming light (Martin, 2014). From the relative magnitude of the water-leaving radiance detected by the different spectral channels of a radiometer, it is possible to estimate the concentration of those water constituents which give the ocean its colour (e.g. chlorophyll, suspended particulate matter and colored dissolved organic matter) (Robinson, 2010) via application of bio-optical algorithms (e.g. Ocean Chlorophyll 4,OC4). In this thesis, four ocean colour products were used, namely the merged product from Ocean Colour (OC) Climate Change Initiative (CCI), and single sensor products from the Medium Resolution Imaging Spectrometer (MERIS), the Ocean and Land Colour Instrument (OLCI) and the Multispectral Instrument (MSI). The used products were already processed until Level 3 (L3, i.e., with applied radiometric and geometric calibration, georeferencing, atmospheric correction and bio-optical algorithms, and mapped onto uniform space-time grids).

OC-CCI

The CCI (http://cci.esa.int/) is an ESA programme contributing to a rapidly expanding body of scientific knowledge due to its long-term global Earth observation archives established over the last 30 years. This program comprises fourteen parallel projects geared to Essential Climate Variables (ECV) data production of which ocean colour is one of them. Of all the marine ECV in the CCI programme, ocean colour is the only one that targets the biological field (Grant et al., 2017). The remote sensing derived chlorophyll-*a* concentration in seawater, from the OC-CCI dataset Version 4.0 (https://rsg.pml.ac.uk/thredds/catalog-cci.html), was generated by SeaWiFS Data Analysis System (SeaDAS) using a blended combination of three algorithms: the ocean colour index (OCI) (Ocean Colour 4v6 (OC4v6) + Colour Index (CI) from Hu et al., 2012), and the band ratio algorithms Ocean Colour 3 (OC3) and Ocean Colour 5 (OC5), depending on water class memberships (Jackson et al., 2017). Fourteen water class memberships are considered, based on their optical properties. Data was accessed via Open-source Project for a Network Data Access Protocol (OPeNDAP). Monthly composites were used with 4 km spatial resolution, with records starting on September 1997 until December 2018.

MERIS

MERIS is an imaging spectrometer on the ESA environmental satellite Envisat. The entire operational period of the Envisat mission, from 9th May 2002 until 8th April 2012, of full spatial resolution (300 m) chlorophyll-*a* concentration was used for the Portuguese Western coast. The MERIS Chl-*a* product was processed by the Plymouth Marine Laboratory (PML) in the scope of the AQUA-Users Project, using the OC5 bio-optical algorithm (Gohin et al., 2008), developed for coastal waters. The full dataset was accessed in Network Common Data Form (NetCDF).

OLCI

Sentinel-3 (S3) is an EO satellite constellation developed by the ESA as part of the Copernicus Programme, which currently consists of two satellites: Sentinel-3A (S-3A, launched in February 2016) and Sentinel-3B (S-3B, launched in April 2018). The OLCI sensor onboard both S-3A and S-3B was developed in part to provide continuity with measurements made previously by the MERIS. Composited L3 Chl-*a* from the OLCI instrument (300 m spatial resolution) were provided by the PML Remote Sensing Group via OPeNDAP, supplied by the Natural Environment Research Council (NERC) Earth Observation Data Acquisition and Analysis Service (NEODAAS). The used Chl-*a* dataset was processed using the Polynomial-based algorithm applied to MERIS (Polymer) v4.12 (Steinmetz et al., 2011), comprising data from the 1st April 2019 until the 10th January 2020.

MSI

Identical to the S3, Sentinel-2 (S2) is an EO mission from the Copernicus Programme, operated by ESA, that systematically acquires optical imagery at high spatial resolution over land and coastal waters. The mission supports a broad range of services and applications, specially land based (e.g. agricultural applications). Nonetheless, it has been successfully applied to water quality of coastal regions. It is also a constellation of two twin satellites (S-2A launched in June 2015 and S-2B launched in March 2017), however only S-2A was used since the used product was not yet available for S-2B. The S-2A aggregated L3 used product was Chl-*a* from the Copernicus Global Land Operations Service under Copernicus Global Land Operations, provided by the PML via OPeNDAP, with 100 m spatial resolution. Chl-*a* was derived using the Ocean Colour 2 algorithm (OC2). Available data for these products extended from the 30th April 2018 until the 10th January 2020.

3.3.3. Satellite turbidity

The RS turbidity product was retrieved from the S-2A MSI sensor. Like the MSI Chl-*a*, turbidity is a L3 product from the Copernicus Global Land Operations Service under Copernicus Global Land Operations, provided by the PML via OPeNDAP, with 100 m spatial resolution. Turbidity was processed by the PML and Brockmann Consult, through pixel-mean derived with Calimnos optical water type dependant blending of total suspended matter algorithms as tuned in the GloboLakes project. Available data for these products extended from the 30th April 2018 until the 10th January 2020.

3.3.4. Remote sensing data analysis

Climatologies

Climatological analysis was performed in different areas both for SST and Chl-*a* RS products. These climatologies were carried out in a downscaling approach, starting from the general panorama of the Western Iberia, to the Western Portuguese coast and finally the ROI centered in Cape Sines (Figure 3.3). The climatologies were materialized through per-pixel averages in the aforementioned areas as detailed in Table 3.5. All SST climatological averages (annual, seasonal and monthly) were performed using the GHRSST product. Concerning Chl-*a*, the annual climatological average used the OC-CCI product while the seasonal and monthly analyses used the MERIS retrieved product. The utilized SST dataset ranged from June 2002 until June 2018, while for Chl-*a* data from September 1997 until June 2018 and from May 2002 until April 2012 was used for the OC-CCI and MERIS products, respectively. Per-pixel standard deviations were also computed for each climatological analysis. For SST, all climatologies were made using the GHRSST products, while for Chl-*a*, the annual climatological average was made using OC-CCI product, and the seasonal and monthly climatologies were made using the MERIS derived Chl-*a*. Regarding the seasonal climatologies, the seasons were considered as follows: summer - June, July and August; autumn - September, October and November; winter - December, January and February; spring - March, April and May.

Table 3.5 – Details about the performed annual, seasonal and monthly climatological averages.

Climatological average	*RS Products*	*Spatial resolution*	*Time interval used*	*Area*
Annual	SST (GHRSST	1 km	June 2002 – June 2018	Western Iberia (Figure 3.3, red square)
	Chl-*a* (OC-CCI)	4 km	September 1997 – June 2018	
Seasonal	SST (GHRSST	1 km	May 2002 - April 2012	Western Portuguese coast (Figure 3.3, green square)
	Chl-*a* (MERIS)	300 m	May 2002 - April 2012	
Monthly	SST (GHRSST	1 km	May 2002 - April 2012	Sines region, i.e. ROI (Figure 3.3, blue square)
	Chl-*a* (MERIS)	300 m	May 2002 - April 2012	

Product comparison of inactive (MERIS) and active (OLCI) ocean colour sensors

The Chl-*a* concentration retrieved from MERIS OC5 and OLCI Polymer algorithms was compared in the ROI by computing the per pixel climatological average of the MERIS product (2002 - 2012) for the available OLCI product dataset (i.e., from the 1st April until the 20th November). Thus, this analysis resulted in the comparison between the climatological average of 1707 L3 processed MERIS Chl-*a* images with 233 L3 OLCI Chl-*a* images. Further, a full dataset Chl-*a* monthly mean time series for both products was computed for a pixel inside the aquaculture region with an area of 1.44 km^2 (Figure 3.3, black square).

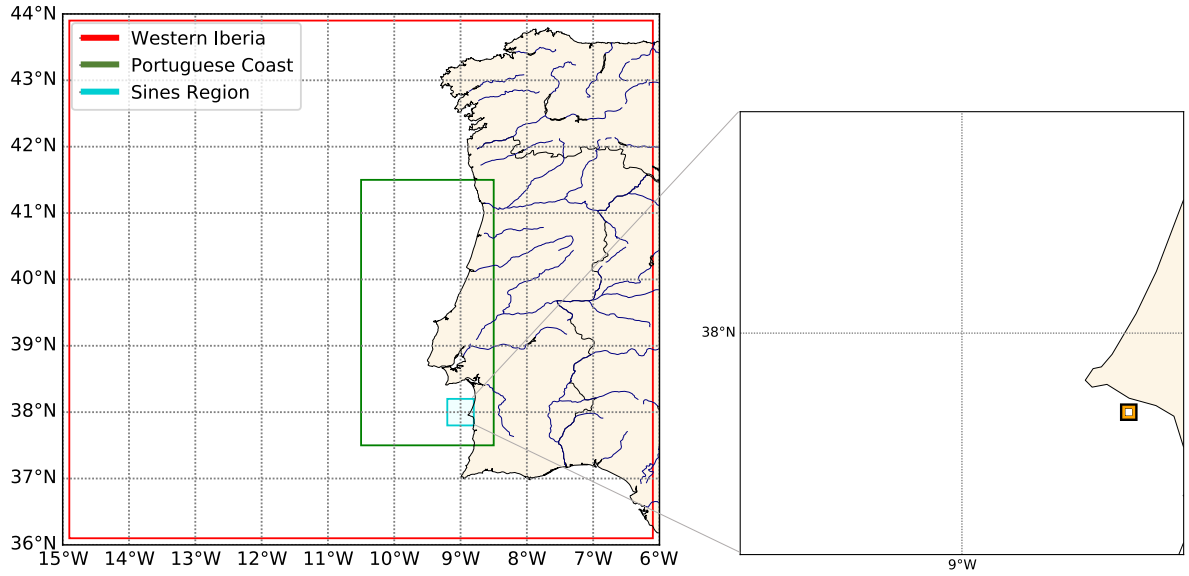

Figure 3.3 - Areas used for climatological and percentile analysis (Chl-*a* and SST). Left subplot - areas used in the climatological analyses: red square - Western Iberia; green square - Portuguese Coast; blue square - Sines region (ROI). Right subplot - areas used in the climatological year and percentile analyses: black square – area averaged for Chl-*a*; orange square – area averaged for SST.

Climatological year and percentile analysis

The analysis of the climatological year was carried out by creating a time series with weekly averages and percentiles 10 (p10) and 90 (p90) of SST (2002 – 2019) and Chl-*a* (2002 - 2012). Then, the same weeks of each year were overlapped. In the ROI, for the SST climatological year and percentile analysis, an area of 1 km^2 (1x1 pixels of 1 km) centered in the aquaculture cage production was used (Figure 3.3, right subplot, orange square). For the analogous Chl-*a* analysis, an area of 1.44 km^2 (4x4 pixels of 300 m) that encompasses all *in situ* sampling stations was averaged (Figure 3.3, right subplot, orange square). The averages for the areas used was obtained in different ways. Regarding SST, the Sentinel Application Platform (SNAP) software version 6.0 was used, namely the Extract Pixel Values tool, averaging the selected area (1x1 pixels centered in the *in situ* sampling stations: Lat 37.928600 Lon -8.849500). For Chl-*a*, the selected area average (4x4 pixels centered in the stations) was performed manually using a Python routine. It should be noted that different areas were obtained (1 km^2 for SST and 1.44 km^2 for Chl-*a*) due to the different spatial resolutions of the products used (1 km for SST and 300 m for Chl-*a*). For Chl-*a*, values higher than three times the standard deviation, throughout the climatological year were discarded.

Comparison of remote sensing products and *in situ data*

Satellite retrieved products, namely Chl-*a*, Turb and SST, were compared with *in situ* data through the overlapping of available time series and matchup analysis. For Chl-*a* and Turb the *in situ* data were obtained in the field campaigns (see section *3.1. In situ data: physical, chemical and biological parameters*). Regarding temperature, besides from the CTD temperature obtained in the field campaigns, *in situ* T from a buoy from the Portuguese Hydrographic Institute (IH) located offshore Sines was used (Lat 37.69167 Lon -9.7250000, the location of the buoy is indicated with a blue cross Figure 3.4). This buoy recorded data hourly, which were sub-sampled to a daily frequency for the time series and matchup comparisons with RS data. This task was performed averaging full 24 h periods.

For the RS products, small scale spatial variability can be expected and therefore multi-pixel areas were used. In the aquaculture vicinity in Sines, this is particularly evident for the SST, since a hot water outflow (water temperatures up to 30 ºC) from a thermoelectric powerplant is located approximately 3 km southwest from the sampling station 4 (see Figure 3.2-A). For this reason, despite the SST being homogeneous in relatively large areas, the minimum area equivalent to just 1 pixel was used to compare the in situ CTD data with RS SST. The areas considered for each comparison are shown in Figure 3.4. Each square delimits the areas for which RS products were averaged to be compared with the *in situ* data. In total seven areas were considered: two areas for *in situ* temperature (CTD and buoy T) and RS SST comparisons; and five areas for *in situ* Turb and Chl-*a* comparisons with the same products retrieved from RS products:

- Orange square (Figure 3.4, left subplot) – 1 km^2 for SST vs CTD T (all stations averaged);
- Grey square (Figure 3.4, left subplot) – 9 km^2 for SST vs buoy T;
- Black square (Figure 3.4, left subplot) – 1.44 km^2 for Chl-*a* and Turb (RS vs *in situ* all stations averaged). This area was also used for the comparison of Poly OC2 (MSI) and Polymer v4.12 (OLCI) retrieved Chl-*a*;
- Red square (Figure 3.4, right subplot) – 1.44 km^2 for Chl-*a* and Turb (RS vs *in situ* station 1);
- Green square (Figure 3.4, right subplot) – 1.44 km^2 for Chl-*a* and Turb (RS vs *in situ* station 2);
- Yellow square (Figure 3.4, right subplot) – 1.44 km^2 for Chl-*a* and Turb (RS vs *in situ* station 3);
- Blue square (Figure 3.4, right subplot) – 1.44 km^2 for Chl-*a* and Turb (RS vs *in situ* station 4).

The CTD T used in the comparison with RS SST corresponds to the surface water temperature of all stations averaged, given the low variations between station (maximum variations of 0.3 °C in 29/06/2018; 0.1 °C both in 25/10/2018 and 12/03/2019; 0.2 °C in 30/04/2019; and 0.7 °C in 29/07/2019). On the other hand, for chlorophyll-*a* and turbidity the comparisons were made using all stations separately.

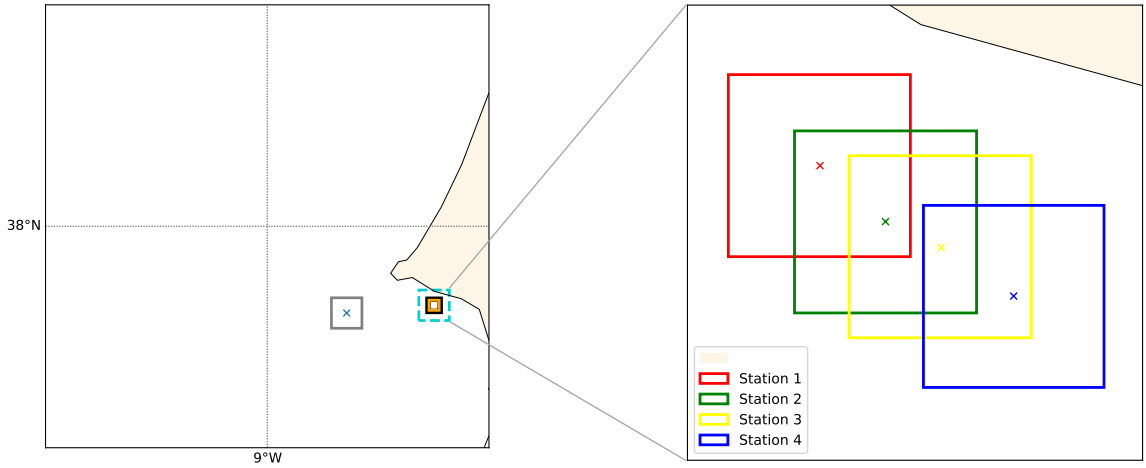

Figure 3.4 – Areas used for the comparison of RS and *in situ* data. Each square delimits the areas for which RS products were averaged to be compared with the *in situ* data. Left subplot: orange square – for comparison of RS SST with CTD T; grey square - for comparison of RS SST with buoy T (blue cross indicates the position of the buoy); black square - for comparison of RS with *in situ* Chl-*a* and Turb (all stations averaged). Right subplot: areas centred in each sampling station for the comparison of RS with *in situ* Chl-*a* and Turb (for each station): red square for station 1, green square for station 2, yellow square for station 3 and blue square for station 4. The coloured crosses indicate the location of the *in situ* sampling stations.

It should be noted that the OLCI Chl-*a* represents the average of both OLCI sensors from S-3A and S-3B. Also, MSI Chl-*a* and Turb were retrieved only from S-2A MSI since S-2B MSI data was not available in the used dataset (see Table 3.4).

For the matchup analysis, several parameters were calculated to evaluate algorithm uncertainty in comparison to *in situ* data. These were linear regression parameters such as the coefficient of determination (r^2), slope and intercept; as well as the mean Relative Percentage Difference (RPD) and the mean Absolute Percentage Difference (APD), calculated as follows:

$$\mathrm{RPD} = \frac{1}{N}\sum_{i=1}^{N}\frac{[Sat]_i - [In\ situ]_i}{[In\ situ]_i} \times 100$$

$$\mathrm{APD} = \frac{1}{N}\sum_{i=1}^{N}\frac{|[Sat]_i - [In\ situ]_i|}{[In\ situ]_i} \times 100$$

Anomalies

Anomalies were computed over space and time in the ROI using different remote sensing products. Chlorophyll-*a* concentration spatial anomalies were determined for three of the six dates where field campaigns were carried out, namely for the 30/04/2019, 23/05/2019 and 29/07/2019. For this task, the average of the last 7 and 14 days was subtracted from the average of 3 days centered on the dates indicated above. The 3-day average was used to represent the three dates to maximize the valid pixels in the area, reducing the effect of cloud contamination (i.e., invalid pixels). This analysis was done using both CCI Chl-*a* (4 km, daily) and OLCI Chl-*a* (300 m, daily) for the entire ROI.

Time series of the SST and Chl-*a* anomalies were calculated for a subset of the ROI (area of 8 km^2), indicated with the black square in Figure 3.5. This area was chosen due to the relatively low resolution of the CCI product (4 km), which did not allow choosing an area centered on aquaculture production in Sines. The upper right corner of this polygon coincides with sampling station 4 (see Figure 3.2 and Figure 3.4). The anomaly time series represent the difference of the year 2019 with historical data, for this specific area. The used products were from GHRSST SST (2002-2019) and CCI Chl-*a* (1997-2019) since historical data were available for them.

For the CCI Chl-*a*, the database had the 8-day composite product available (see Table 3.4). On the other hand, for the GHRSST SST, the 8-day averages were computed from the daily dataset using a Python routine. The 2019 SST anomaly time series is not complete since data were only available until the end of July 2019.

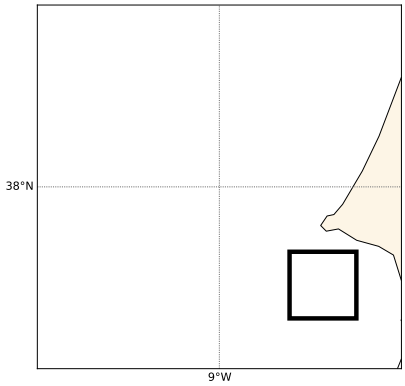

Figure 3.5 – Entire area: ROI; back square: area averaged for the anomaly time series analysis.

4. Results

4.1. Region of interest characterization with satellite data: SST and Chl-*a* variability

Climatological annual averages

The climatological annual averages for sea surface temperature (daily SST, GHRSST) and surface chlorophyll-*a* concentration (monthly Chl-*a,* OC-CCI) computed from 16 and 21 years of remote sensing data, respectively, along Western Iberia are shown in Figure 4.1. The standard deviation (Std) and the number of observations (N) that contributed to the climatology are also shown. The number of observations of SST are uniform along the entire area as they were derived from L4 data (i.e., combination of remote sensing and *in situ* data), in contrast to the L3 Chl-*a* data where a higher number of observations along the coast can be observed.

The climatological annual SST average along the West Iberian coastal and oceanic waters (Figure 4.1. top) indicates a latitudinal gradient, with higher temperatures in the southern domain (≈19 °C) and lower temperatures in the northern domain (≈16 °C). Along the Portuguese western coast, an evident coast-offshore gradient is observed, with lower SST values in coastal waters when compared to oceanic waters at the same latitude. The variability of temperature is also lower adjacent to the coast (std ≈1.8 °C) than in oceanic waters (std ≈2.8 °C). The southern coast of Portugal, including the Cadiz Gulf, shows a less marked coast-offshore gradient, and presents the highest average temperatures of the whole area considered (19.6 °C). The variability in this region is the highest along with the coastal region of the Bay of Biscay (both regions with std ≈3.5 °C).

The climatological annual average of phytoplankton biomass (Figure 4.1. bottom), indexed as chlorophyll-*a* concentration, also shows latitudinal and coast-offshore gradients. Unlike SST, higher Chl-*a* concentrations are found at higher latitudes and along the entire coastal waters. Oceanic waters evidence an oligotrophic character, i.e. they contain very low concentrations of Chl-*a*, especially in the southern domain of the considered area. Also contrasting with the SST pattern, higher variability of Chl-*a* is found in coastal waters (std ≈0.8 mg m^{-3}) and lower in the oceanic domain (std 0.1 - 0.4 mg m^{-3}).

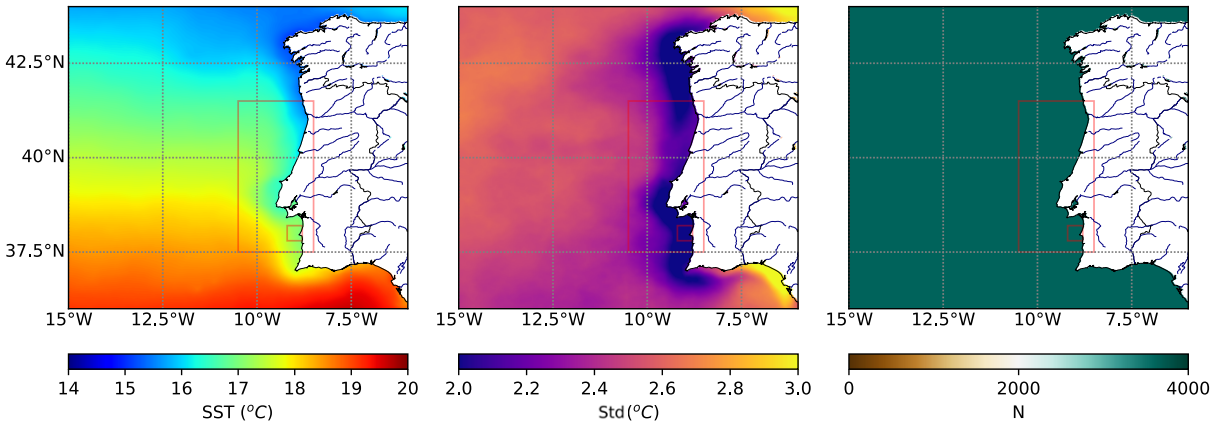

Figure 4.1 - Climatological annual average (June 2002 until June 2018 for SST; September 1997 until June 2018 for Chl-*a*) of sea surface temperature (SST, top) and chlorophyll-a concentration (Chl-*a*, bottom – next page), standard deviation (Std) and number of observations (N) off the Western Iberian Coast. Daily SST data is from GHRSST, 1 km resolution; and monthly Chl-*a* data is from OC-CCI, 4 km resolution.

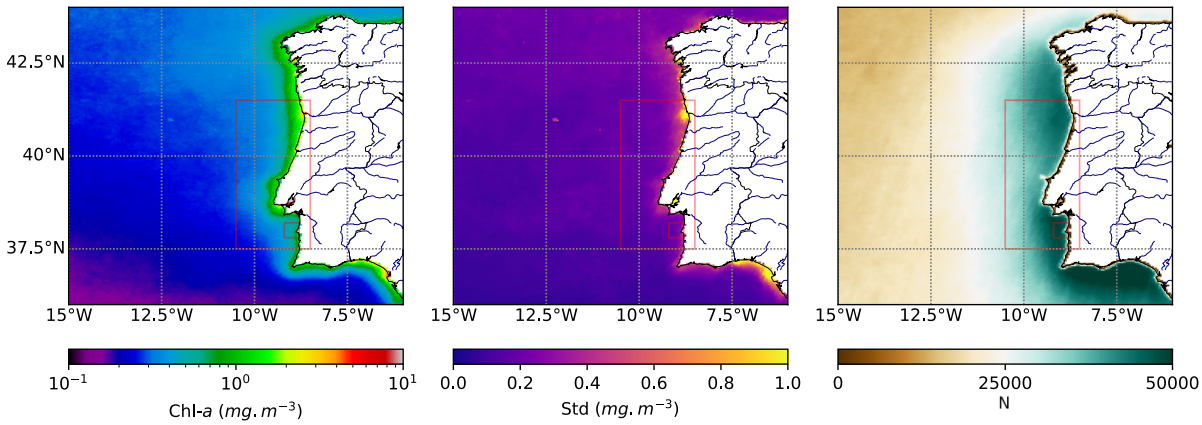

Figure 4.1 – Continued.

Climatological seasonal averages

The seasonal climatological averages of SST (daily, GHRSST) and Chl-*a* (daily, MERIS) computed from 10 years (May 2002 – April 2012) of remote sensing data for the Portuguese Western Coast are shown in Figure 4.2. Seasons were grouped considering the following: summer - June, July and August; autumn - September, October and November; winter - December, January and February; spring - March, April and May. For the entire area considered, the climatological SST average varies between 17.30 °C and 20.39 °C in summer (std 0.67 °C); 16.75 °C and 20.50 °C in autumn (std 0.78 °C); 13.56 °C and 16.36 °C in winter (std 0.61 °C); and 14.25 °C and 16.55 °C in spring (std 0.52 °C). As evidenced by the annual climatological average, all seasons indicate higher water temperatures in the southern oceanic domain of the considered area, and lower temperatures along the coast (Figure 4.2, left).

Analogous to the pattern verified in the annual climatology, all seasons show a stronger Chl-*a* signal in coastal waters, and a marked coast-offshore gradient of phytoplankton biomass (Figure 4.2, right). The number of observations that contributed to the climatological averages are shown in Figure A.1 of the Appendix. Overall, spring is the most productive and variable season over the entire area throughout the 10 years (2002 - 2012). Offshore waters mark a clear seasonal spring maximum and summer/autumn minimum. In these waters, variability of Chl-*a* along the years is low in summer and autumn (std close to 0 mg m^{-3}); and higher in winter and spring (std 0.5 – 1.5 mg m^{-3}). In the coastal domain, the highest Chl-*a* concentrations (≥ 10 mg m^{-3}) are found north of 40 °N in summer and autumn; and south of 38.5 °N in spring. These regions of high Chl-*a* concentration appear to be the most variable over the years (std > 2.5 mg m^{-3}).

Climatological monthly averages

Zooming into the Sines region, monthly climatological averages and standard deviations of SST (daily, GHRSST) and Chl-*a* (daily, MERIS) are shown in Figure 4.3 and Figure 4.4, respectively. The scales used for SST are adjusted to the minimum and maximum values found for each monthly climatological average and standard deviation. Over the months, temperatures are lower close to the coast, particularly in the area where the aquaculture units are located (south of Cape Sines), where a relatively colder water plume persists throughout the year. February is the month with the lowest temperatures (14.44 – 15.07 °C), followed by March (14.76 – 15.29 °C) and January (14.96 – 15.65°C). Throughout spring, temperatures rise until summer and fall, where the highest temperatures over the entire area are found in August (19.00 – 19.47 °C), September (18.86 – 19.57 °C) and October (18.79 – 19.51 °C). In the remaining months, the range of climatological temperatures found was 15.68 –

15.91 °C for April; 16.59 – 17.05 °C for May; 18.33 – 18.59 °C for June; 18.29 – 18.76 °C for July; 17.41 – 18.06 °C for November; and 15.87 – 16.47 °C for December. Temperature variability over 10 years in each month is low: November is the most variable month over the 10 years (std 1.15 – 1.40 °C), especially south of Cape Sines where the aquaculture is located. On the other hand, the less variable month is March (0.56 – 0.68 °C).

Regarding the climatological monthly averages of Chl-*a* (Figure 4.4.), there is a well-defined maximum over the entire area from March until May, with higher concentrations along the entire coast (≈ 8 mg m^{-3}) and extending to offshore areas (≈ 2 mg m^{-3}). This maximum persists until September in the coastal region, particularly south of Cape Sines where the width of this most productive waters is larger. The lowest Chl-*a* concentrations (≈ 0.4 mg m^{-3}) are found offshore in December, January and February. The variability of Chl-*a* along the 10 years is always greater close to the coast, especially in the months where Chl-*a* is higher. October, November and December are the less variable months in the coastal regions.

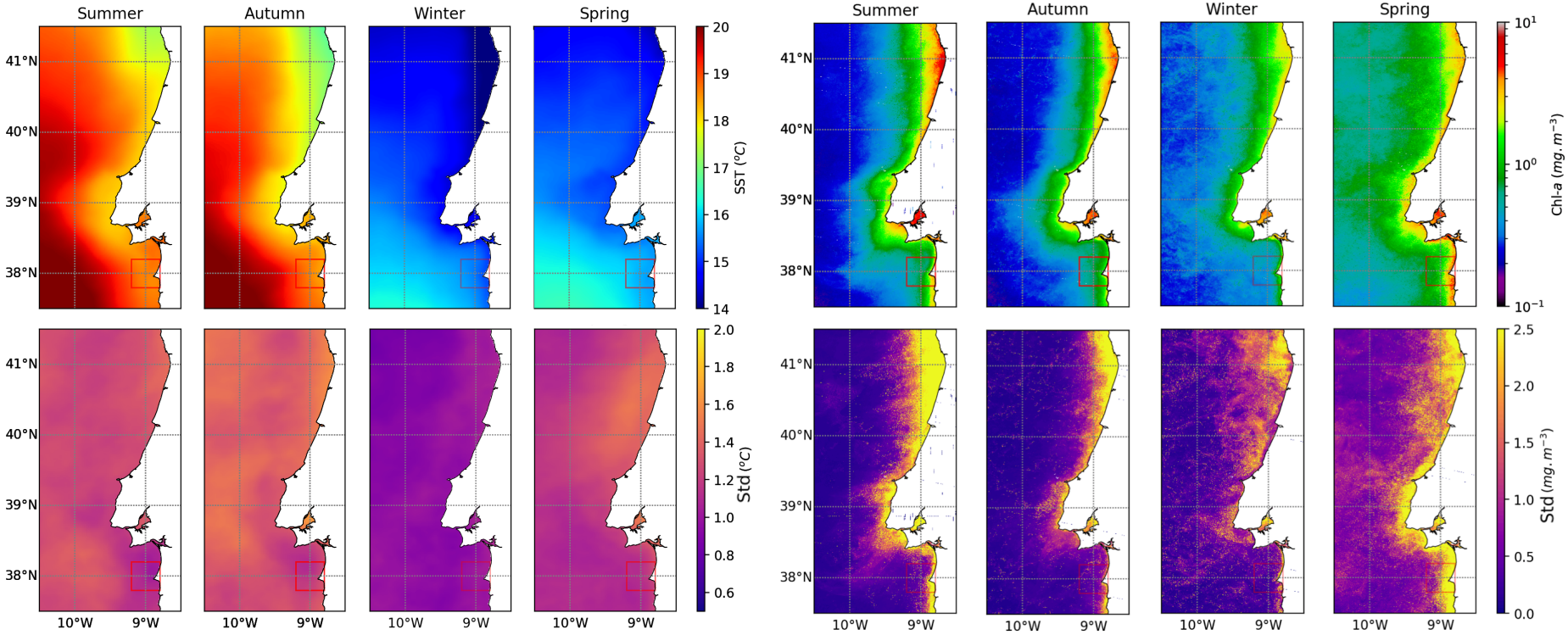

Figure 4.2 - Climatological seasonal average (May 2002 – April 2012) for sea surface temperature (SST, left) and chlorophyll-a concentration (Chl-*a*, right), and standard deviation (std) off the Portuguese western coast. Daily SST data from GHRSST, 1 km resolution. Daily Chl-*a* data from MERIS, 300 m resolution. Summer – June, July and August; autumn – September, October and November; winter – December, January and February; spring – March, April and May.

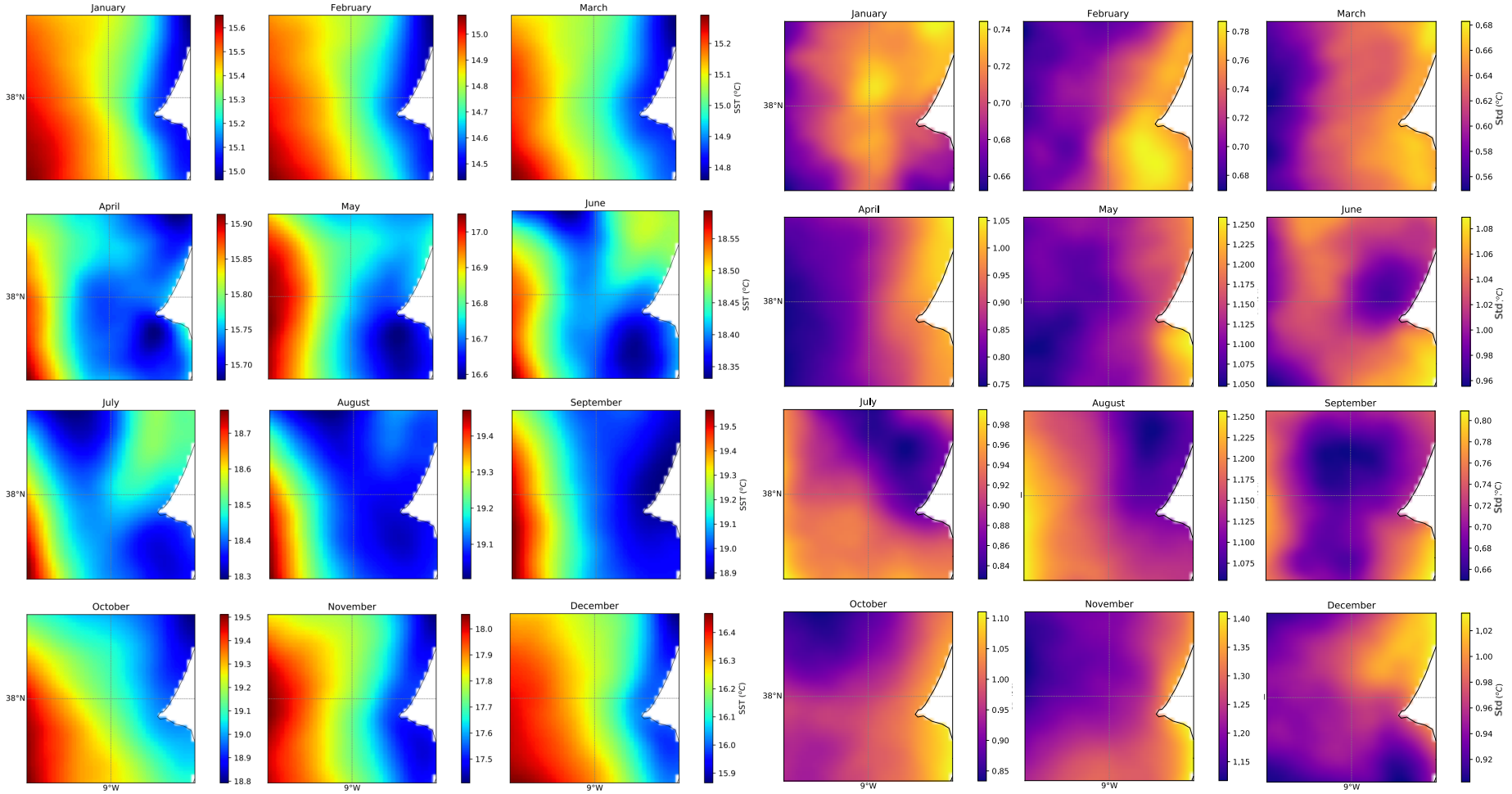

Figure 4.3 - Climatological monthly average (May 2002 – April 2012) for SST (left) and standard deviation (right) in Sines region (area centered on Cape Sines). The scale of each subplot (SST and std) is adjusted to the minimum and maximum found in the area.

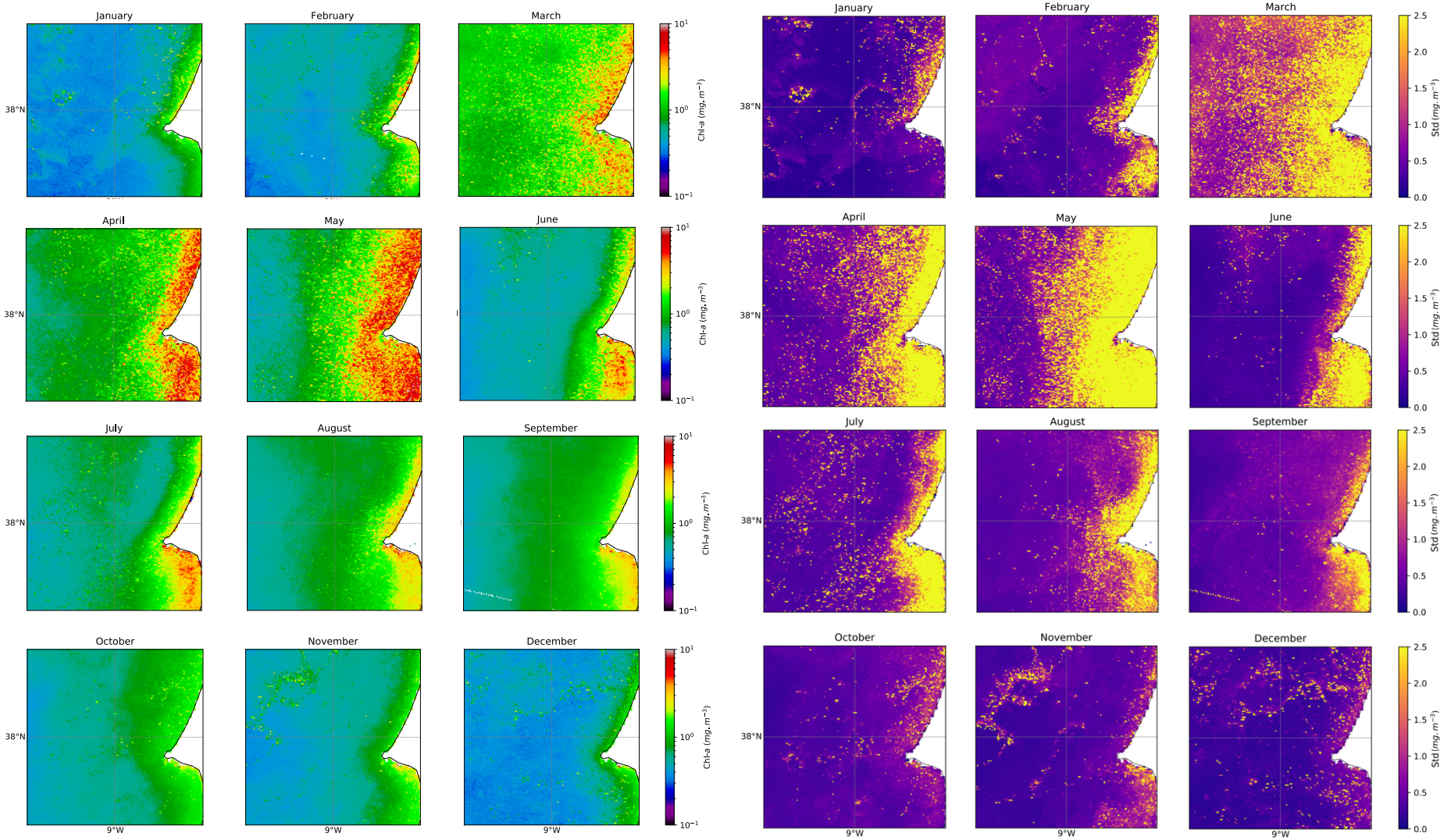

Figure 4.4 - Climatological monthly average (May 2002 – April 2012) for Chl-*a* (left) and standard deviation (right) in Sines.

4.2. *In situ* water quality monitoring

The water quality parameters obtained will be presented in detail in the following subsections. Section 4.2.4 (*4.2.4 Summary of water quality parameters*) presents a summary table (Table 4.10) which compiles these parameters by averages per campaign (all stations averaged) and maxima found for each campaign.

4.2.1. Physical parameters

Temperature and salinity

Temperature and salinity are indicators of the presence or absence of stratification along the water column which in turn is related to the local water renewal. Therefore, they are included as water quality parameters. Water temperature (Figure 4.5 top) was lower in spring (14.78 ± 0.27 °C in May, 15.16 ± 0.18 °C in March and 15.16 ± 0.23 °C in April), followed by summer (15.84 ± 0.40 °C in June), and higher in autumn (17.80 ± 0.37 °C in October). The T ranges (minimum and maximum) in each field campaign (Table 4.1), indicate an absolute minimum in May (14.35 °C) and an absolute maximum in October (18.44 °C). In all campaigns, the T profiles along the water column in the different stations did not show great disparity. The maximum difference between stations was in May at the surface, concerning stations 2 and 4 (difference of 0.74 °C). The highest water temperatures were found at the surface, decreasing slightly with depth where temperatures of all sampling stations converge. The maximum surface bottom T difference was 1.35 °C found in station 4 in May. In average, T decreased 0.74 °C along the water column.

Salinity varied from 35.72 ± 0.03 in summer (June) to 36.05 ± 0.03 in spring (March) (Table 4.10). October, April and May showed spatial salinity averages (stations averaged) of 36.01 ± 0.02, 35.95 ± 0.03 and 35.88 ± 0.05, respectively. The S ranges found in each campaign are shown in Table 4.1 and indicate an absolute minimum and maximum in June (35.62) and March (36.08), respectively. Like for temperature, in all campaigns the salinities profiles obtained along the water column in the different stations were similar. Between stations, the highest S differences were found in May, both between stations 2 and 4 at ≈2 m depth, and stations 3 and 4 also at ≈2 m depth (S difference of 0.21 for both cases). Along the water column, the highest S difference (0.26) was found in May in station 4 between subsurface and bottom waters (Figure 4.5 bottom). The average variation of salinity along the water column was 0.10.

Table 4.1 – Temperature and salinity range (minimum and maximum) in each sampling campaign.

T (°C)	*29/06/2018*	*25/10/2018*	*12/03/2019*	*30/04/2019*	*23/05/2019*	*29/07/2019*
Range	15.36 – 16.66	17.08 – 18.44	14.88 – 15.62	14.78 – 15.51	14.35 – 15.71	NC
S (PSU-78)						
Range	35.62 – 35.76	35.94 – 36.06	35.94 – 36.08	35.85 – 36.01	35.68 – 35.95	NC

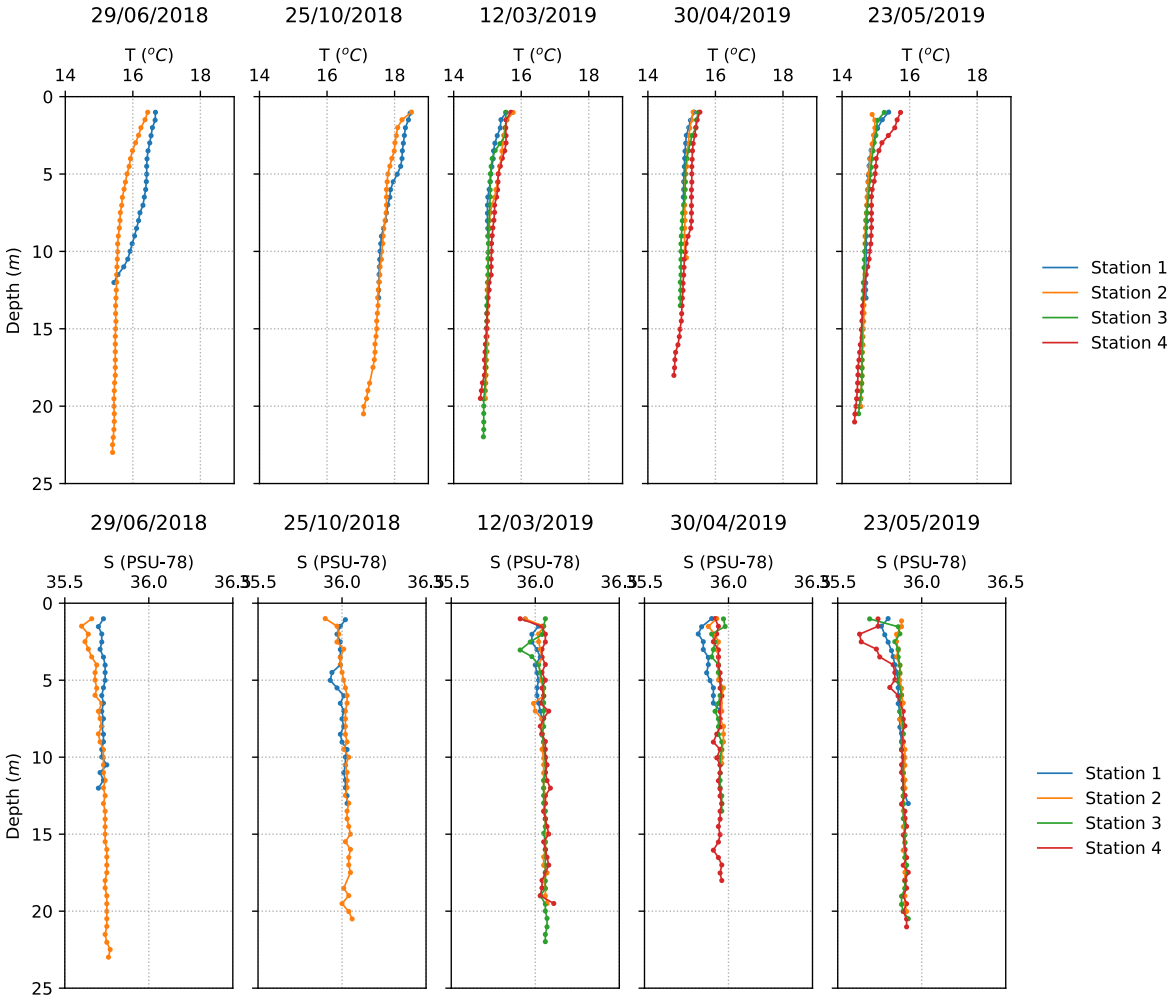

Figure 4.5 - Temperature (top) and salinity (bottom) vertical profiles obtained with the CTD in all stations and along the sampling campaigns. In 29/06/2018 and 25/10/2018 only stations 1 and 3 were sampled.

Water clarity

Water clarity parameters, i.e. turbidity and light in the water column (Secchi depth , light extinction coefficient and euphotic depth) are shown in Figure 4.6 and Table 4.2. Similar to SPM, turbidity (Turb) presented higher values in the bottom of each station than at the surface (except in April at station 4). The differences between surface and bottom (all stations averaged) are given in Table 4.2. Turb ranged between 0.38 NTU and 1.35 NTU in the surface (total average 0.77 ± 0.26 NTU), while at the bottom values ranged between 0.76 NTU and 7.61 NTU (total average 2.06 ± 1.84 NTU). The highest turbidity in the water was found at the bottom in March, at stations 2 and 3, where turbidity exceeded the average plus twice the standard deviation (6.74 and 7.61 NTU, respectively). Seasonally, Turb increased from June (0.96 ± 0.38 NTU) to October (1.15 ± 0.45 NTU) and March (2.59 ± 2.89 NTU); and then decreased in April (1.18 ± 0.66 NTU) and May (1.09 ± 0.87 NTU). In July, Turb increased again (1.17 ± 0.37 NTU).

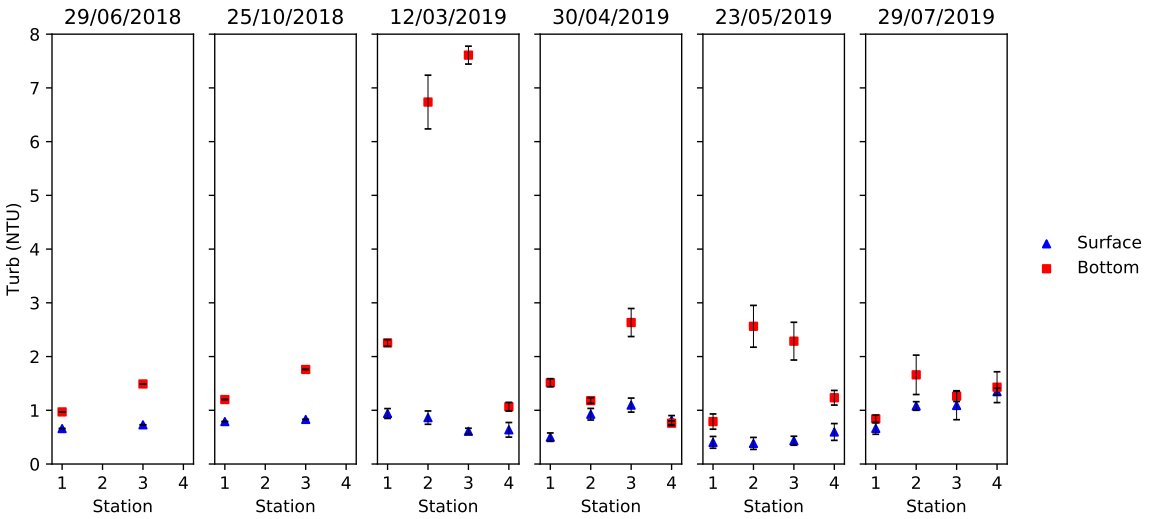

Figure 4.6 - Turbidity in all stations along the sampling campaigns. In 29/07/2018 and 25/10/2018 only stations 1 and 3 were sampled.

The Secchi depth, light attenuation coefficient and euphotic depth are presented in Table 4.2 and indicate the average of stations 1 and 3 for each sampling campaign (since radiometry profiles were performed at these two stations only). The light attenuation coefficient (K_d) average varied between 0.15 m^{-1} in October, and 0.48 m^{-1} in March. The Z_{eu}, depth at which 1% of the surface light remains, was higher than the average depth of both stations (19.5 m) in June and October (22.68 and 33.55 m, respectively), meaning that light penetrated throughout the entire water column. In April the euphotic depth was the lowest (13.56 m), but still, light penetrated about 70% of the whole water column.

Suspended particulate matter

Suspended particulate matter in all stations and along the sampling campaigns is shown in Figure 4.7. The surface bottom difference of SPM (all stations averaged), ranges and stations where extremes were found are given in Table 4.3. The total average SPM was 1.93 ± 1.54 mg L^{-1}. Throughout the year, all stations showed higher SPM at the bottom (total average of 2.97 ± 1.69 mg L^{-1}) than at the surface (total average of 1.06 ± 0.45 mg L^{-1}). Seasonally, April showed the highest SPM concentrations at the surface (average of all surface samples: 1.64 ± 0.38 mg L^{-1}) and included the absolute surface maximum (1.97 mg L^{-1} at station 2). Despite that, at the bottom, the maximum occurred in March (average of all bottom samples: 3.81 ± 2.72 mg L^{-1}), with an absolute bottom maximum at station 3 (6.80 mg L^{-1}). Considering the SPM obtained in each campaign (all stations averaged, Table 4.10), summer presented the lowest values: June (0.63 ± 0.11 mg L^{-1}) and July (1.17 ± 0.48 mg L^{-1}); followed by autumn: October (2.02 ± 1.15 mg L^{-1}); and the highest SPM was found in spring months: March (2.30 ± 2.41 mg L^{-1}), April (2.24 ± 1.00 mg L^{-1}), and May (2.32 ± 1.79 mg L^{-1}).

The percentages of organic and inorganic fractions of the SPM are depicted in Figure 4.8. The spatial average of all stations (of both fractions) in each sampling campaign are given in Table 4.3. The surface stations were dominated by the organic fraction, with 65.78 ± 10.56% of particulate organic matter; while bottom stations were dominated by the inorganic fraction, with an average of 56.85 ± 15.38% of particulate inorganic matter.

Table 4.2 – Water clarity parameters: turbidity, Secchi depth, light extinction coefficient, and euphotic depth along sampling campaigns. Values correspond to the spatial average of the surface and bottom stations and their standard deviation. The minimum and maximum values are also given (the values in brackets (#) indicate the stations where extremes were found). S – surface; B – bottom.

Turb (NTU)	*29/06/2018*	*25/10/2018*	*12/03/2019*	*30/04/2019*	*23/05/2019*	*29/07/2019*
Average (Std)	S: 0.69 (0.05) B: 1.23 (0.38)	S: 0.81 (0.03) B: 1.48 (0.40)	S: 0.76 (0.16) B: 4.42 (3.24)	S: 0.84 (0.25) B: 1.52 (0.80)	S: 0.45 (0.10) B: 1.72 (0.84)	S: 1.05 (0.28) B: 1.30 (0.35)
Range	S: 0.66 (#1) – 0.73 (#3) B: 0.97 (#1) – 1.49 (#3)	S: 0.79 (#1) – 0.83 (#3) B: 1.20 (#1) – 1.76 (#3)	S: 0.61 (#3) – 0.94 (#1) B: 1.07 (#4) – 7.61 (#3)	S: 0.50 (#1) – 1.10 (#3) B: 0.76 (#4) – 2.63 (#3)	S: 0.38 (#2) – 0.60 (#4) B: 0.79 (#1) – 2.56 (#2)	S: 0.66 (#1) – 1.35 (#4) B: 0.84 (#1) – 1.66 (#2)
SD (m)						
Average (Std)	10.8 (2.0)	8.3 (0.4)	9.1 (2.3)	5.1 (0.5)	7.4 (2.2)	8.5 (1.9)
Range	9.5 (#3) – 13.0 (#1)	8.5 (#1) – 8.0 (#3)	6.5 (#2) – 12.0 (#4)	4.5 (#2) – 5.5 (#3 & #4)	4.5 (#2) – 9.5 (#4)	7.0 (#2 & #3) – 11.0 (#1)
K_d (m^{-1})						
Average	0.20	0.15	0.48	0.36	0.26	0.26
Z_{eu} (m)						
Average	22.68	33.55	17.30	13.56	18.54	18.38

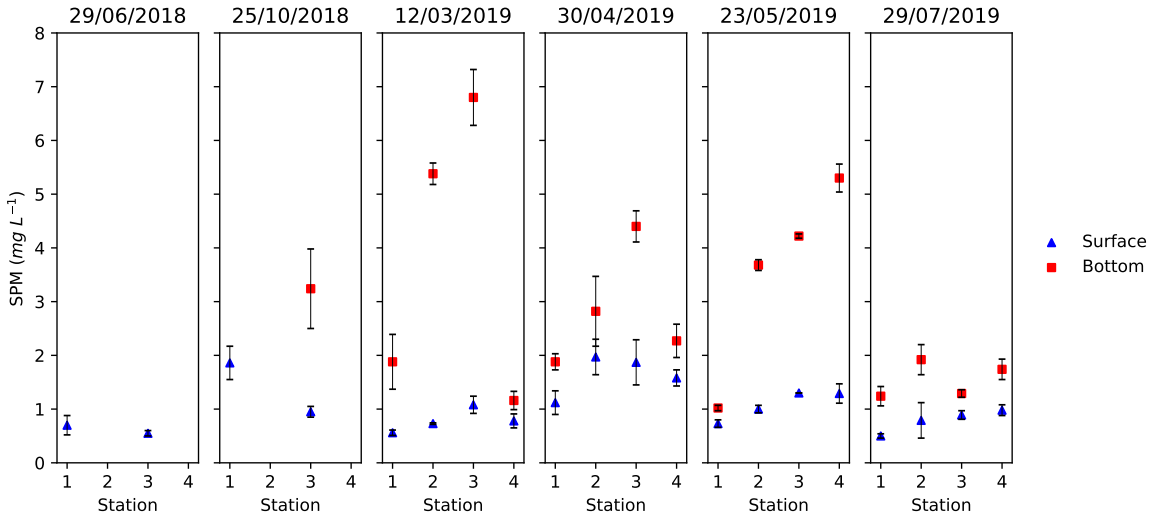

Figure 4.7 - Suspended particulate matter in all stations along the sampling campaigns. In 29/06/2018 and 25/10/2018 only stations 1 and 3 were sampled.

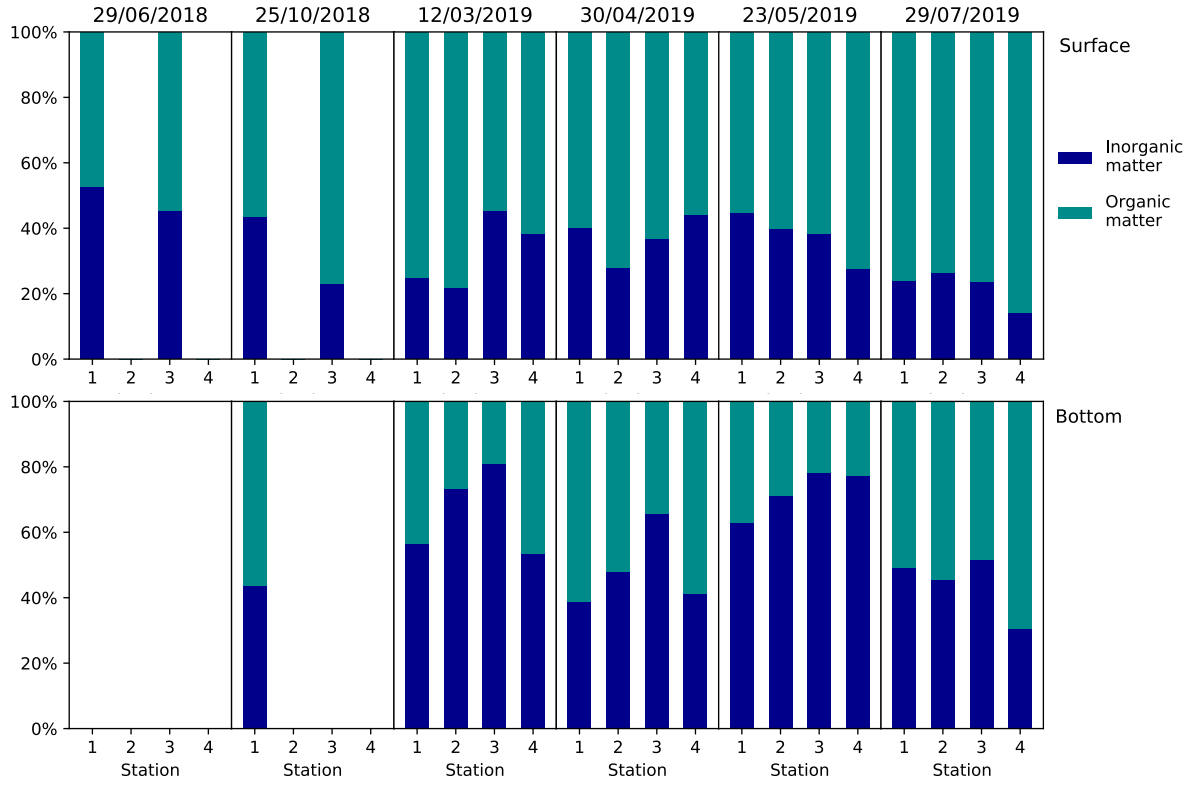

Figure 4.8 - Organic and inorganic fractions of the SPM at the surface (top) and bottom (bottom) stations along the sampling months. In 29/06/2018 and 25/10/2018 only stations 1 and 3 were sampled.

Table 4.3 - Suspended particulate matter, organic matter and inorganic matter along sampling months (spatial average of surface and bottom stations), standard deviation, and range (minimum and maximum). Values in brackets (#) indicate stations where the extremes were found. S – surface; B – bottom; NC – not collected.

SPM (mg L^{-1})	*29/06/2018*	*25/10/2018*	*12/03/2019*	*30/04/2019*	*23/05/2019*	*29/07/2019*
Average (Std)	S: 0.63 (0.11) B: NC	S: 1.41 (0.64) B: NC	S: 0.79 (0.22) B: 3.81 (2.72)	S: 1.64 (0.38) B: 2.84 (1.11)	S: 1.08 (0.27) B: 3.56 (1.82)	S: 0.79 (0.21) B: 1.55 (0.34)
Range	S: 0.55 (#3) - 0.70 (#1) B: NC	S: 0.95 (#3) - 1.86 (#1) B: NC	S: 0.56 (#1) - 1.08 (#3) B: 1.16 (#4) - 6.80 (#3)	S: 1.12 (#1) - 1.97 (#2) B: 1.88 (#1) - 4.40 (#3)	S: 0.73 (#1) – 1.30 (#3) B: 1.02 (#4) - 5.30 (#4)	S: 0.50 (#1) - 0.98 (#4) B: 1.24 (#1) - 1.92 (#2)
OM (%)						
Average (Std)	S: 50.84 (5.23) B: NC	S: 66.65 (14.42) B: 56.50 (-)	S: 67.31 (11.09) B: 33.98 (13.26)	S: 62.73 (6.90) B: 51.60 (12.23)	S: 62.23 (7.17) B: 27.70 (7.09)	S: 77.88 (5.38) B: 55.85 (9.46)
Range	S: 47.14 (#1) – 54.55 (#3) B: NC	S: 56.45 (#1) – 76.84 (#3) B: 56.50 (#1) (single value)	S: 54.63 (#3) – 78.08 (#2) B: 19.10 (#3) – 46.60 (#4)	S: 55.90 (#4) – 72.10 (#2) B: 34.20 (#3) – 61.20 (#1)	S: 55.20 (#1) – 72.20 (#4) B: 21.80 (#3) – 37.20 (#1)	S: 73.40 (#2) – 85.70 (#4) B: 48.40 (#3) – 69.50 (#4)
IM (%)						
Average (Std)	S: 49.16 (5.23) B: NC	S: 33.35 (14.42) B: 43.50 (-)	S: 32.69 (11.09) B: 66.02 (13.26)	S: 37.28 (6.90) B: 48.40 (11.94)	S: 37.78 (7.17) B: 72.30 (7.09)	S: 22.13 (5.38) B: 44.15 (9.46)
Range	S: 45.45 (#3) – 52.86 (#1) B: NC	S: 23.16 (#3) – 43.55 (#1) B: 43.50 (#1) (single value)	S: 21.82 (#2) – 45.37 (#3) B: 53.40 (#4) – 56.40 (#1)	S: 27.90 (#2) – 44.10 (#4) B: 38.80 (#1) – 65.20 (#3)	S: 27.80 (#4) – 44.80 (#1) B: 62.80 (#1) – 78.20 (#3)	S: 14.30 (#4) – 26.60 (#2) B: 30.50 (#4) – 51.60 (#3)

4.2.2. Chemical parameters

Dissolved oxygen

The variation of dissolved oxygen concentrations along the water column in the stations throughout the field campaigns is given in Figure 4.9. Table 4.4 gives the DO concentration and saturation average of the vertical profiles of each station. The total average of DO was 8.15 ± 0.52 mg L^{-1} (102.21 ± 6.37 % of saturation). Overall, higher DO concentrations and saturations are found at the subsurface, decreasing towards greater depths (except at station 3 in June, and at stations 1 and 4 in March, where higher DO is found at the surface; and station 3 in October where the maximum is found at 7.5 m). The DO average (all stations averaged, Table 4.10) was 7.99 ± 0.38 mg L^{-1} in June, 7.60 ± 0.33 mg L^{-1} in October, 8.07 ± 0.44 mg L^{-1} in March and 8.43 ± 0.52 mg L^{-1} in April. In the field campaigns carried out in March and April, where all stations were sampled, station 4 always presented the highest oxygen concentrations (absolute maximum 9.65 mg L^{-1}; 121.3% in April at 2.2 m depth). In March, station 2 clearly had the lowest concentrations of oxygen, although it is never less than 7.23 mg L^{-1}. Nonetheless, the absolute minimum was found at station 3 in October (6.92 mg L^{-1} at 9.8 m depth). Although October shows the lower average DO concentration and saturation (99.90 ± 4.86%) and includes the absolute minimum concentration, the absolute minimum saturation is found at station 2 in March (89.4% at 12.6 m).

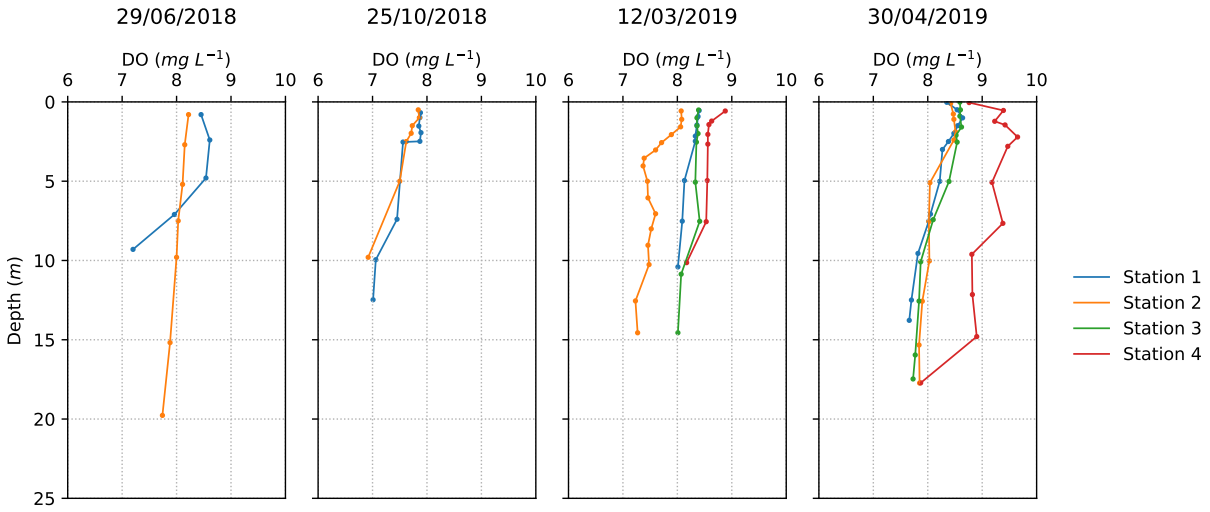

Figure 4.9 - Dissolved oxygen concentration in all stations along the sampling months. In 29/06/2018 and 25/10/2018 only stations 1 and 3 were sampled.

pH

The pH displays an increase throughout the sampling campaigns (stations averaged, Table 4.10), varying from 8.25 ± 0.03 in June, to 8.42 ± 0.05 in October, and to 8.77 ± 0.10 in April. No pH data were obtained in March, May and July. Along the water column, the pH variation was in the order of hundredths (except in station 3 in April, where the variation was in the order of tenths). The total average for all stations over the sampling months was 8.57 ± 0.24 (minimum 8.16 in June, station 1; maximum 8.96 in April, station 4).

Table 4.4 - Dissolved oxygen concentration and saturation averages for each vertical profile along the sampling months. In 29/06/2018 and 25/10/2018 only stations 1 and 3 were sampled. NC – not collected.

DO (mg L^{-1})		*29/06/2018*	*25/10/2018*	*12/03/2019*	*30/04/2019*
Average (Std)	Station 1	8.15 (0.59)	7.60 (0.36)	8.25 (0.15)	8.21 (0.33)
	Station 2	NC	NC	7.60 (0.28)	8.19 (0.28)
	Station 3	8.02 (0.17)	7.60 (0.32)	8.30 (0.15)	8.26 (0.37)
	Station 4	NC	NC	8.56 (0.19)	9.11 (0.38)
DO saturation (%)					
Average (Std)	Station 1	102.96 (8.24)	100.14 (5.43)	102.29 (2.21)	101.85 (4.19)
	Station 2	NC	NC	94.22 (3.80)	101.74 (3.67)
	Station 3	100.86 (2.64)	99.59 (4.43)	102.91 (2.20)	103.17 (5.04)
	Station 4	NC	NC	106.55 (2.90)	113.82 (5.09)

Nutrients

The surface and bottom concentrations of nitrites and nitrates, phosphates and ammonia are given in Figure 4.10 - Figure 4.12. Silicates and nitrites were also quantified; however, all the samples were below the determined detection limits. Therefore, it might be assumed that the sum of nitrites and nitrates constitutes mainly nitrates. Generally, there is no clear pattern of nutrient concentrations between the stations and along the water column. Except N, all nutrients present high percentages of samples below the DL (100% for Si; 87% for NH_4^+; 58% for P), denoting low concentrations. The maximum concentrations of N, P and NH_4^+ were 19.68 μmol L^{-1} (bottom station 1, March), 0.72 μmol L^{-1} (bottom station 3, October), and 1.64 μmol L^{-1} (bottom station 2, March), respectively.

Table 4.5 summarizes the results obtained in each sampling campaign. N showed higher concentrations in March (9.94 ± 2.31 μmol L^{-1} in the surface samples and 14.98 ± 3.56 μmol L^{-1} in the bottom samples). P concentrations were higher in October (0.61 ± 0.15 μmol L^{-1} in the surface and 0.37 ± 0.16 μmol L^{-1} in the bottom samples). At the surface, all NH_4^+ samples were below the DL. At the bottom, only stations 2 and 3 which are closer to the aquaculture cages showed values above the DL, ranging between 0.95 μmol L^{-1} (October, station 3) and 1.64 μmol L^{-1} (March, station 2).

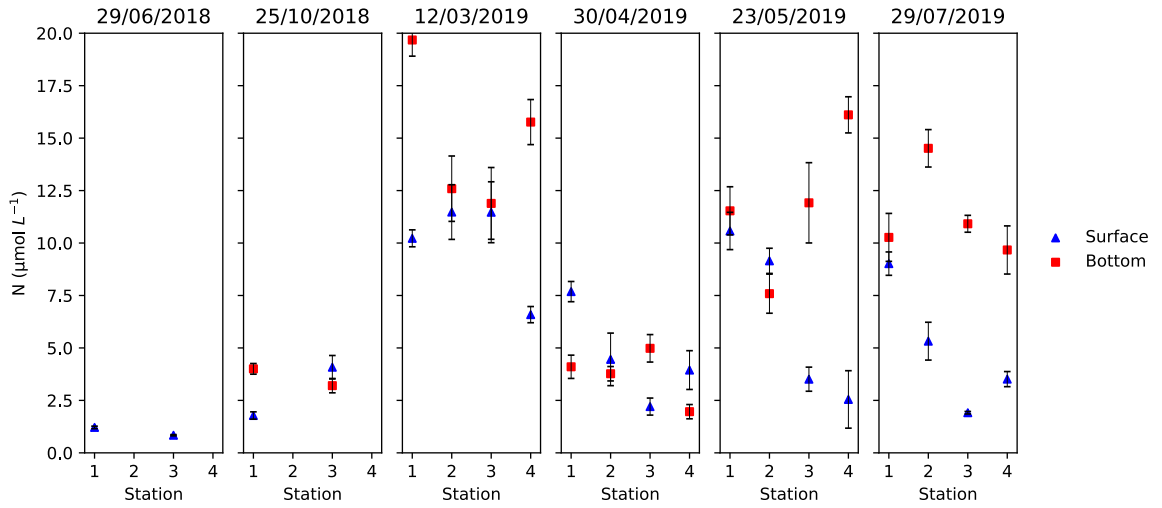

Figure 4.10 – Nitrites and nitrates concentration in all stations along the sampling months. In 29/06/2018 and 25/10/2018 only stations 1 and 3 were sampled.

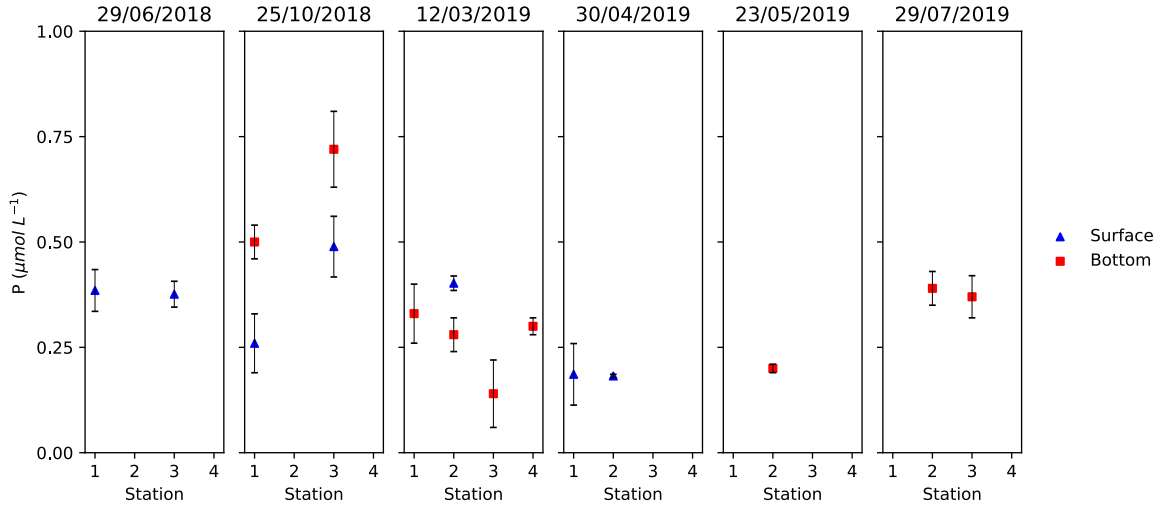

Figure 4.11 - Phosphates concentration in all stations along the sampling months. In 29/06/2018 and 25/10/2018 only stations 1 and 3 were sampled.

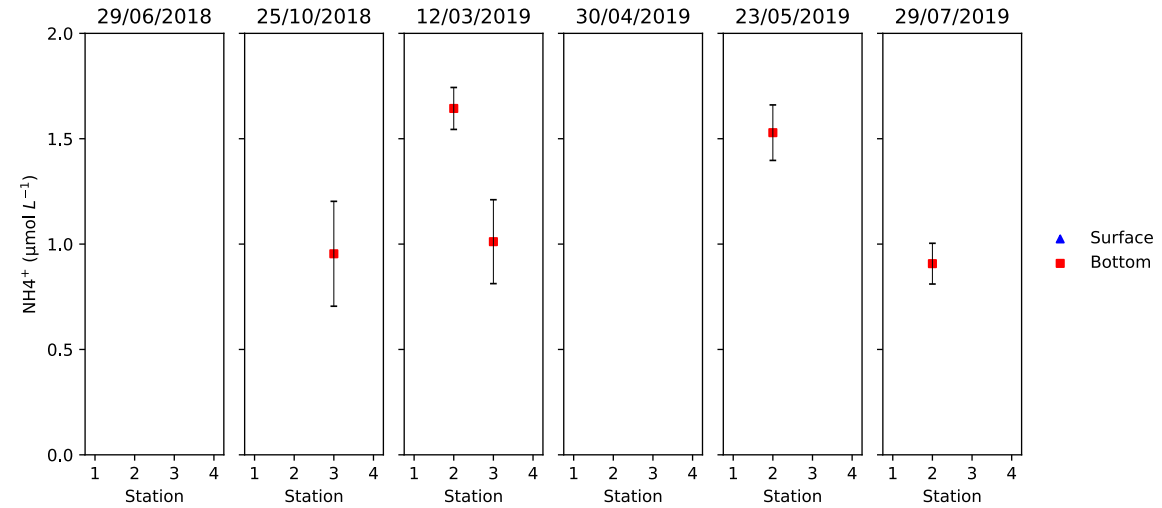

Figure 4.12 - Ammonia concentration in all stations along the sampling months. In 29/06/2018 and 25/10/2018 only stations 1 and 3 were sampled. All surface samples were above the detection limit of the used method.

Table 4.5 - Nutrient concentrations along sampling months. Values correspond to the spatial average of the surface and bottom stations and their standard deviation. The minimum and maximum values are also given (the values in brackets (#) indicate the stations where extremes were found). DL – detection limit; NC – not collected. < DL is the percentage of samples above the detection limit determined for each used method.

N (µmol L^{-1})	*29/06/2018*	*25/10/2018*	*12/03/2019*	*30/04/2019*	*23/05/2019*	*29/07/2019*
Average (Std)	S: 1.03 (0.26) B: NC	S: 2.93 (1.63) B: 3.60 (0.57)	S: 9.94 (2.31) B: 14.98 (3.56)	S: 4.57 (2.29) B: 3.70 (1.27)	S: 6.45 (4.01) B: 11.79 (3.48)	S: 4.94 (3.05) B: 11.34 (2.18)
Range	S: 0.84 (#3) - 1.21(#1) B: NC	S: 1.78 (#1) – 4.08 (#3) B: 3.20 (#3) – 4.00 (#1)	S: 6.59 (#4) – 11.48 (#2) B: 11.89 (#3) – 19.68 (#1)	S: 2.21 (#3) – 7.69 (#1) B: 1.96 (#4) – 4.98 (#3)	S: 2.55 (#4) – 10.58 (#1) B: 7.59 (#2) – 16.11 (#4)	S: 1.91 (#3) – 9.02 (#1) B: 9.67 (#4) – 14.51 (#2)
< DL	S, B: 0%, NC	S, B: 0%	S, B: 0%	S, B: 0%	S, B: 0%	S, B: 0%
P (µmol L^{-1})						
Average (Std)	S: 0.38 (0.01) B: NC	S: 0.37 (0.16) B:0.61 (0.15)	S: 0.40 (-) B: 0.26 (0.08)	S: 0.18 (0.00) B: DL	S: DL B: 0.20 (-)	S: DL B: 0.38 (0.01)
Range	S: 0.38 (#3) – 0.39 (#1) B: NC	S: 0.26 (#1) – 0.49 (#3) B: 0.50 (#1) – 0.72 (#3)	S: 0.40 (#3) (single value) B: 0.14 (#3) – 0.33 (#1)	S: 0.18 (#2) – 0.19 (#1) B: DL	S: DL B: 0.20 (2#) (single value)	S: DL B: 0.37 (#3) – 0.39 (#2)
< DL	S: 0% B: NC	S: 0% B: 0%	S: 75% B: 0%	S: 50% B: 100%	S: 100% B: 75%	S: 100% B: 50%
Si (µmol L^{-1})						
Average (Std)	S, B: DL	S, B: DL	S, B: DL	S, B: DL	S, B: DL	S, B: DL
Range	S, B: DL	S, B: DL	S, B: DL	S, B: DL	S, B: DL	S, B: DL
< DL	S, B: 100%	S, B: 100%	S, B: 100%	S, B: 100%	S, B: 100%	S, B: 100%
NH_4^+ (µmol L^{-1})						
Average (Std)	S: DL B: NC	S: DL B: 0.95 (-)	S: DL B: 1.33 (0.45)	S: DL B: DL	S: DL B: 1.53 (-)	S: DL B: 0.91 (-)
Range	S: DL B: NC	S: DL B: 0.95 (#3) (single value)	S: DL B: 1.01 (#3) – 1.64 (#2)	S: DL B: DL	S: DL B: 1.53 (#2) (single value)	S: DL B: 0.91 (#2) (single value)
< DL	S: 100% B: NC	S: 100% B: 50%	S: 100% B: 50%	S: 100% B: 100%	S: 100% B: 75%	S: 100% B: 75%

4.2.3. Biological parameters

Phytoplankton pigments

The HPLC pigment analysis provided qualitative analysis of 28 different pigments, and quantitative analysis of 26 of them. In the Table 4.6 all pigments detected and quantified are listed, along with their abbreviation that will be used henceforth (according to Roy et al., 2011) and the average retention time. An example of an obtained chromatogram can be seen in Figure A.2 of the annexes. The maximum concentration of each pigment is also shown in Table 4.6, along with its month and sampling site of occurrence. Maximum pigment concentrations vary between 0.03 μg L^{-1} (Diato) and 7.38 μg L^{-1} (Chl-*a*).

Table 4.6 – List of pigments detected and quantified via HPLC, and the abbreviation (* according to Roy et al., 2011) and average retention time of each one. For each pigment the maximum concentration and month and station of occurrence are given. S – surface; B – bottom. QL – quantification limit.

Peak number	*Pigment*	*Abbreviation **	*Retention time (min)*	*Detected*	*Quantified*	*Limit of quantification (μ g)*	*Max. concentration found (μ g L^{-1})*	*Month of maximum concentration*	*Site of max. concentration*
1	Chlorophyll c_3	Chl-*c_3*	7.20	Yes	Yes	0.05	0.40	May 2019	2 (B)
2	Chlorophyllide a	Chlide	9.40	Yes	Yes	0.11	0.28	May 2019	3 (S)
3	Mg-2,4-divinyl pheoporphyrin a_5 monomethyl ester	MgDVP	9.96	Yes	Yes	0.05	0.20	April 2019	1 (B)
4	Chlorophyll c_2	Chl-*c_2*	10.29	Yes	Yes	0.05	1.03	April 2019	2 (B)
5	Chlorophyll c_1	Chl-*c_1*	10.88	Yes	No	-	-	-	-
6	Peridinin	Peri	12.72	Yes	Yes	0.14	0.46	July 2019	4 (B)
7	Pheophorbide a	Pheide	14.92	Yes	Yes	0.05	0.22	October 2018	3 (B)
8	19'-Butanoyloxyfucoxanthin	But-fuco	16.11	Yes	< QL	0.09	< QL	-	-
9	Fucoxanthin	Fuco	16.93	Yes	Yes	0.07	2.58	July 2019	3 (S)
10	Neoxanthin	Neo	17.90	Yes	Yes	0.05	0.05	March 2019	3 (S)
11	Prasinoxanthin	Pras	18.66	Yes	Yes	0.07	0.09	May 2019	2 (B)
12	Violaxanthin	Viola	19.47	Yes	< QL	0.05	< QL	May 2019	3 (S)
13	19'-Hexanoyloxyfucoxanthin	Hex-fuco	19.69	Yes	Yes	0.07	0.18	July 2019	3 (S)
14	Diadinoxanthin	Diadino	21.83	Yes	Yes	0.04	0.24	July 2019	3 (S)
15	Antheraxanthin	Anth	22.73	Yes	< QL	0.05	< QL	-	-
16	Alloxanthin	Allo	23.80	Yes	Yes	0.03	0.09	October 2018	1 (S)
17	Diatoxanthin	Diato	24.50	Yes	Yes	0.03	0.03	July 2019	4 (B)
18	Zeaxanthin	Zea	25.07	Yes	Yes	0.03	0.12	July 2019	3 (S)
19	Myxoxantophyll	Myxo	25.47	Yes	< QL	0.10	< QL	-	-
20	Lutein	Lut	25.72	Yes	< QL	0.02	< QL	October 2018	3 (B)
21	Dehydroluthein	Dehydro Lut	27.91	Yes	No	-	-	-	-
22	Echinenone	Echin	29.85	Yes	< QL	0.03	< QL	-	-
23	Chlorophyll b	Chl-*b*	29.89	Yes	Yes	0.05	0.08	July 2019	3 (S)
24	Divinyl Chlorophyll a	DV Chl-*a*	29.94	Yes	Yes	0.05	0.05	April 2019	3 (S)
25	Chlorophyll a	Chl-*a*	30.47	Yes	Yes	0.08	7.38	April 2019	2 (B)
26	Pheophytin a	Phe	32.77	Yes	Yes	0.04	0.12	April 2019	2 (B)
27	α-carotene	α-Car	33.21	Yes	< QL	0.03	< QL	April 2019	2 (B)
28	β-carotene	β-Car	33.57	Yes	Yes	0.04	0.18	July 2019	3 (S)

Phytoplankton biomass and degradation products

The concentrations of phytoplankton biomass (Chl-*a*) and degradation products of chlorophyll pigments (phaeopigments, Phaeos, representing Chlide plus Pheide and Phe) are shown in Figure 4.13, in all stations along the sampling campaigns. The obtained phaeopigment concentrations are markedly lower (total average 0.17 ± 0.12 µg L^{-1}) than Chl-*a* concentrations (total average 2.82 ± 2.17 µg L^{-1}). Table 4.7 shows the monthly averages of Chl-*a* and Phaeos obtained in the surface and bottom stations, the Phaeos to Chl-*a* ratios as well as percentage of Chl-*a* degradation. The Chl-*a* concentrations present higher values during the months of April (5.52 ± 1.66 µg L^{-1}), May (2.96 ± 1.39 µg L^{-1}) and July (3.44 ± 1.87 µg L^{-1}). The highest values of degradation pigments occur in April and May, with concentrations of 0.23 ± 0.09 µg L^{-1} and 0.26 ± 0.14 µg L^{-1}, respectively. Due to the low concentrations of the degradation pigments, the chlorophyll-*a* degradation percentages are low (never exceeding 1.32%) as are the Phaeos to Chl-*a* ratios.

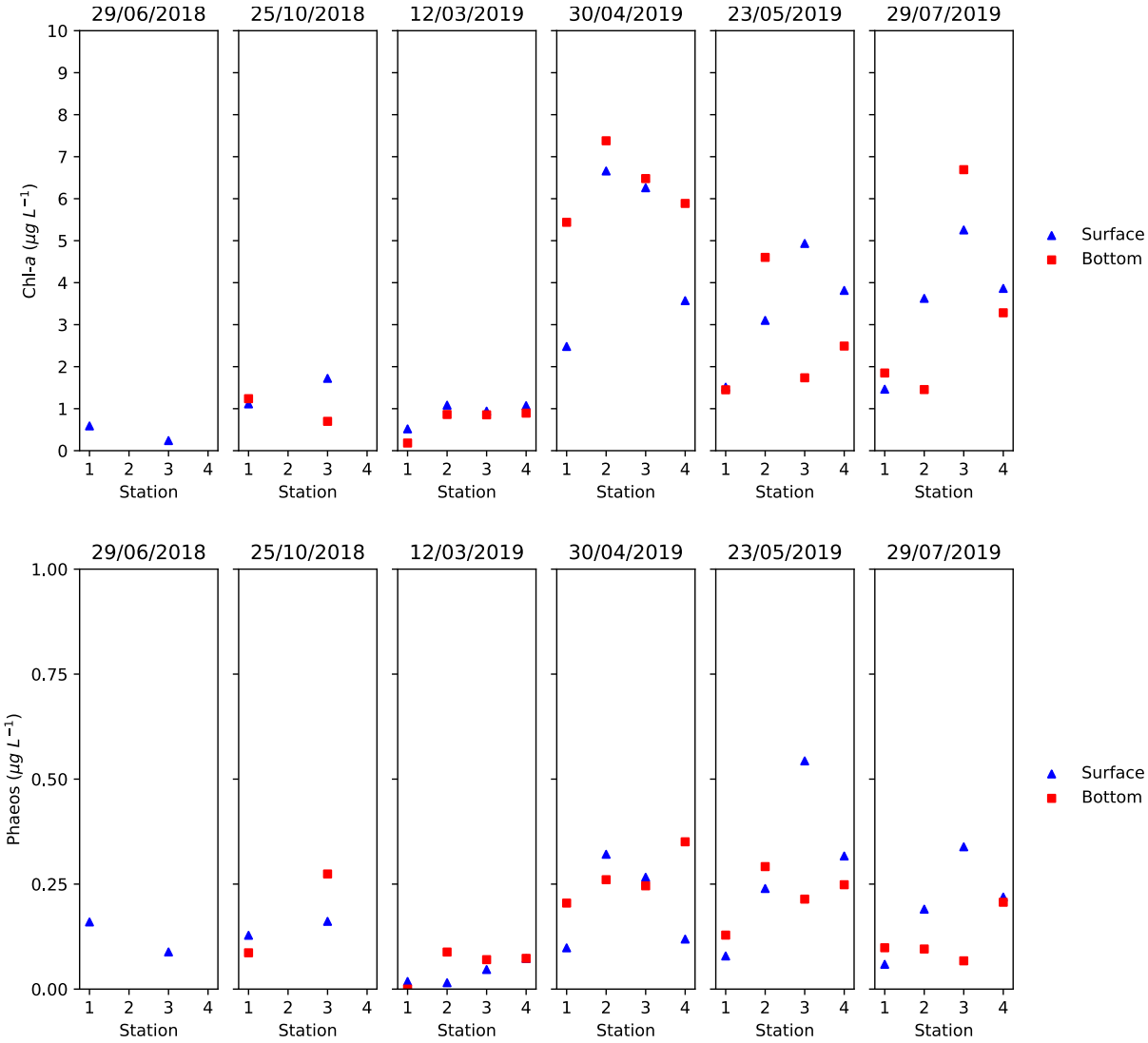

Figure 4.13 - Chlorophyll-*a* (top) and phaeopigments (bottom) concentration (µg L^{-1}) the surface (S) and bottom (B) of all stations along the sampling months. NC – not collected.

Table 4.7 –Chl-*a* and phaeopigment (Phaeos: Chlide, Pheide and Phe) concentration (μg L^{-1}) average (of all stations), standard deviation and range along sampling months. Values in parentheses in the range indicate station where extremes were found. The pigment ratio of Phaeos to Chl-*a* is averaged for the surface and bottom stations.

Chl-*a* (μg L^{-1})	*29/06/2018*	*25/10/2018*	*12/03/2019*	*30/04/2019*	*23/05/2019*	*29/07/2019*
Average (Std)	S: 0.42 (0.25)	S: 1.42 (0.43)	S: 0.91 (0.26)	S: 4.74 (2.04)	S: 3.34 (1.43)	S: 3.55 (1.57)
	B: NC	B: 0.97 (0.38)	B: 0.70 (0.38)	B: 6.30 (0.84)	B: 2.57 (1.42)	B: 3.32 (2.38)
Range	S: 0.24 (3) – 0.59 (1)	S: 1.11 (1) – 1.72 (3)	S: 0.52 (1) – 1.01 (2)	S: 2.48 (1) – 6.66 (2)	S: 1.51 (1) – 4.94 (3)	S: 1.46 (1) – 5.26 (3)
	B: NC	B: 0.70 (3) – 1.24 (1)	B: 0.18 (1) – 0.89 (4)	B: 5.44 (1) – 7.38 (2)	B: 1.45 (1) – 4.60 (2)	B: 1.46 (2) – 6.69 (3)
Phaeos (μg L^{-1})						
Average (Std)	S: 0.12 (0.05)	S: 0.14 (0.02)	S: 0.04 (0.03)	S: 0.20 (0.11)	S: 0.29 (0.19)	S: 0.20 (0.11)
	B: NC	B: 0.18 (0.13)	B: 0.06 (0.04)	B: 0.27 (0.06)	B: 0.22 (0.07)	B: 0.12 (0.06)
Range	S: 0.09 (3) – 0.16 (1)	S: 0.13 (1) – 0.16 (3)	S: 0.02 (2) – 0.07 (4)	S: 0.10 (1) – 0.32 (2)	S: 0.08 (1) – 0.54 (3)	S: 0.06 (1) – 0.34 (3)
	B: NC	B: 0.09 (1) – 0.27 (3)	B: 0.00 (1) – 0.09 (2)	B: 0.20 (1) – 0.35 (4)	B: 0.13 (1) – 0.29 (2)	B: 0.07 (3) – 0.21 (4)
Phaeos / Chl-*a*						
	S: 0.32	S: 0.10	S: 0.04	S: 0.04	S: 0.08	S: 0.05
	B: NC	B: 0.23	B: 0.07	B: 0.04	B: 0.09	B: 0.05
Chl-*a* degradation (%)						
	S: 1.32%	S: 1.10%	S: 1.04%	S: 1.04%	S: 1.08%	S: 1.05%
	B: NC	B: 1.23%	B: 1.07%	B:1.04%	B: 1.09%	B: 1.05%

Phytoplankton communities

Relative abundance results, derived from HPLC (Figure 4.14), indicate that diatoms (as estimated by the Fuco/TPigments index from HPLC) dominated the phytoplankton assemblages in all samples. The results do not indicate substantial changes in the community structure along the stations nor throughout the sampling campaigns. The different stations (surface and bottom) show similar pigment compositions along the carried-out campaigns. June and July display the same phytoplankton groups in all samples; October and May as well, except for both stations 3B where haptophytes (Hex-fuco/TPigments) and dinoflagellates (Peri/TPigments) were absent, respectively; March shows the same groups in all surface stations and 4B station while stations 1B, 2B and 3B presented 100% of diatoms; April showed small variations of chlorophytes (Chl-*b*/TPigments) and dinoflagellates between the stations – absence of chlorophytes at stations 1S, 1B and 4S, and peridin-containing dinoflagellates only present at stations 2B, 4S and 4B.

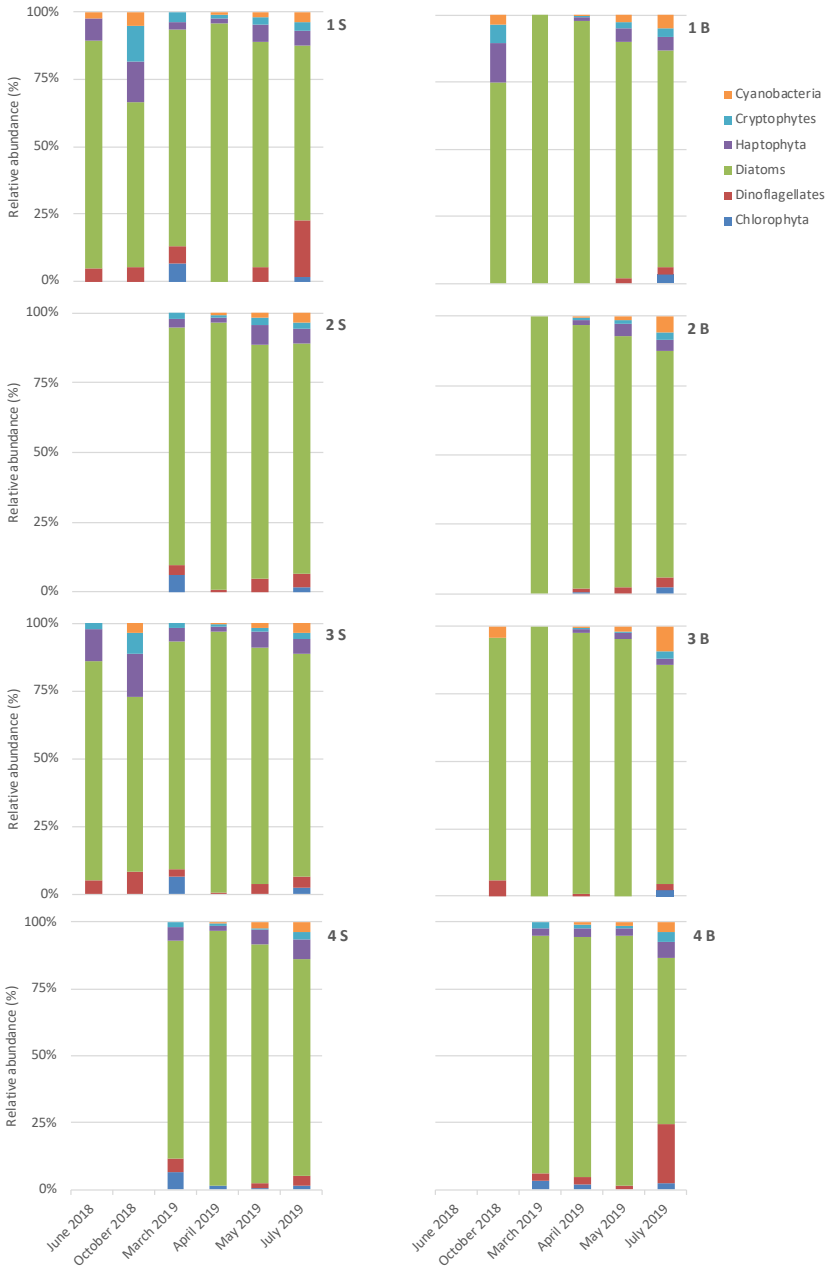

Figure 4.14 - Relative abundance (%) of main phytoplankton groups derived from HPLC data in each station along the sampling campaigns. S – surface; B – bottom.

The results from microscopic analysis (Figure 4.15, left) also indicate that micro-sized phytoplankton, namely diatoms i.e. Bacillariophyceae class, were the major contributors to the phytoplankton biomass in all stations and campaigns (Table 4.8). The dominance of diatoms (79.1%) is followed by dinoflagellates (18.7%), i.e. Dinophyceae class, according to the microscopy results. On the other hand, HPLC derived results indicate a dominance of 83.1% of diatoms, and 4.34% of peridin-containing dinoflagellates.

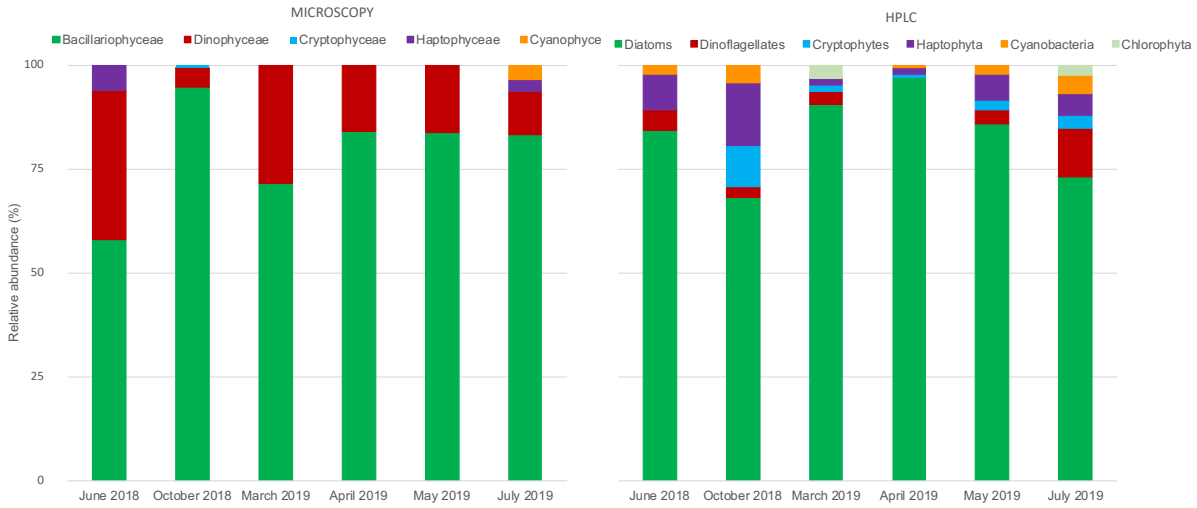

Figure 4.15 - Relative abundance (%) of phytoplankton classes obtained through microscopic (left) and HPLC (right) analysis. Microscopy results refer to net samples, i.e. phytoplankton net used vertically along the water column at station 1. HPLC data correspond to the average of the relative abundance of surface and bottom samples of station 1.

From the microscopic analysis, the percentage of toxic or potentially toxic species present in each class are shown in Table 4.8. In June and October 2018, no toxic or potentially toxic algae were found. On the other hand, in July 2019, 83.10% of the diatoms and 14.11% of the dinoflagellates found were toxic or potentially toxic. These were mainly *Pseudo-nitzschia spp.* and *Dinophysis spp*. In the remaining sampling campaigns toxic or potentially toxic diatoms percentage varied from 14.29% in March 2019 (*Pseudo-nitzschia spp.*), to 0.24% in April 2019 (*Pseudo-nitzschia spp.*) and 0.85% in May 2019 (*Pseudo-nitzschia spp.*). Harmful or potentially harmful dinoflagellates showed higher percentages than diatoms, namely 10.66% for March 2019 (*Dinophysis spp.*), 5.98% in April 2019 (*Alexandrium spp. and Dinophysis acuminata*) and 22.5% in May 2019 (*Alexandrium spp*., *Dinophysys acuminate*, *Dinophysys acuta*, *Dinophysys caudata*, *Phalacroma rotundatum* and *Prorocentrum micans*).

Table 4.9 lists all the identified species in the observed samples. The most abundant genera/species identified were *Pseudo-nitzschia spp.* and *Chaetoceros spp*. Some toxic or potentially toxic species were identified, namely diatoms such as *Pseudo-nitzschia spp.*, and dinoflagellates such as *Alexandrium spp.*, *Dinophysis acuminate*, *Dinophysis acuta*, *Phalacroma rotundatum*, *and Prorocentrum micans*. For the Haptophyceae, Cyanophyceae and Prasinophyceae classes only one species was found for each class, namely *Phaeocystis spp*., *Oscillatoria spp*., and *Pterosperma cristatum*, respectively.

Table 4.8 - Relative abundance (%) of phytoplankton classes obtained through microscopic analysis, in station 1 (phytoplankton net used vertically along 10 m of the water column) along the sampling months; and percentage of toxic and/or potentially toxic algae found in each class.

Relative abundance	*29/06/2018*	*25/10/2018*	*12/03/2019*	*30/04/2019*	*23/05/2019*	*29/07/2019*
Bacillariophyceae	57.83%	94.66%	71.44%	84.07%	83.70%	83.12%
Dinophyceae	35.96%	4.71%	28.56%	15.93%	16.30%	10.62%
Euglenophyceae	0.00%	0.30%	0.00%	0.00%	0.00%	0.00%
Cryptophyceae	0.00%	0.61%	0.00%	0.00%	0.00%	0.00%
Haptophyceae	6.16%	0.00%	0.00%	0.00%	0.00%	2.87%
Cyanophyceae	0.00%	0.00%	0.00%	0.00%	0.00%	3.39%
Prasinophyceae	0.12%	0.00%	0.00%	0.00%	0.00%	0.00%
Percentage of toxic or potentially toxic algae for each class						
Bacillariophyceae	0.00%	0.00%	14.29%	0.24%	0.85%	83.10%
Dinophyceae	0.00%	0.00%	10.66%	5.98%	22.5%	14.11%
Euglenophyceae	-	0.00%	-	-	-	-
Cryptophyceae	-	0.00%	-	-	-	-
Haptophyceae	0.00%	-	-	-	-	0.00%
Cyanophyceae	-	-	-	-	-	0.00%
Prasinophyceae	0.00%	-	-	-	-	-

Table 4.9 – List of species identified through microscopic analysis. * Toxic or potentially toxic species.

Class	*Species*		
Bacillariophyceae	*Bacteriastrum furcatum* *Corataulina pelágica* *Chaetoceros curvisetus* *Chaetoceros spp.* *Coscinodiscus wailesii* *Conscinodiscus spp.* *Cylindrotheca closterium* *Detonula pumila* *Guinardia flácida*	*Guinardia striata* *Lauderia annulata* *Leptocylindricus danicus* *Leptocylindricus minimus* *Licmophora spp.* *Meuniera membranácea* *Neocalyptrella robusta* *Paralia sulcata* *Podosira stelligera*	*Proboscia indica* *Pseudo-nitzschia australis** *Pseudo-nitzschia delicatissima** *Pseudo-nitzschia spp. ** *Rhizosolenia styliformis* *Rhizosolenia spp.* *Stephanopyxis turris* *Skeletonema spp.*
Dinophyceae	*Alexandrium spp.** *Azadinium caudatum* *Ceratium furca* *Ceratium fusus* *Ceratium horridum* *Ceratium tripos* *Ceratium lineatum* *Cochlodinium spp.* *Dinophysis acuminata** *Dinophysis acuta** *Dinophysis caudata*	*Dinophysis fortii* *Ensiculifera spp.* *Gonyaulax spinifera* *Gymnodinium catenatum* *Karenia spp.* *Katodinium glaucum* *Noctiluca scintillans* *Noctiluca spp.* *Phalacroma rotundatum ** *Podolampas palmipes* *Polykrikos kofoidii*	*Polykrikos schwartzii* *Prorocentrum cordatum* *Prorocentrum micans** *Protoceratium reticulatum* *Protoperidinium depressum* *Protoperidinium divergens* *Protoperidinium globosus* *Protoperidinium stainii* *Protoperidinium spp.* *Pyrophacus horologium*
Haptophyceae	*Phaeocystis spp.*		
Cyanophyceae	*Oscillatoria spp.*		
Prasinophyceae	*Pterosperma cristatum*		

4.2.4. Summary of water quality parameters

To conclude the *in situ* water quality parameters monitored along the six field campaigns (from June 2018 until July 2019) are summarized in Table 4.10. The obtained parameters and indicators are shown here as spatial averages of the all sampled stations per campaign.

Table 4.10 – Average and standard deviation of water quality parameters and indicators, i.e. spatial average of stations for each sampling campaign. DL – detection limit.

Parameter	*29/06/2018*	*25/10/2018*	*12/03/2019*	*30/04/2019*	*23/05/2019*	*29/07/2019*
Number of stations sampled	2	2	4	4	4	4
T (°C)	15.86 (0.40)	17.80 (0.37)	15.15 (0.23)	15.17 (0.18)	14.78 (0.27)	-
S (PSU-78)	35.72 (0.03)	36.01 (0.02)	36.05 (0.03)	35.95 (0.03)	35.88 (0.05)	-
Turb (NTU)	0.96 (0.38)	1.15 (0.45)	2.59 (2.89)	1.18 (0.66)	1.09 (0.87)	1.17 (0.32)
SD (m)	10.8 (2.0)	8.3 (0.4)	9.1 (2.3)	5.1 (0.5)	7.4 (2.2)	8.5 (1.9)
SPM (mg L^{-1})	0.63 (0.11)	2.02 (1.15)	2.30 (2.41)	2.24 (1.00)	2.32 (1.79)	1.17 (0.48)
pH	8.25 (0.03)	8.42 (0.05)	-	8.77 (0.10)	-	-
DO (mg L^{-1})	7.99 (0.38)	7.60 (0.33)	8.07 (0.44)	8.43 (0.52)	-	-
DO saturation (%)	100.58 (5.49)	99.90 (4.86)	100.11 (5.80)	105.03 (6.77)	-	-
N (µmol L^{-1})	1.03 (0.26)	3.27 (1.07)	12.46 (3.87)	4.14 (1.77)	9.12 (4.50)	8.14 (4.21)
P (µmol L^{-1})	0.38 (0.01)	0.49 (0.19)	0.29 (0.10)	0.18 (0.00)	0.20 (-)	0.38 (0.01)
Si (µmol L^{-1})	DL	DL	DL	DL	DL	DL
NH_4^+ (µmol L^{-1})	DL	0.95 (-)	1.33 (0.45)	DL	1.53 (-)	0.91 (-)
Chl-a (*µg L^{-1}*)	0.42 (0.25)	1.19 (0.42)	0.80 (0.31)	5.52 (1.66)	2.96 (1.39)	3.44 (1.87)

4.3. Complementary tools for aquaculture

4.3.1. Product comparison of inactive (MERIS) and active (OLCI) ocean colour sensors

For the comparison of chlorophyll-*a* concentration derived from the MERIS and OLCI sensors, the climatological average of MERIS (2002-2012) was computed for the time range of available OLCI data (1st April until 12th January) (Figure 4.16). Similar to the pattern found in the annual, seasonal and monthly climatologies (shown in section 4.1), a coast-offshore gradient is evident both in the MERIS and OLCI derived Chl-*a*. However, the climatological MERIS Chl-*a* shows a stronger zonal gradient caused by higher concentrations in waters adjacent to the coast (3 - 4 mg m^{-3}). In these waters, OLCI average show Chl-*a* concentrations ranging between 1 - 2 mg m^{-3}. It should be noted that the MERIS product reflects the 10-year average of data while the OLCI represents only the 2019 - early 2020 average (1st April 2019 until 12th January 2020).

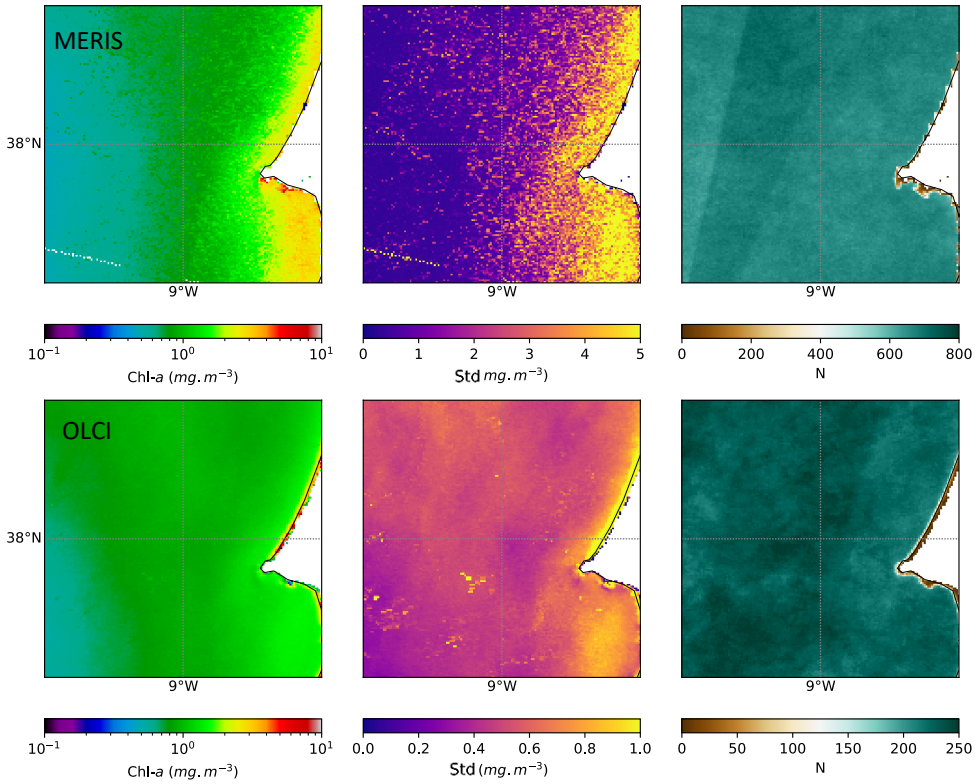

Figure 4.16 - Climatological average of MERIS OC5 Chl-*a* (top), standard deviation and number of observations for the period between the 1st April and 12th January (2002-2012). Average of OLCI Polymer Chl-*a* (bottom), standard deviation and number of observations for the period between the 1st April and 12th January 2020.

The full time series for both products (MERIS and OLCI retrieved Chl-*a*) is depicted in a monthly average time series in Figure 4.17, for an area inside the aquaculture production region in Sines (Figure 3.4, black square). The time series of the MERIS Chl-*a* shows great inter and intra-annual variability. In the entire time series, 45% of the monthly averages fall within the Chl-*a* range of [0.45, 2.39] mg m^{-3}, 23% between [2.39, 5.30] mg m^{-3} and 2% between [5.30,10.15] mg m^{-3}. From the monthly averages above 2.39 mg m^{-3} (25% of the months), 34% of these occurrences were in winter, 28% in autumn, 21% in summer and 17% in spring. On the other hand, the OLCI derived Chl-*a* shows a very low variation over the months, with 70% of data in the range of [1.11, 1.59] mg m^{-3}, and 30% between [1.59, 2.07] mg m^{-3}. In the spring and summer months, phytoplankton biomass concentration is slightly below average, while in autumn and winter the opposite is verified.

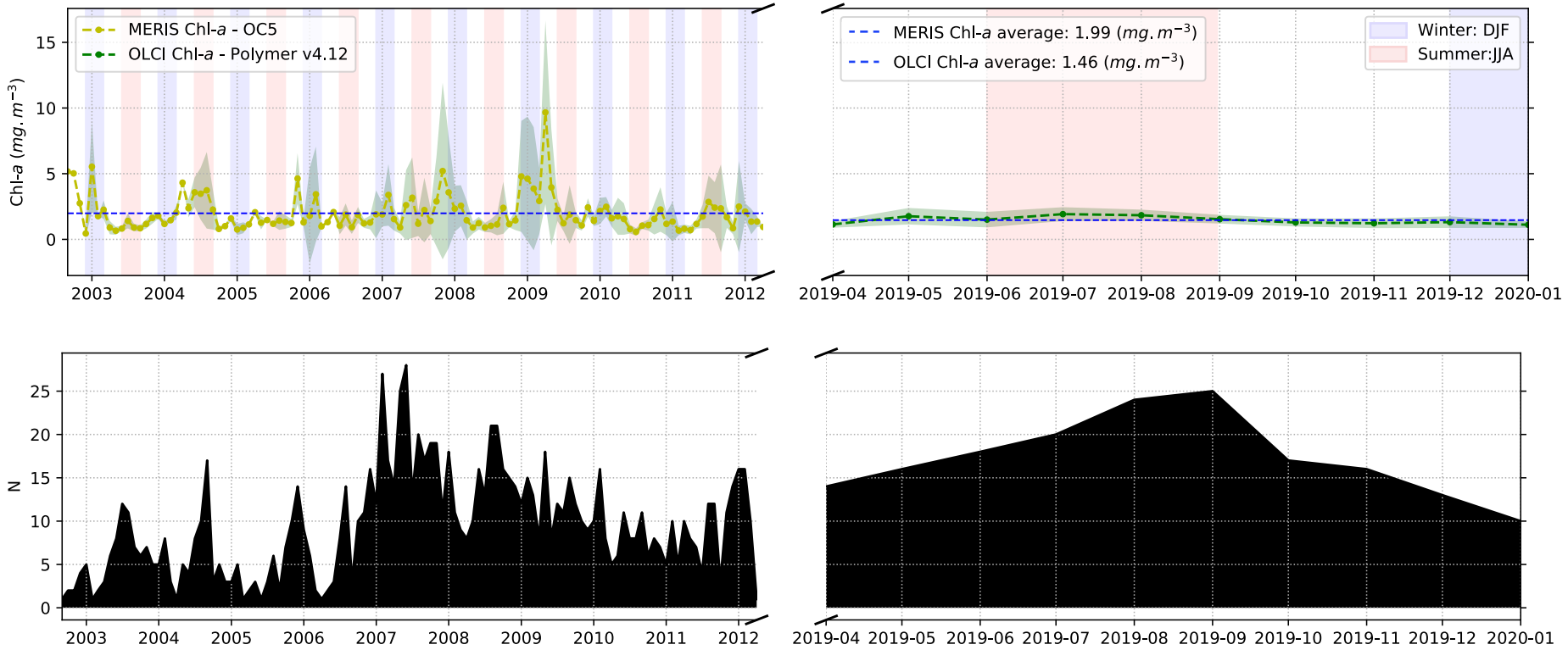

Figure 4.17 - Chl-*a* concentration monthly averages (top) for area inside aquaculture region (1.44 km^2), derived from MERIS (OC5) and OLCI (Polymer) sensors. MERIS time series start on September 2002 and ends in March 2012. Light green bars along time series represent spring (March, April and May). Light orange bars represent autumn (September, October and November). OLCI time series spans from April 2019 until January 2020. For each month the number of observations that contributed to the monthly mean are shown (bottom).

4.3.2. SST and Chl-a climatological year and percentiles for the aquaculture region

The climatological years (weekly averages) of SST and Chl-*a* for the aquaculture production area in Sines are shown in Figure 4.18 and Figure 4.19, as well as the *in situ* data, the p10 and p90, and the observations that contributed to the weekly averages. The SST climatological year (2002 – 2019) for the area of 1 km^2 centered in the aquaculture cages (Figure 3.4, orange square) is characterized by an average SST of 16.79 °C, that varies 4.82 °C throughout the climatological year. SST shows a clear seasonal pattern, with temperatures in the following ranges:

- Winter (weeks 1 - 9 and 49 - 52): [14.20, 16.05] °C;
- Spring (weeks 10 - 22): [14.42, 17.11] °C;
- Summer (weeks 23 - 35): [17.39, 19.03] °C;
- Autumn (36 - 48): [16.35, 18.96] °C;

Hereupon, the SST climatological year analysis shows that the aquaculture region commonly presents higher temperatures (> 18 °C) from summer until mid-autumn, and lower temperatures (< 14 °C) from mid-winter to early spring. The *in situ* T (all stations averaged) fall within the normal temperatures for the region in April (30/04/2019) and October (25/10/2018). In March (12/03/2019), the *in situ* T overlaps with the RS determined 90th percentile value. In May (23/05/2019) and June (29/06/2018), the *in situ* T was below the normal range for the area.

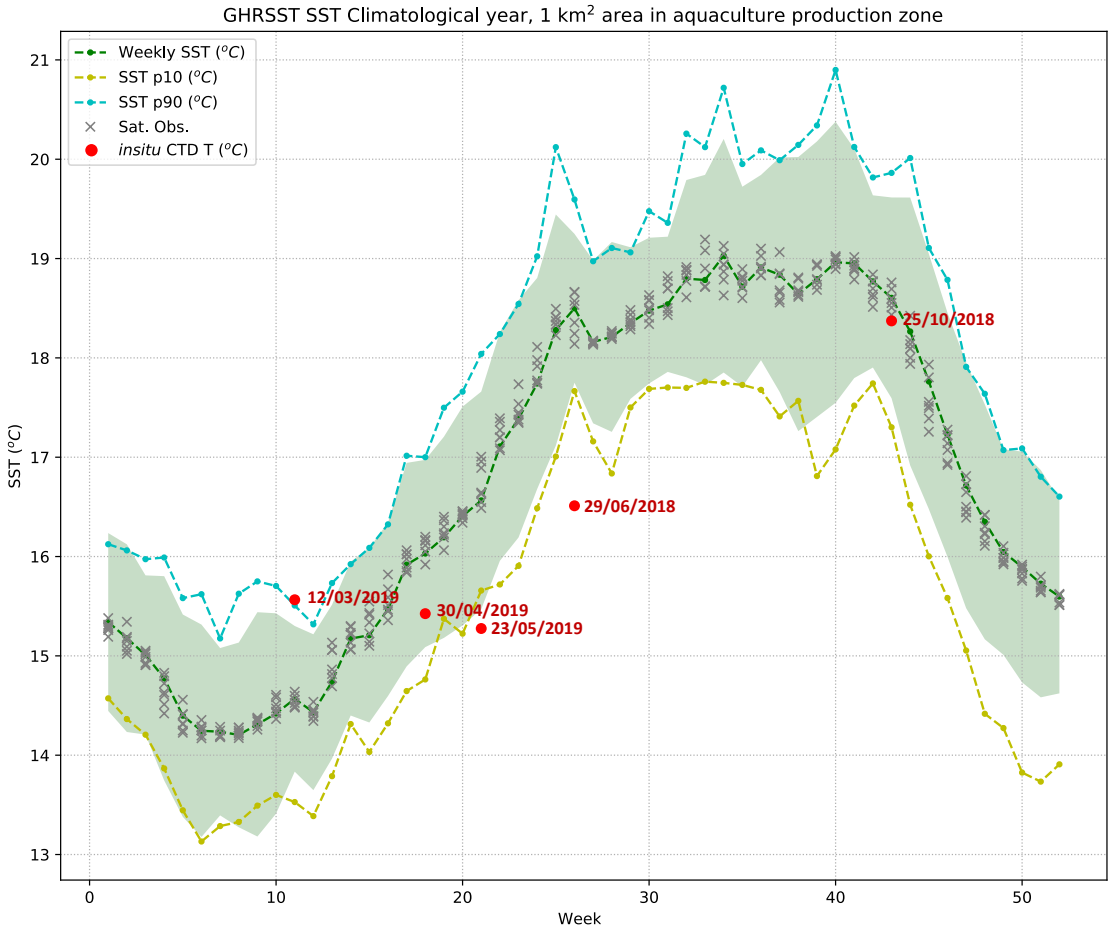

Figure 4.18 – SST climatological year (weekly average, 2002-2019) for the aquaculture production area in Sines, and p10 (light green dashed line) and p90 (blue dashed line). The green filled area represents the standard deviation. Red dots indicate the *in situ* T obtained with the CTD probe (all sampling stations averaged).

The climatological year of Chl-*a* (2002 – 2012, Figure 4.19) for an area of 1.44 km^2 centered in the aquaculture cages (Figure 3.4, black square), is characterized by a high variability over the year and a less clear seasonal pattern than SST. The climatological year average is 1.94 mg m^{-3} varying 3.35 mg m^{-3} throughout the year. The ranges of Chl-*a* weekly averages by season are as follows:

- Winter (weeks 1 - 9 and 49 - 52): [0.88, 2.30] mg m^{-3};
- Spring (weeks 10 - 22): [1.09, 4.23] mg m^{-3};
- Summer (weeks 23 - 35): [1.39, 3.41] mg m^{-3};
- Autumn (weeks 36 - 48): [1.05, 2.84] mg m^{-3}.

Winter is the less variable season, followed by autumn, summer and spring (most variable season). The *in situ* Chl-*a* falls within the natural variability of the area (i.e., within the standard deviation range). However, the *in situ* data collected in April (30/04/2019) is placed at the upper limit of the standard deviation reflecting high phytoplankton biomass conditions. Nevertheless, this Chl-*a* concentration is still below the 90th percentile of the respective week of the year. On the other hand, the *in situ* Chl-*a* of June (29/06/2018) is located in the lower limit of the standard deviation which is coincident with the 10th percentile for the respective week of the year, reflecting a low phytoplankton biomass condition.

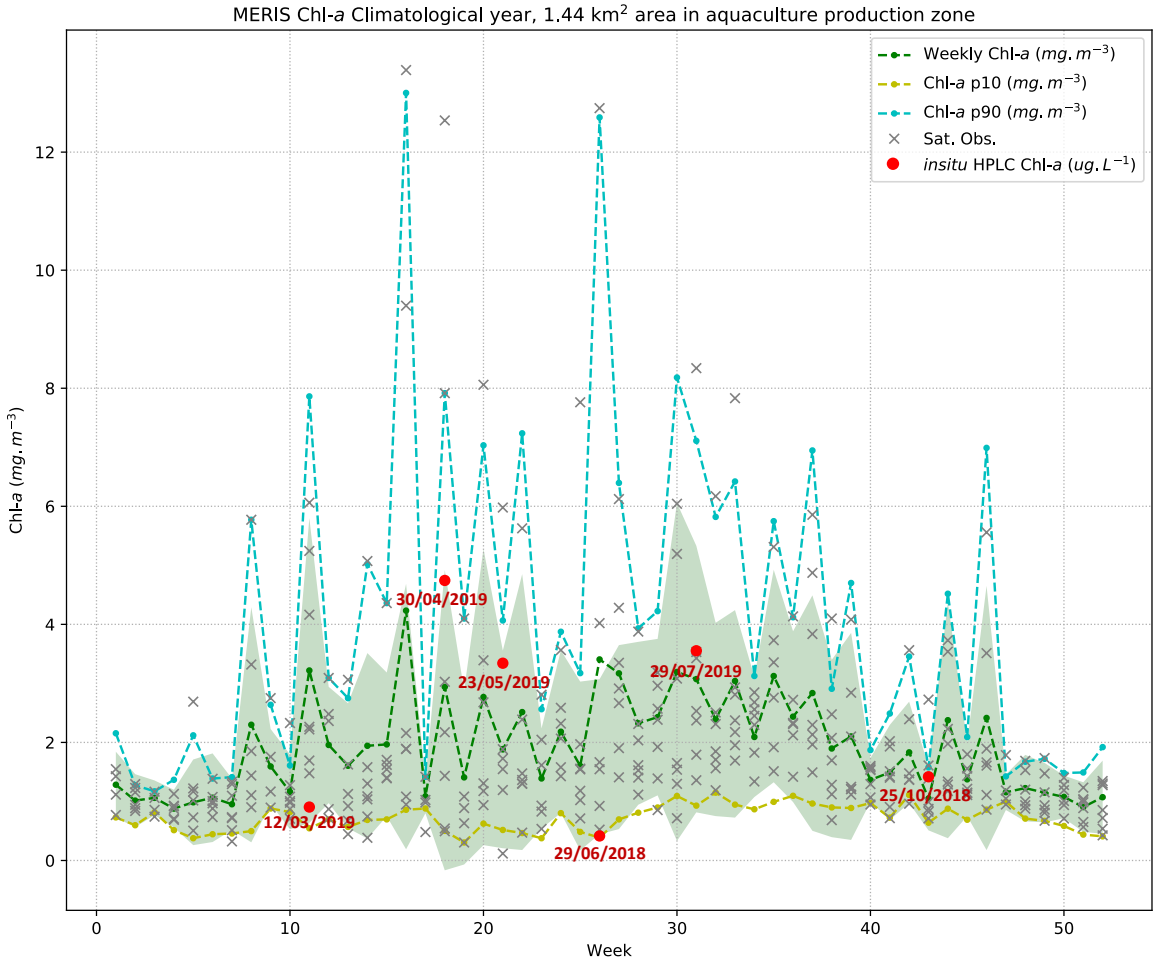

Figure 4.19 – Chl-*a* climatological year (weekly average, 2002-2012) for the aquaculture production area in Sines, and p10 (light green dashed line) and p90 (blue dashed line). The green filled area represents the standard deviation. Red dots show the *in situ* Chl-*a* data obtained through HPLC (all sampling stations averaged).

4.3.3. Comparison of remote sensing and in situ data for Sines

The comparison of RS and *in situ* data was conducted for the SST, Turb and Chl-*a* variables using several RS products (GHRSST for SST; S3 OLCI and S2 MSI Chl-*a*; S2 MSI turbidity) and two *in situ* data sources (collected in the field campaigns and data from a buoy located offshore of the aquaculture region). These comparisons were made in two ways, overlapping the time series and performing matchups. The details of matchups can be found in Table 4.11.

Table 4.11 - Details of the matchups between RS and *in situ* data.

Variable	*Product/ Sensor*	*In situ*	*Within*		*N*	r^2	Slope	Intercept	RPD (%)	APD (%)
			Time	Space						
T (°C)	GHRSST	CTD	1 day	500 m	16	0.71	0.91	1.71	2.02	3.07
T (°C)	GHRSST	Buoy	1 day	1500 m	3189	0.91	1.06	-0.78	1.27	2.73
Chl-*a* (mg m^{-3})	MSI	HPLC	3 h	600 m	0	-	-	-	-	-
Chl-*a* (mg m^{-3})	OLCI	HPLC	3 h	600 m	8	0.22	-0.08	2.57	-15.62	50.48
Turb (NTU)	MSI	Turbidimeter	3 h	600 m	0	-	-	-	-	-

GHRSST SST and *in situ* T: CTD and buoy data

The RS SST and *in situ* T (CTD and buoy) time series and matchups are presented in Figure 4.20 and Figure 4.21, respectively. In the time series, the indicated CTD data represents the average of surface temperature of the four sampling stations. On the other hand, the matchups were conducted considering the T data of each station separately. The areas for which the RS pixels were averaged for these comparisons are shown in Figure 3.4. The CTD temperature and RS derived temperatures yielded results which were similar between them (differences of less than 0.6 °C), except in June (29/06/2018) where the difference was 1.52 °C. Moreover, the coefficient of determination between both datasets (N = 16) was 0.71. Regarding the buoy temperature data, these show high agreement with the satellite data, visible through the similar seasonal pattern in the time series, and through a high coefficient of determination (N = 3189, R^2 = 0.91) in the matchup plot.

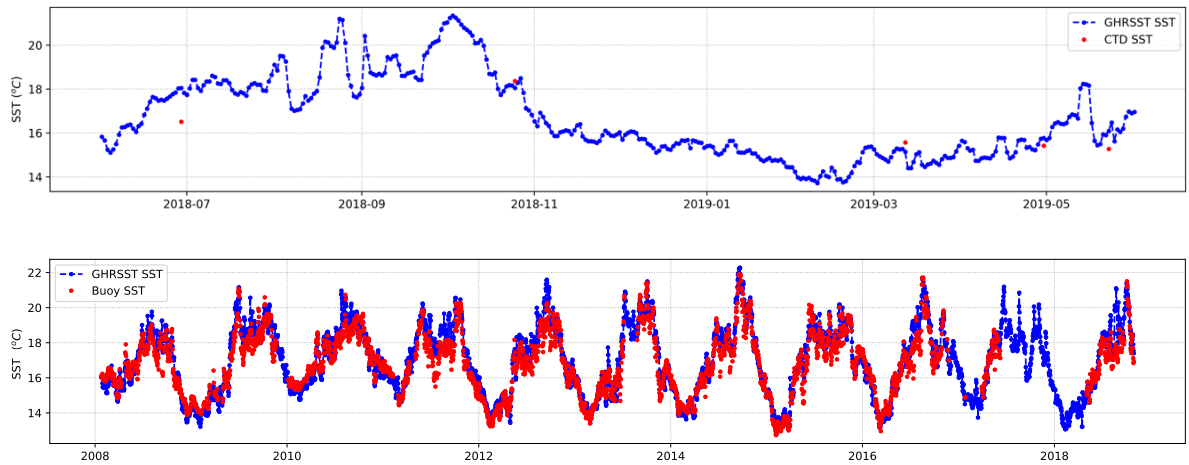

Figure 4.20 – RS SST (GHRSST, blue dashed line and dots) and *in situ* T (CTD – top, buoy – bottom; red dots) time series.

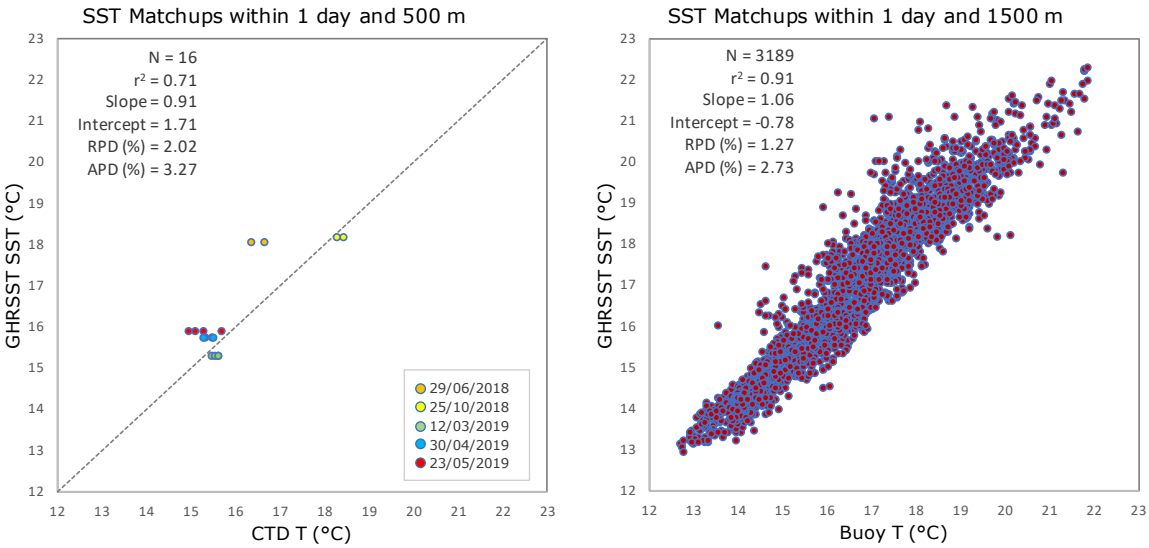

Figure 4.21 – Comparison of GHRSST RS data and *in situ* CTD T (left) and buoy T (right).

S2, S3 and *in situ* Chl-*a*

The phytoplankton biomass (indexed as Chl-*a* concentration) comparison between Poly OC2 (S2 MSI), Polymer v4.12 (S3 OLCI) and *in situ* HPLC Chl-*a* is shown in the time series of Figure 4.22 for each sampling station. The areas for which the RS pixels were averaged for these comparisons are shown in Figure 3.4. The same comparison but with the averaged *in situ* data (i.e., average all sampling stations) is shown in Figure A.3 of Annexes. Considering the time series, station 1 shows the best agreement between the RS and *in situ* Chl-*a*. Nevertheless, since only two dates matched for HPLC and OLCI Polymer v4.12 Chl-*a* (23/05/2019 and 29/07/2019), only two datapoints of each station were available for the matchups, not allowing further analysis of the difference between stations. Regarding the MSI Poly OC2 Chl-*a*, no matchups were available since two field campaigns coincided with the overpass of the S-2B sensor (not yet incorporated in the database used, which consists only in data from S-2A); and the field campaign with the S-2A overpass (29/06/2018) presented cloudy meteorological conditions not giving any valid pixels for OC-RS data retrieval.

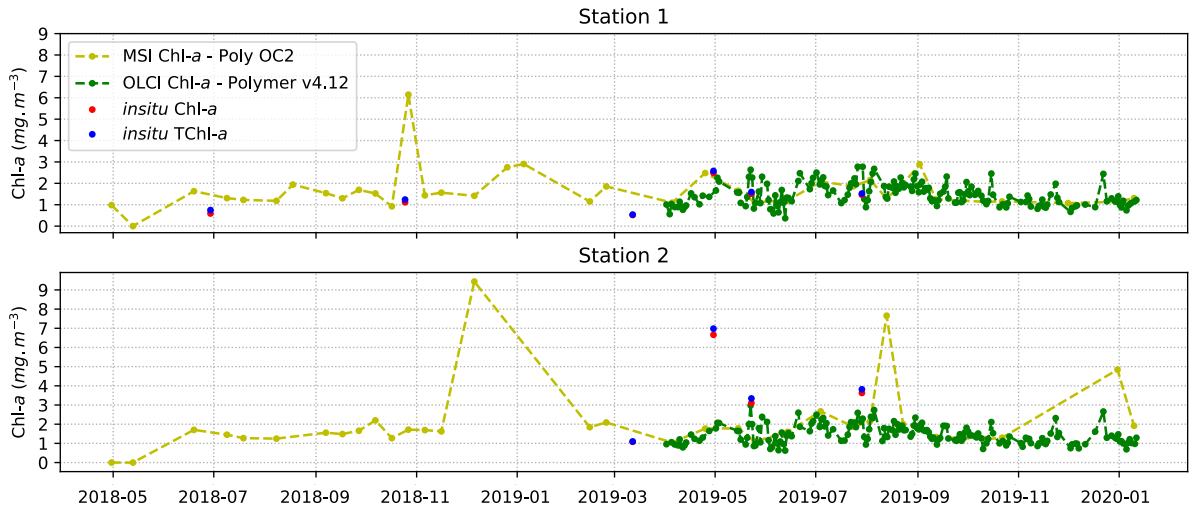

Figure 4.22 – RS Chl-*a* (MSI – light green dashed line and dots; OLCI – dark green dashed line and dots) and *in situ* Chl-*a* (HPLC – red dots) and TChl-*a* (HPLC – blue dots) time series for each sampling station.

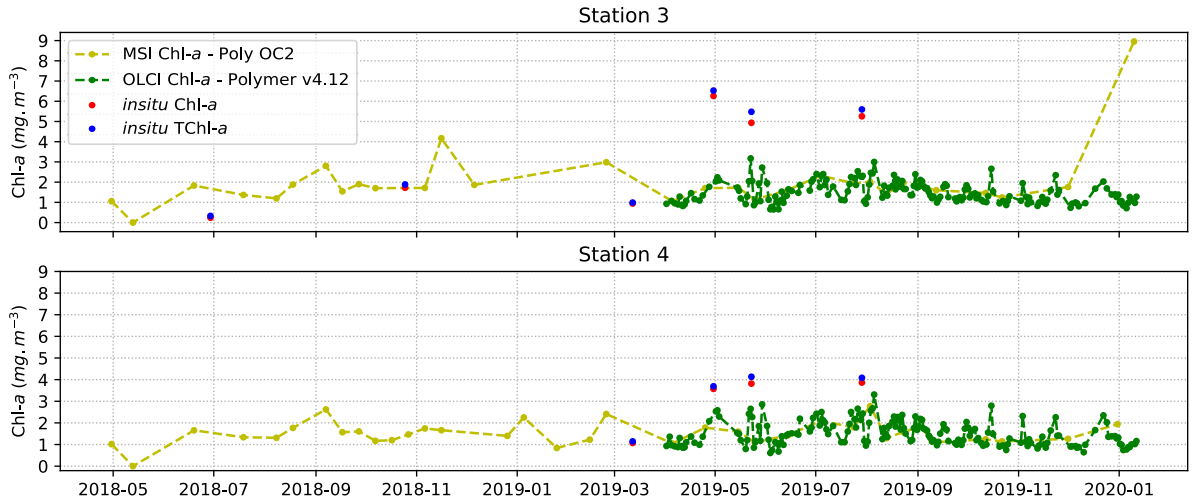

Figure 4.22 – Continued.

As an example, the comparison between the Chl-*a* obtained from the satellite and the pigment analysis are shown in Figure 4.23. As aforementioned, these results show a low number of concomitant samples (N = 8), and a coefficient of determination of 0.22. Both matchups located above the identity line, indicating an overestimation of RS Chl-*a*, correspond to station 1. For the remaining stations, the matchups indicate an underestimation of RS Chl-*a*.

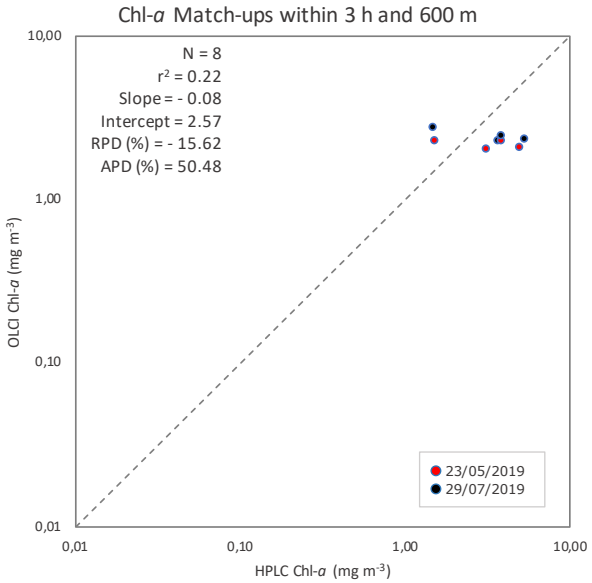

Figure 4.23 – Comparison of OLCI and *in situ* HPLC Chl-*a* (left).

In addition, Chl-*a* retrieved from both MSI (Poly OC2) and OLCI (Polymer v4.12) were compared. The coincident Chl-*a* data in time (within 3 h) and space (same spatial windows) for both products is shown in the Figure 4.24. For the two products, 52 datapoints matched, from the 1st April 2019 until the 10th January 2020 considering the four sampling stations separately. These points show a coefficient of determination of 0.76. For this comparison, Chl-*a* values higher than three times the standard deviation, considered as outliers, were discarded.

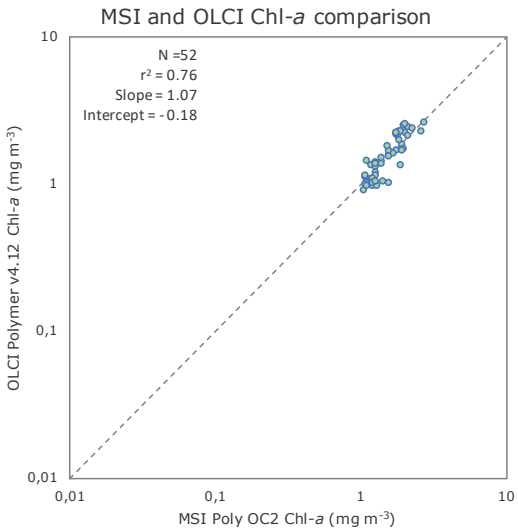

Figure 4.24 - Comparison between the Chl-*a* product from OLCI (S3) and MSI (S2) sensors using Polymer v4.12 and Poly OC2 algorithms, respectively.

S2 and *in situ* Turb

As for MSI Chl-*a*, the MSI retrieved turbidity did not present any coincident data in space and time with the *in situ* Turb. Therefore, only the comparison in the overlapping time series was done (Figure 4.25). Even so, except for a few occasional peaks, the variation of the RS Turb seems to capture the variability of turbidity in the region since values from both data sources for close dates appear to have concordant results. The same comparison but with the averaged *in situ* data (i.e., average all sampling stations) is shown in Figure A.4 of Annexes.

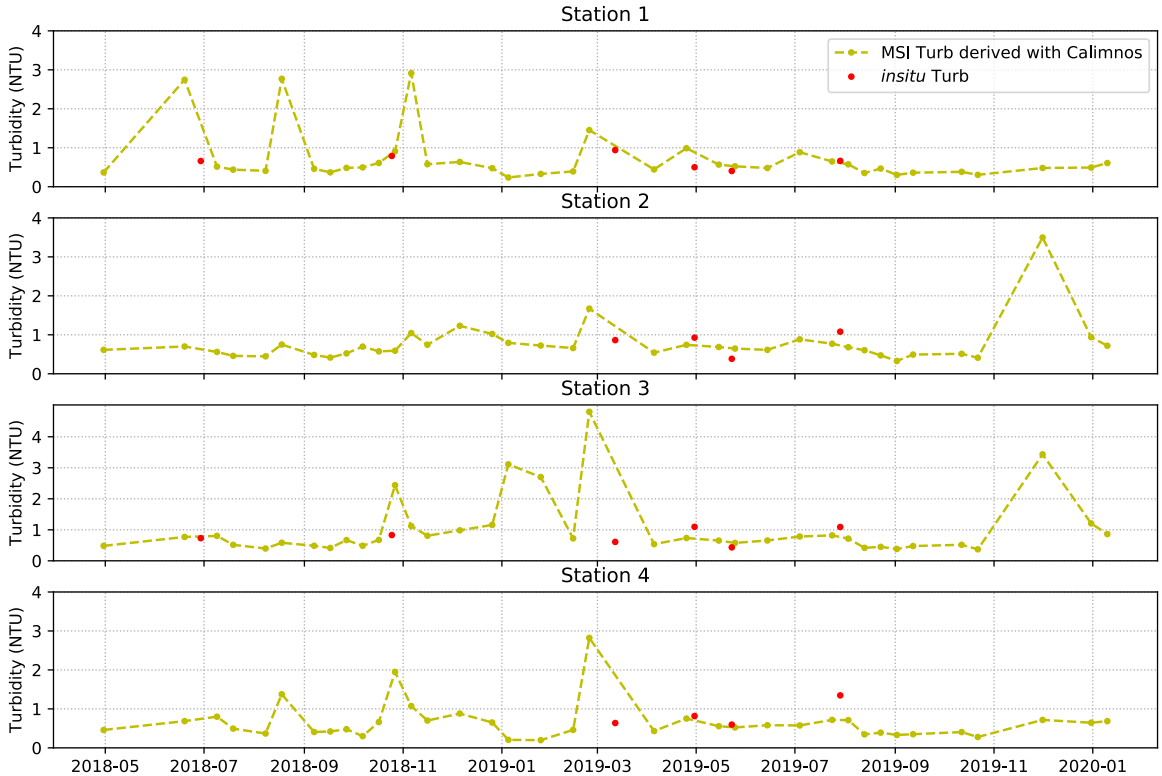

Figure 4.25 – RS Turb (MSI – light green dashed line and dots) and *in situ* Turb (red dots) time series for each sampling station.

4.3.4. SST and Chl-a anomalies in the ROI and aquaculture vicinity

The chlorophyll-*a* anomalies over the entire ROI are shown in Figure 4.26, for three specific days, which coincide with the collection of *in situ* samples in the aquaculture area (30/04/2019, 23/05/2019 and 29/07/2019). These were calculated using both the CCI and OLCI retrieved Chl-*a*. Comparing the two products, the visible difference in resolution (4 km for CCI, 300 m for OLCI) highlights the inability of the CCI product to capture data from areas adjacent to the coastline. This fact is particularly relevant for this work, since the CCI product does not allow data to be obtained for the aquaculture region, south of Cape Sines.

Concerning the Chl-*a* for each date compared to the last 7 and 14 days, in general, the two products show the same spatial anomaly pattern throughout the ROI. For the subset of the ROI closer to aquaculture production, the two products are concordant in relation to the anomaly signal (Table 4.12), although an exception occurs on 23/05/2019 where CCI does not capture the negative anomaly detected by OLCI. For instance, on 30/04/2019 higher chlorophyll values were observed in the aquaculture region (through *in situ* data). Despite this, the area selected to capture data from the CCI indicates that this day was less productive than the last 7 and 14 days (mean negative anomaly obtained from CCI and OLCI products). Calculating this same anomaly for the area overlapping aquaculture production in Sines, the data indicates a positive Chl-*a* anomaly compared to the last 7 and 14 days, evidencing local higher productive waters.

The comparison of the three dates with the last 7 and 14 days, allows to understand if higher productivity and/or phytoplankton blooms occurred in those dates, or if they occurred in the last 1 and/or 2 weeks and weakened towards those specific dates. In Table 4.12, the anomalies for the area overlapping the aquaculture production are also shown. In this case, it is possible to verify that on the 30/04/2019 a great positive anomaly occurred around the aquaculture (as verified in the *in situ* data), that most likely started on that date. On the 23/05/2019, a negative anomaly is verified. The magnitude of the anomaly weakens comparing with the last 7 days, meaning that 2 weeks previous to this date, productivity was higher in the aquaculture vicinity. Lastly, 29/07/2019 showed slightly higher productivity regarding the last 1 and 2 weeks, meaning that waters were becoming more productive around that date.

Table 4.12 – Comparation of mean anomalies obtained for Chl-*a* (CCI and OLCI retrieved) in ROI subset close to aquaculture production; and OLCI Chl-*a* aquaculture area.

*Mean Chl-a anomaly (mg m^{-3}) for **area close to production** (see Figure 3.5)*	***14 days***		***7 days***	
	CCI	OLCI	CCI	OLCI
30/04/2019	-0.31	-0.25	-0.42	-0.20
23/05/2019	0.33	0.23	0.15	-0.07
29/07/2019	0.37	-0.07	0.01	-0.05
*Mean Chl-a anomaly (mg m^{-3}) for **aquaculture area** (see Figure 3.4 black square)*	***14 days***		***7 days***	
	OLCI			
30/04/2019	0.57		0.54	
23/05/2019	-0.15		-0.41	
29/07/2019	0.06		0.05	

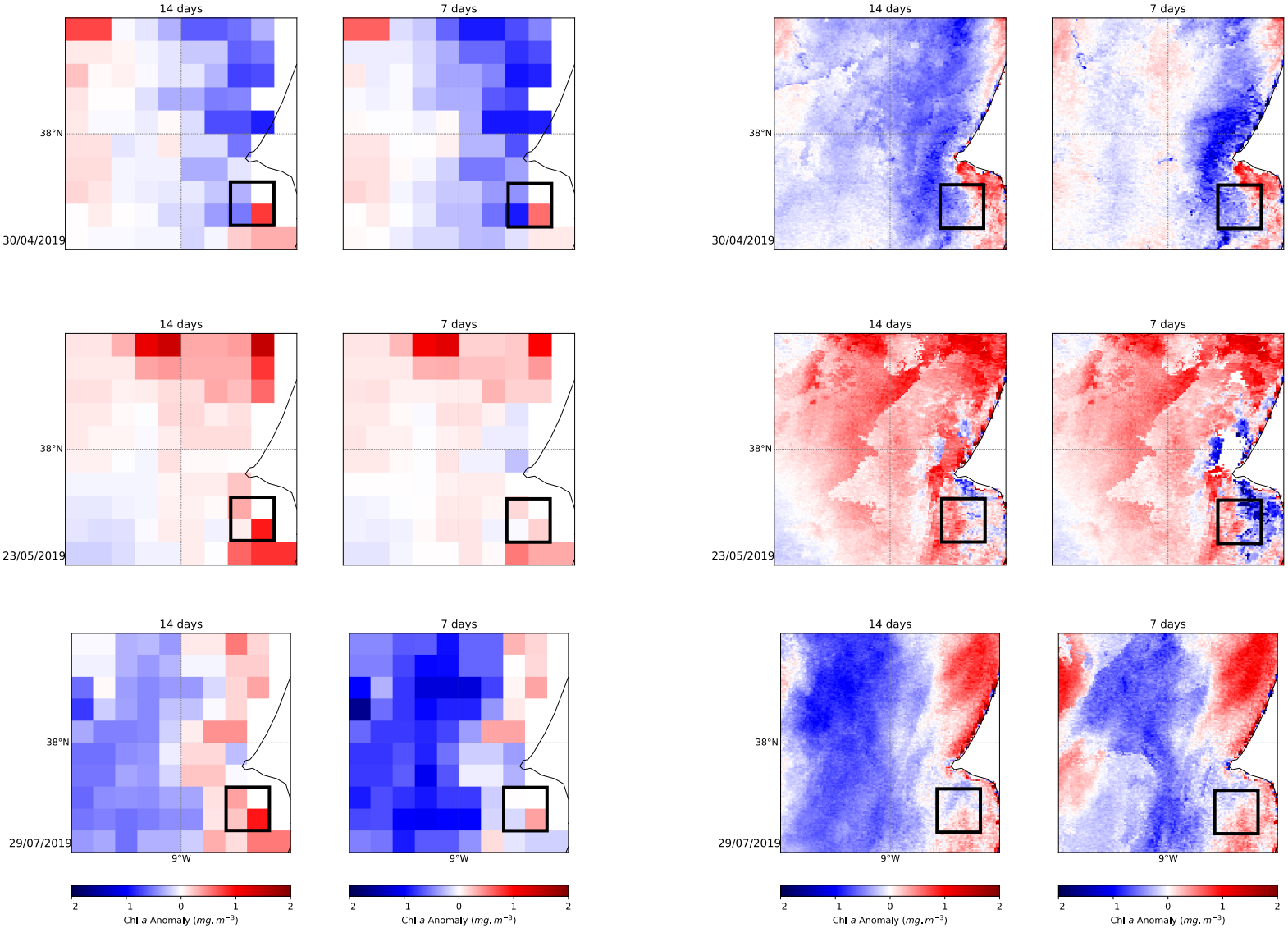

Figure 4.26 – Chl-*a* anomalies in the ROI (CCI left, OLCI right) for 3 days centred in 30th April, 23rd May and 29th July 2019 regarding the last 14 and 7 day. Black squares indicate the area used for anomaly time series analysis.

In order to understand whether the Chl-*a* anomalies verified in the spatial analysis are a common feature, and to understand if these are related to SST variations, the weekly anomalies of 2019 (compared to historical data) were computed (Figure 4.27). Due to the high SST and Chl-*a* variability over the ROI area, evident both in the climatological analysis (Figure 4.3, Figure 4.4 and Figure 4.16) and anomaly analysis (Figure 4.26), the selected ROI subset was as close as possible to the production area, taking into account the spatial resolution of the products used (see Figure 3.5, this area is also indicated as back squares in Figure 4.26).

The time series of the anomalies of 2019 regarding historical data indicates that the week encompassing the 30/04/2019 (23-30 April) was more productive than the average of this same week for the last 22 years. This positive Chl-*a* anomaly was accompanied by a negative temperature anomaly that started 3 weeks before. In the 7 weeks between 17th May and 11th July 2019, a persistent negative sea surface temperature anomaly occurred, which was followed by a Chl-*a* anomaly that persisted for 8 weeks between 20th July and 21st September 2019 close to the aquaculture in Sines. Contrarily, on the week encompassing 23/05/2019, a negative Chl-*a* anomaly was observed, which was associated with a negative SST anomaly in the same week, and a strong positive anomaly in the week before.

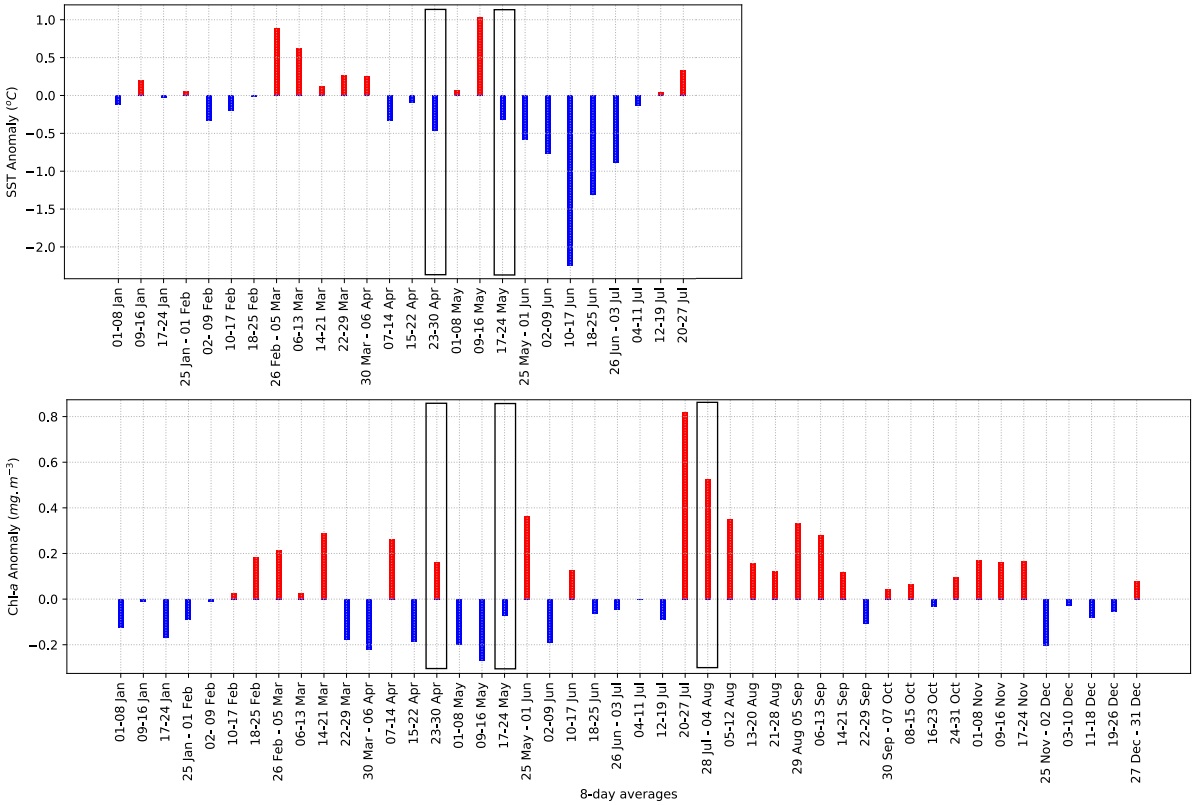

Figure 4.27 – SST (top) and Chl-*a* (bottom) anomalies of 2019 compared to the 2002-2018 (for SST) and 1997-2018 (for Chl-*a*) climatological average. The anomaly was calculated from the spatial averages of an area close to the aquaculture production (see Fig. 3.5). Black rectangles indicate the weeks that encompass the dates 30/04/2019, 23/05/2019 and 29/07/2019 when *in situ* data was collected.

5. Discussion

5.1. Water quality and impact assessment

The water quality parameters monitored over six field campaigns will be discussed in two different perspectives. On one hand, comparing the measured and analytically determined water quality parameters with the acceptable and optimum values for marine finfish production, specified in the literature overview. On the other hand, to assess the impact of aquaculture in the receiving medium, the parameters directly influenced by aquaculture production will be compared with typical values for Sines (prior to the aquaculture production in the region), to understand their relation to the regional background levels.

5.1.1. References for marine fish aquaculture: water quality assessment

The results presented in this thesis reveal a scenario of good local water quality for the intense sea bass production in Sines. This is evidenced by the fact that nearly all the obtained water quality parameters were within the acceptable ranges for marine aquaculture. Considering the parameters merged by campaign (sampling stations averaged), all fall within the acceptable range for finfish production. Considering the parameters separately (i.e. vertically at different depths in the water column, horizontally between the different sampling stations and over time throughout the various sampling campaigns), the phosphate concentration was slightly above (14%, 0.9 μmol L^{-1}) the ideal threshold (according to Stone and Thomforde, 2003) at station 3 in October. Also, the absolute minimum of the Secchi depth at the station between the aquaculture cages (station 2) was 10% (0.5 m) below the reference value defined by Prema (2013), both in April and May. Despite this, it should be noted that this ideal value is referred to the annual average, which the obtained annual average Secchi depth exceeds (8.2 ± 1.9 m). All the remaining water quality parameters and indicators were within acceptable and optimal values for marine fish production.

5.1.2. Comparison to background conditions: impact assessment

Aquaculture activities are commonly associated with detrimental environmental effects on its surroundings, with its magnitude determined by the type of aquaculture and the hydrodynamic and biogeochemical features of the site. Direct impacts of fish production on the water column include decrease of water clarity; nutrient enrichment; increase of aquaculture effluents high in biological oxygen demand (therefore reducing the dissolved oxygen along the water column); and increase of local primary productivity triggered by nutrient enrichment. Studies have analyzed the distribution of some of the primarily affected water quality parameters (e.g., dissolved oxygen, nutrients, and phytoplankton biomass and composition) along the Portuguese coast encompassing Sines region (e.g., Cabrita et al., 2015; Moita, 2001; Sá, 2013). The results from these studies will further be compared with the ones obtained in this thesis. Regarding water clarity parameters, to date, there are no studies that characterize the variation of the suspended matter and turbidity in the coastal waters off Sines. There is a vast number of studies focusing not only but also these parameters in estuaries in Portugal (e.g., Valente and Silva 2009). Also, some available literature addresses water clarity at bottom morphologies such as marine canyons (e.g., Guerreiro et al., 2014), and coastal areas under strong influence of riverine runoff (e.g.,

Oliveira et al., 1999). The above-mentioned studies will also be used to discuss the results obtained in this thesis.

Water clarity

The mean values of Secchi depth obtained in this thesis (8.2 ± 1.9 m), as a measure of water transparency in the water column, was higher than the value determined by Cabrita et al. (2015) along the coastal waters between Cape Sagres and Peniche (7.9 ± 2.5 m), suggesting clear waters in the aquaculture site even when comparing to surrounding areas. Regarding turbidity in Portuguese waters, Voelker et al. (2014), for instance, collected turbidity data over the oceanic waters, and found values ranging between ~ 0.01 – 0.2 NTU about 120 km offshore southwest of Cape Sines. Guerreiro et al. (2014) collected turbidity data along a coast-offshore transect in the Nazaré Canyon between in March 2010. Their results showed low turbidity levels in this region, ranging between 0.02 and 0.19 NTU. It should be noted that this submarine canyon was observed to be a conduit for advection of oceanic waters into nearshore areas, which explains the little turbid waters even close to the coast. Oliveira et al. (1999) characterized turbidity and total suspended matter in the northwest Portuguese coast using data collected during winter of 1996. Suspended particulate matter results obtained for the inner shelf (< 50 m) went up to 3 mg L^{-1} at surface waters (5 m) and up to 13 mg L^{-1} at the bottom. On the other hand, turbidity ranged from ~0.25 and ~7 NTU in the inner shelf waters. It is noteworthy that the sampled area in this study has influence of five rivers and that the sampling took place in winter, so that the results present high river discharge conditions.

Regarding the data collected and analyzed in the present thesis, the turbidity along the sampling campaigns went up to 1.35 NTU at the surface; and up to 7.61 NTU at the bottom. Total suspended matter went up to 1.97 mg L^{-1} at the surface and to 6.80 mg L^{-1} at the bottom. The aforementioned bottom maximums refer to isolated situations in the stations that are closer to the fish cages. At the stations located in the extremities, this signal was no longer visible, which might be an indicator of rapid local dispersion. As expected, turbidity and total suspended matter is higher on the Sines coastal waters than in oceanic waters, and higher at the bottom than at the surface. However, the lack of data for the Sines area does not allow these results to be further explored. When compared to the values obtained in presumably extreme turbidity and suspended matter conditions by Oliveira et al. (1999), the results obtained here are below those mentioned above. Moreover, the obtained dominance of the inorganic matter fraction in bottom waters indicates a stronger influence of the substrate than organic matter originated from aquaculture activity in the region. These results suggest that there is good mixing and renewal of water promoting high dispersion, even in the innermost area of fish farming.

Dissolved oxygen

Dissolved oxygen concentrations obtained in the aquaculture zone do not evidence oxygen depletion or a sharp decrease in the aquaculture vicinity, a frequent occurrence at such sites (Wu et al., 1994a; Sarà, 2007; Sriyasak et al., 2015). For instance, in summer when the respiration and metabolic rates of fish increase, the oxygen saturation in the water was still above 100%. These observations suggest that the organic matter produced by fish feces or unconsumed feed, the major causes of oxygen consumption at aquaculture sites (Wu et al., 1994a; Pérez et al., 2014), and fish metabolic activities are not promoting anoxia. According to Moita (2001), using data collected during four cruises between the summer of 1985 and the spring of 1986 along the Portuguese coast, surface waters (first 100 m) in Sines show high oxygenation typically ranging between 7 – 8 mg L^{-1}. The obtained results were within or higher than the aforementioned range. Cabrita et al. (2015) also points that Portuguese coastal waters are well oxygenated; and determined a DO 10^{th} percentile of 7.4 mg L^{-1} for the coastal area spanning

from Peniche until Lagos (encompassing Sines), using data collected between 1998 and 2000. The percentile 10 of the *in situ* data determined in the present thesis was higher (7.47 mg L^{-1}), showing good oxygenation conditions at the aquaculture site.

Phytoplankton biomass and nutrients

Phytoplankton biomass usually respond to the nutrient-rich waters at aquaculture sites by having concentrations above background levels (Sarà et al., 2011). The Chl-*a* results here presented are contrary to this, considering that the determined values fall within the typical range observed for the Portuguese coastal area (0.01 – 10.15 µg L^{-1}; Sá, 2013). The nutrient background levels for the coastal area encompassing Sines were described in Cabrita et al. (2015), to support the determination of the eutrophication state of the Portuguese waters. In this study, nutrient enrichment was observed in coastal waters, mostly related to river plume influence. The reference station to set background nutrient levels chosen for the southwestern Portuguese coast is located north of Cape Sines. The nutrient background levels for this station were 2.5, 0.18 and 2.2 µmol L^{-1} for dissolved inorganic nitrogen (DIN, sum of NO_3^-, NO_2^- and NH_4^+), phosphates and silicates, respectively. Moreover, the spatial nutrient average from data collected between 1995 and 2008 (Cabrita et al., 2015), showed mean annual concentrations of 4.8, 0.30 and 2.9 µmol L^{-1} for DIN, P and Si along the southwest Portuguese coast that encompasses Sines region. Portuguese waters naturally present low concentrations of phosphates. Nonetheless, according to Cabrita et al. (2015), the Sines region showed stronger P concentrations (~ 0.6 µmol L^{-1}) in relation to the nearest coastal areas, resembling the discharge areas of large rivers (e.g., Tagus river). This value is also within the range determined by Moita (2001) for Sines. Moita (2001) obtained nutrient ranges along the year in Sines of [3, 10] µmol L^{-1} of N, [0.2, 0.8] µmol L^{-1} of P [1, 4] µmol L^{-1} of Si, according to data collected during four cruises between the summer of 1985 and the spring of 1986.

The results obtained in the present thesis, showed nutrient averages of 6.67, 6.27 and 0.32 µmol L^{-1} for DIN, N and P, respectively. Si concentrations were all below the detection limit, denoting low concentrations. Regarding phosphates, the concentrations obtained in the aquaculture vicinity are within the normal range for the region, taking into account the above-mentioned natural ranges for Sines. N in Sines fall within the range obtained by Moita (2001) while DIN exceed the concentrations obtained in Cabrita et al. (2015). Nevertheless, the determined DIN concentrations in the aquaculture surroundings were 9% above the winter conditions in Sines (month of maximum concentrations according), where average DIN was 6.1 µmol L^{-1}. It is important to highlight that the contribution of ammonia (product excreted by fish) to DIN is weak. Despite the concentrations of DIN above the threshold for Sines region, the fact that coastal areas have been successively enriched in nutrients (Cabrita et al., 2015) does not allow to infer if this is a direct consequence of aquaculture or an effect of the increasing pressure that has been occurring in coastal areas in Portugal, including Sines.

Phytoplankton species composition

The distribution and variety of phytoplankton taxa is controlled by a combination of abiotic and biotic factors being the upwelling identified as the major source of seasonal and spatial variability of phytoplankton biomass and composition (Moita, 2001; Loureiro et al., 2005). In the Portuguese coast, the assemblage associated with upwelling is primarily composed of chain-forming diatoms like *Chaetoceros* and *Pseudo-nitzschia spp*. (Abrantes and Moita, 1999; Moita, 2001). Accordingly, the most abundant species identified on the samples collected in the aquaculture in Sines were from the genera *Pseudo-nitzschia* and *Chaetoceros*.

Some species of the diatom genus *Pseudo-nitzschia* produce domoic acid, known as the amnesic shellfish toxin (e.g., Bates et al., 1989; Garrison et al., 1992). This toxin is specially accumulated in filter-feeding organisms (e.g., bivalves); however, studies indicate that planktivorous fish are also

effective vectors of the toxin transfer through the pelagic food chain (e.g., Lefebvre et al., 2002). Moreover, the hypothesis that they also affect fish of higher trophic levels is considered in some studies (e.g., Delegrange et al., 2015). Delegrange et al. (2015) analysed the effects of juvenile sea bass to the exposure of *Pseudo-nitzschia delicatissima* (i.e. needle shaped diatom and potential domoic acid producer) and found no impacts on fish growth rates. However, they observed that these diatom species could induced a mechanical stress, affecting gill functions.

On the same token, some *Chaetoceros* are considered to be harmful due to the rigid (heavy silicified) nature of its setae which can irritate the gills of fish causing excessive mucous production or, in intense cases, cause direct physical damage to the gills (Helleren, 2016). Several species of *Chaetoceros* (*Chaetoceros concavicornis, Chaetoceros convolutus, Chaetoceros danicus, Chaetoceros densus, Chaetoceros eibenii, Chaetoceros pendulum, Chaetoceros wighami*) have been reported as the primary causative factor in many fish mortality events globally, generally associated with caged or penned fish in aquaculture farms (e.g., Treasurer et al., 2003; Rensel and Whyte, 2004). However, these events typically involve a combination of other aggravating factors such as low dissolved oxygen concentrations, abnormally high water temperatures, pollution and or pathogens (Helleren, 2016). It is a combination of two or more of these factors that lead to the mortality events rather than any one in isolation. In Sines, a bloom of *Chaetoceros* was identified in the aquaculture vicinity on the 30th April 2019. Despite this, temperatures were low (15.17 ± 0.18 °C) and dissolved oxygen in the water was high (8.43 ± 0.55 mg L^{-1}). To our knowledge, no harm effect was detected in the fish productions after such events.

In June and October 2018, there were no occurrences of toxic or potentially toxic phytoplankton species in the aquaculture vicinity. In the remaining campaigns, in addition to *Pseudo-nitzschia spp.*, there were occurrences of toxic or potentially toxic dinoflagellates, namely *Dinophysis acuta, Dinophysis acuminata*, *Alexandrium spp., Prorocentrum micans and Phalacroma rotundatum*. All of the identified species occur naturally in Portuguese waters (e.g. Pinto and Silva, 1956; Palma, 1998; Moita and Vilarinho, 1999; Moita, 2001; Vale et al., 2008); therefore, their incidence is not considered an indirect effect of aquaculture production in Sines.

Impact assessment

Sines is a highly industrialized city and, therefore, its coastal area is inevitably under intense human pressure. Even so, the apparent undetectable impacts of the aquaculture on the monitored parameters may be promoted by dilution triggered by rapid dispersion and mixing processes due to the hydrodynamic regime. The strong influence of the costal hydrodynamics, together with the tide, the wide entrance and the relatively shallow depth of the port, promote a low residence time of the water at the cage sites (Correia et al., 2019) i.e., fast renewal of the water in the system. This feature of a well-mixed system is also evident in the temperature and salinity vertical profiles, denoting the absence of stratification in the water column in all four sampling stations, for all campaigns. As such, the good water quality observed in all field campaigns can be explained by intense flushing and water renewal at the site. The feeding at the aquaculture units in Sines is done continuously through a pressurized pipe system. The amount of feed delivered is adjusted according to the environmental conditions and fish behavior, which are monitored using T and DO sensors and underwater cameras installed at the cages. Therefore, feed waste as well as potential environmental effects caused by unconsumed pellets are minimized. Hence, the lack of detrimental impact of the production units on local water quality also points to the fact that the feeding strategy is not imposing a stress on the receiving waters.

5.2. Complementary tools for aquaculture management

5.2.1 Climatological characterization: downscaling approach

Large-scale climatologies

Site characterization is relevant to support daily operations of marine cage productions by increasing the knowledge of spatio-temporal variability of abiotic and biotic variables of interest for aquaculture users, such as SST and Chl-*a*. Considering oceanic waters, in the seasonal climatologies a clear Chl-*a* maximum is evident in spring due to the North Atlantic spring bloom – a massive growth of phytoplankton that occurs annually during the spring season in mid and high latitudes (Kuhn et al., 2015). Also in offshore regions, the lowest Chl-*a* values found during summer and autumn reflect the oligotrophic nature of eastern North Atlantic Subtropical Gyre province (Longhurst, 2007). In terms of temperature, the offshore waters present higher temperatures than the colder coastal waters due to upwelling, a feature that is commonly associated to the Eastern boundary currents such as the Portugal current (Talley et al., 2011). The aforementioned results were obtained through using a 1 km spatial resolution SST product (GHRSST) and a lower spatial resolution product for Chl-*a* (CCI 4 km) which uses a blended combination of three algorithms (OCI, OC3 and OC5, depending on optical water types), designed to optimise the chlorophyll-*a* product across a range of optical environments. Both products seem to reproduce correctly the large-scale dynamics over the southwestern Iberia waters (Ferreira et al., 2019; Valente et al., 2019).

Coastal regions display high spatial complexity and temporal variability, making the use of remote sensing derived variables particularly useful in these areas. However, the chlorophyll-*a* retrieval from OC sensors is challenging since coastal waters contain suspended sediments, dissolved organics, and other substances, in addition to chlorophyll. To identify Chl-*a* in these optically complex waters requires more sophisticated algorithms than the empirical regression models used in the open ocean (e.g., Sá, 2013). Therefore, a higher spatial resolution product (MERIS 300 m) derived from a regional bio-optical algorithm (OC5), was chosen for the seasonal and monthly climatologies and further for the climatological year analysis (discussed in section *5.2.2.* Tools to assess the impact of the environment on aquaculture: alert conditions). For the SST, all the performed analyses used the same product (GHRSST 1 km) since the basis of RS SST retrieval does not alter in coastal waters making the products suitable over these highly variable areas.

In the coastal domains along the Portuguese coast, the climatological SST and Chl-*a* (MERIS 300 m) averages showed the presence of colder and more productive waters in the inner shelf, especially during spring months. Such evidences that the phytoplankton biomass distribution is closely related to the nutrient increase due upwelling along the coast (Moita, 2001; Loureiro et al., 2005; Santos et al., 2007); also verifying the suitability of the used products to characterize large-scale dynamics. Regarding Chl-*a*, both CCI and MERIS products require caution when used in coastal waters with strong riverine influences, due to higher concentrations of sediments that can mistakenly yield higher concentrations of phytoplankton biomass. Both in the annual and seasonal climatologies, stronger Chl-*a* concentrations are found close to great estuaries (for instance, areas adjacent to Douro river). When approaching the ROI of this study, Sines, higher resolution products are needed and will be discussed below.

Climatologies for Sines

Typical years in Sines exhibit dominance of northerly winds (Salgueiro et al., 2015), making the outcropping of cold nutrient-rich waters not restricted to spring and summer seasons. The Sines coastal

domain does not have strong influence of continental freshwater outflows nor prominent topographic irregularities. Therefore, the intensity and persistence of coastal upwelling conditions is seemingly the main controller of phytoplankton dynamics in the region. Figure 5.1 shows the upwelling indexes along the year in Sines, which seem to be closely related to the months of higher productivity. When upwelling favorable conditions start to prevail in March, higher Chl-*a* concentrations are found. Near Cape Sines the inorganic matter composition clearly reflect the marine origin (Alt-Epping et al., 2007), evidencing the lack of continental nutrient sources in the ROI. According to Alt-Epping et al. (2007), Sines reflects a close proximity to seasonal upwelling centers which are stronger further south. This pattern can be seen in the monthly climatological sea surface temperature, where a colder water temperature plume persists throughout the year. Moreover, persistent higher phytoplankton biomass signal in the southern domain of the ROI are most likely to be related to stronger destratification cycles providing nutrients to surface waters through vertical mixing. A study performed off central Portugal coast to investigate the behavior of SST, Chl-*a* and advection patterns during a strong upwelling event (first week of July 2005) also evidenced a wider front of high phytoplankton biomass south of Cape Sines before, during and after the event (Oliveira et al., 2009).

Comparing the SST and Chl-*a* monthly climatological averages (GHRSST 1km and MERIS 300 m) with the *in situ* data collected in the field campaigns (CTD T and HPLC Chl-*a*), both show the same qualitative intra-annual variation. Quantitatively, the temperatures obtained with the CTD in the aquaculture area were lower (except in March) than the monthly climatological SST averages for the aquaculture surroundings (- 1.79 °C for June; - 0.63 °C for October; + 0.66 °C for March; - 0.27 °C for April; and - 1.32 °C in May). This could mean that during the sampling year, temperatures were lower than in the past years, i.e. than the monthly climatological average of the last 17 years. It can also be indicative that the presence of the thermoelectric plant south of the aquaculture zone, which discharges hot water, may be accounted in the sensed area yielding higher SST values. When the *in situ* values are compared with this same satellite product in a more refined grid (1 km^2 centred at each sampling station), both show good agreement. Regarding phytoplankton biomass, it has a large coefficient of variation (> 2.5 mg m^{-3}) especially along the coast in the months of higher productivity (spring months). Nonetheless, qualitatively the interannual variability of the phytoplankton biomass seemed to be well captured. In a more detailed analysis, *in situ* and RS products will be further compared using higher temporal resolutions (weekly averages) for the aquaculture vicinity in the next section (*5.2.2 - Tools to assess the impact of the environment on aquaculture: alert conditions*).

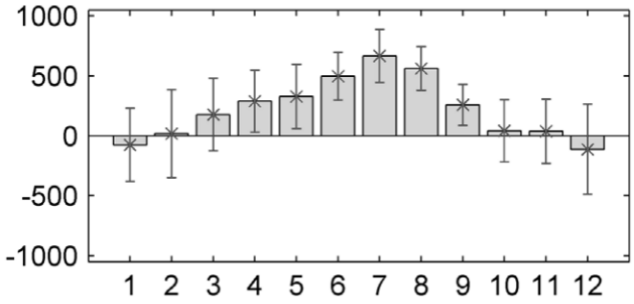

Figure 5.1 - Monthly distribution of upwelling index intensity (m^3 s^{-1} km^{-1}) with associated errors for Sines, computed from data between 1967 and 2009. Source: Ramos et al., (2013).

5.2.2 Tools to assess the impact of the environment on aquaculture: alert conditions

Climatological year

Climatological data with respective statistics may provide useful information for alert conditions to site managers. In this context, climatological weekly averages, coefficients of variation, as well as the 10th and 90th percentiles of SST and Chl-*a* were provided for the aquaculture vicinity in Sines using products with 1 km (SST) and 300 m (Chl-*a*) resolutions. This knowledge can further contribute for a more efficient management through introduction of new fish in the cages in the ideal time of the year; harvesting fish at ideal times; predicting fish growth rates; and preventing the loss of fish stock due to anomalous conditions.

The temperature showed a stable inter and intra annual variation for the aquaculture vicinity area. On the 12/03/2019 the *in situ* T was coincident with the 90th percentile for that time of the year, showing anomalous high temperatures. This could also be evidenced by a positive anomaly in the anomalies time series on the week from the 6th until the 13th March 2019, as well as in the previous week. If the aquaculture producer would compare near-real time *in situ* temperature measurements with historical climatological data on this date, this would be an alert to monitor other critical parameters (e.g., dissolved oxygen concentrations) to minimize possible negative impacts on the fish stock.

All HPLC Chl-*a* determined from the samples collected in the aquaculture fall within the variability range of the region, according to historical MERIS Chl-*a*. On the 30/04/2019, date on which a bloom was detected in the region (according to *in situ* data and confirmed with OLCI anomaly analysis), the obtained Chl-*a* (5.52 ± 1.66 μg L^{-1}) was within the standard deviation of that area for that time of year. Nonetheless, considering the average 90th percentile for the area (4.10 mg m^{-3}), the bloom situation HPLC Chl-*a* was above this threshold. In the remaining campaigns, the values of Chl-*a* were below the average p90. Therefore, for the Sines region, given the high variability of phytoplankton biomass, the use of the mean 90th percentile as a threshold to detect anomalous conditions seems to be more appropriate than the climatological weekly percentile.

The MERIS sensor provided 10 years of high-resolution data (300 m) of great importance, especially for the complex coastal areas (e.g. Kratzer et al., 2008 used MERIS to monitor coastal waters in the northwestern Baltic Sea). Nevertheless, since MERIS mission ended in 2012 a direct comparison of *in situ* and MERIS retrieved data could not be done. OLCI sensor (aboard S3) was built on MERIS heritage with similar radiometric setup and quality to ensure continuity between these sensors. On this account, both times series derived from MERIS (inactive) and OLCI (active) sensors with 300 m spatial resolution were compared for the aquaculture region in Sines. This time series analysis compared the 10 years of MERIS Chl-*a* with almost 1 year of OLCI Chl-*a* (1st April 2019 until 12th January 2020 available to date). Both products, despite being obtained using different bio-optical algorithms (OC5 for MERIS and Polymer v4.12 for OLCI), yielded similar total averages (1.99 mg m^{-3} for MERIS; 1.46 mg m^{-3} for OLCI). The OLCI time series available did not include data for the beginning of spring (i.e., March), which, as we verified through climatologies is the month in which productivity begins to increase in Sines. This fact might have contributed to the lower OLCI average. Still, the OLCI derived chlorophyll appears to have less variability throughout the year, than the highly variable MERIS product. This may be related to improvements in atmospheric correction and/or in the algorithm used. That in the OLCI product used accounts for the chlorophyll retrieval with high accuracy in the presence of sun glint conditions. The atmospheric correction algorithm applied to OLCI, named Polymer, was designed to recover ocean colour parameters in the whole sun glint pattern, which is a major issue at sub-tropical latitudes (Steinmetz et al., 2011). Common atmospheric correction algorithms are not

designed to work in these observation conditions, reducing the spatial coverage and data retrieval accuracy at such latitudes.

Anomalies

Anomalies were analysed in two different perspectives. In one hand, comparing the ROI on specific dates (matching with field campaigns) with the previous 7 and 14 days, thus being able to obtain information about the beginning of higher phytoplankton biomass periods. On the other hand, comparing the weekly phytoplankton biomass of 2019 with historical data, thus obtaining information on whether it was a more or less productive year.

The spatial anomaly analysis confirmed that the bloom that occurred on the 30th April 2019 was a local event, that occurred along the coast South of Cape Sines, and started between the 29th and the 30th April. This result shows that the analysis of daily satellite images compared to previous days can provide crucial information on bloom occurrences and alert for decision making. A rather opposing situation was verified on the 23rd May 2019, where the previous 7 and 14 days were more productive. In this situation a negative anomaly of that day regarding the last 14 days was verified, which was intensified considering the previous 7 days. This result can be indicative that a bloom occurred in the area more than two weeks before. Lastly, on the 29th July 2019, the anomaly remained constant regarding the previous 1 and 2 weeks. In this situation, despite the fact that high concentrations of phytoplanktonic biomass could be occurring, unchanging conditions persisted.

The Chl-*a* anomaly time series analysis required the use of an active remote sensing product with available historical data. Since neither MERIS nor OLCI meets these requirements, as MERIS is inactive and OLCI is still quite recent, the Climate Change Initiative multi-sensor Chl-*a* product was used (4 km spatial resolution). The CCI Chl-*a* was also compared to OLCI Chl-*a* for the entire ROI, through anomalies of three specific dates (matching field campaign) regarding the last 7 and 14 days. Despite the evident difference in resolution, both sensors captured very similar anomaly signals throughout the ROI. This comparison has highlighted the importance of using higher resolution products, especially for areas such as the aquaculture region in which this study has focused, since the CCI could not acquire data overlying the aquaculture production area, limiting its use in coastal waters.

The SST anomalies of 2019 regarding historical data were also computed to understand their relation to Chl-*a* anomalies. In fact, although further analysis is needed to understand their relation, positive anomalies of phytoplanktonic biomass are preceded by persistent negative temperature anomalies. For instance, in 2019 a 7-week persistent negative SST anomaly in the aquaculture surroundings was followed by an 8-week positive Chl-*a* anomaly in the area. These results show that there is very likely a lag period between the response of phytoplankton to the upwelling of cold nutrient rich waters in the region. This occurrence has been verified in several studies, for example in the Baltic Sea, Uiboupin et al. (2012) found lower Chl-*a* were recorded in the upwelled water in the Gulf of Finland, and the highest were observed about two weeks after the upwelling peak along the coast.

5.2.3 Tools to support evaluation of the impacts of aquaculture: optimization of monitoring

With the growth of the aquaculture industry, research of its impacts on the environment gained relevance. As this industry developed, it has been demonstrated that there are some short- and medium-temporal effects in marine aquaculture (Enell and Loef, 1983; Philips and Beveridge, 1986; Wu et al., 1994b; Wu, 1995; Rosa et al., 2002). As previously mentioned, the aquaculture site in Sines is characterized by low water residence time and therefore fast renewal in the system. Such evidences emphasize the need for high temporal and spatial resolution monitoring for impact assessment, which

can be provided by satellite remote sensing products. It is a fact that not all water quality parameters can be measured from space, partially limiting the use of satellite data. Also RS products need to be coupled with field-based observations for operational applications, meaning that they should not be used singly. That said, the use of RS to support aquaculture will be discussed here as a tool to target and optimize on-site sampling.

In this thesis, only final processed satellite products were used (that is, with algorithms already applied) and thus no independent assessment of atmospheric correction or bio-optical algorithm validation was performed. However, the products used for Sines (GHRSST SST; OLCI Chl-*a*; MSI Chl-*a*; and MSI Turb) were compared with the values obtained *in situ* (through time series and matchups) to make a first assessment on their suitability for this region. *In situ* water temperatures obtained both with the CTD in the aquaculture region and with a buoy offshore Sines were compared with the GHRSST SST product. These comparisons yielded good agreement (r^2 = 0.71 for CTD vs GHRSST; r^2 = 0.91 for buoy vs GHRSST), with small overestimations by the satellite products (RPD = 2.02 % for CTD vs GHRSST; RPD = 1.27 % for buoy vs GHRSST). It should be noted that the fact that GHRSST SST is a merged product (i.e., with the contribution of several sensors) increases the data available for comparison since daily data is available (N = 16 for CTD vs GHRSST; N = 3189 for buoy vs GHRSST). For the *in situ* and RS Chl-*a* comparison, there was no matchup for the MSI (also valid for Turb), while for OLCI only 8 matchups were identified. Hence, a first comparison between *in situ* and OLCI Chl-*a* resulted in poor agreement (r^2 = 0.22) reflecting an overall underestimation of the OLCI retrieved Chl-*a* (RPD = -15.62 %) and high error (ADP = 50.48 %). Of the few data available for the Chl-*a* matchup (*in situ* vs OLCI), the fact that the regression slope is close to zero (slope = - 0.08) is indicative that the OLCI does not detect the spatial variation of the *in situ* data along the 4 sampling stations. This result is important for monitoring purposes in the area of aquaculture and will be discussed below.

The monitoring of areas relative to their natural variability should alert to abnormal conditions. Through the *in situ* data obtained and determined in the present work, it was possible to evaluate the variability of different parameters along a transect with 4 sampling stations throughout the aquaculture production facility. Regarding the measurable water quality parameters from space used in this study (i.e., SST, Chl-*a* concentration and Turb), temperature and turbidity show weak spatial gradients between all stations. Also, their seasonal variability seems to be well captured by the RS products (evidenced in the time series overlapping *in situ* and RS data). This indicates that to analyse these water quality parameters *in situ*, sampling at a representative point of the aquaculture zone should be sufficient for monitoring purposes. Notwithstanding, no matchups occurred for the Turb product since field campaigns matched the overpass of S-2B which was not yet included in the used dataset. Therefore, the inclusion of the MSI retrieved turbidity from both S-2A and S-2B would represent an asset for future analysis of this subject. Contrary to temperature and turbidity, *in situ* Chl-*a* showed high variability between the four stations, meaning that a station cannot be used as representative of the whole aquaculture zone. Also, as previously discussed, the matchups (OLCI and HPLC Chl-*a*) showed that the OLCI was not able to detect spatial variability over the aquaculture production (only seasonal variability). This reinforces the fact that there is a need to use sensors with higher spatial resolution (e.g., MSI), especially to monitor phytoplankton biomass given its high variability in coastal areas.

This work enabled the analysis of different satellite products for the Sines area and underlines the need for high spatial and temporal resolutions for applications to coastal areas. The use of satellite data requires validation with *in situ* data. On the other hand, the complexity of and extension of coastal waters makes efficient *in situ* monitoring difficult, highlighting the potential of RS products to provide cost-effective tools for these purposes. With that being said, there is an inherent complementarity of the use of *in situ* and satellite data so that the richest harvest of new knowledge comes from the combination of both approaches.

A noteworthy result of the present work was obtained by comparing the Chl-*a* product retrieved from both OLCI (Polymer v4.12) and MSI (Poly OC2 mean) sensors. When comparing the values from these two products for the aquaculture area in Sines, they yielded a good agreement ($r^2 = 0.76$) and a nearly 45° slope (slope = 1.07) for the 52 matching overpass dates for the available datasets. These results highlight the potential of the MSI sensor (developed for land-based applications) to be applied to coastal regions. This is particularly relevant due to the higher resolution of MSI (up to 10 m depending on the spectral bands).

6. Conclusions and future work

Portugal is among the countries in the world with the highest fish consumption per capita, yet aquaculture and fisheries represent low contributions to total European production (EC, 2018). In response to the limited potential to increase wild fishery catches, rising demand for seafood, and improved technology, alternative food supplies such as aquaculture have been emerging. In Portugal, the growth potential of the aquaculture sector is acknowledged, being considered one of the value chains of the sea economy. The ENM reinforces that conditions must be created to attract national and international investment in this sector, and the PEAP identifies the need for development of national aquaculture to enhance its contribution to the fish market. Defined measures to boost the Portuguese aquaculture sector and promote its sustainable development encompass, among others, the need for good environmental conditions in culture areas, and the need to support this industry with scientific research. Indeed, scientific knowledge is a key aspect for the expansion of marine aquaculture in the highly attractive extensive Portuguese coast.

The main objective of this thesis was to provide elements that can support a marine sea bass cage production in Sines, Portugal, considering the end user requirements which focus on decreasing the costs involved in production (increasing profitability) while reducing environmental impacts. Such was supported by resolving the three specific objectives: (1) to characterize the aquaculture site using satellite data through a downscaling approach; (2) to assess the water quality and impacts of the site using *in situ* data; and (3) to combine both *in situ* and satellite approaches providing end users with tools to support the activity. All objectives were met, as detailed below.

Spatio-temporal reference values were given for the Sines region, through the establishment of annual, seasonal, and monthly climatological averages of sea surface temperature and phytoplankton biomass (indexed as Chl-*a*). Understanding local dynamics allows producers to target crucial activities, for instance adjusting feed administered and therefore optimizing production. Further crossing of the results obtained herein with production variables (e.g., fish growth and mortality, feed administration) would contribute for valuable knowledge of the interaction between the caged fish and the environmental conditions. Moreover, if the expansion of the aquaculture would be aimed, the provided knowledge on regional variability could further be used to select the most optimal production sites in Sines, with conditions that support maximum productivity combined with minimized environmental impact.

Water quality was assessed for the aquaculture vicinity. Overall good local water quality with all the parameters (parameters averaged per sampling campaign) within the acceptable for marine fish culture were found in the production surroundings. This is particularly relevant since aquaculture relies on a healthy environment to provide quality and safe products. Future efforts to sample extreme conditions in the aquaculture region would help to establish the worst-case scenario for water quality conditions. These should be late summer and neap tide circumstances due to higher temperatures (higher stratification), higher metabolic rates for fish (higher excretion rates and higher oxygen consumption), and lower water currents in the area.

Sines is a highly industrialized city and, therefore, its coastal area is inevitably under intense human pressure. Even so, no critical impacts of the aquaculture on the monitored parameters were found. Further analysis of the contribution of the urban and industrial activities to the deterioration of coastal waters is necessary to distinguish it from the potential contribution of the aquaculture (for instance, regarding eutrophication). Hereafter, the use of RS data (once validated), is a promising tool since high resolution products with data prior to production until today are available.

Through the combination of *in situ* and satellite approaches, tools to support the aquaculture in Sines were provided. Besides allowing the characterization of the natural variability in the area (SST and Chl-*a*), these also included information on extreme SST and Chl-*a* conditions, detection of anomalies in the area, and providing information for the optimization of local monitoring. Hence, the aforementioned tools have the potential to support decision making.

Finally, it is noteworthy that many of the results obtained here were preliminarily analyzed motivating future work. Relevant themes for future work would focus on the establishment of links between water quality parameters and the response of fish, which could form the basis for robust indicators to build into monitoring services and products, in order to reduce losses and optimize resources. Analysis of covariation between the different environmental parameters could provide more insight on the regional dynamics. For instance, it was found that phytoplankton high biomass events were preceded by negative temperature anomalies. Since SST is more clearly retrieved from RS products (as opposed to Chl-*a* in optically complex waters), determining the relationship between both variables could help early warnings for blooms in the aquaculture region. This work could also be complemented with phenology analysis for Sines region to understand bloom timings and durations. Also, further assessments of RS products suitability for Sines, which require more *in situ* data, would allow exploring novel sensors (e.g., S2 and S3) applied to the aquaculture region. It would be interesting to use RS retrieved Chl-*a* data before and after the beginning of sea bass production in 2016, to study possible influences of the activity on the local productivity.

References

Abrantes, F., and Moita, M. T. (1999). Water column and recent sediment data on diatoms and coccolithophorids, off Portugal, confirm sediment record of upwelling events. *Oceanol. Acta* 22, 318–336. doi:10.1016/s0399-1784(99)90007-5.

Agência Portuguesa do Ambiente (2019). Aquaculture production. *Relatório do Estado do Ambiente.* Available at: https://rea.apambiente.pt/content/aquaculture-production?language=en [Accessed January 12, 2020].

Aguilar-Manjarrez, J., Lovatelli, A., and Soto, D. (2013). Expanding mariculture farther offshore: technical, environmental, spatial and governance challenges. *FAO Fisheries and Aquaculture Proceedings No. 24*. doi:10.13140/RG.2.1.2989.1927.

Alaska Department of Environmental Conservation (2016). Listing Methodology for Determining Water Quality Impairments from Turbidity. Alaska.

Almeida, C., Karadzic, V., and Vaz, S. (2015). The seafood market in Portugal: Driving forces and consequences. *Mar. Policy* 61, 87–94. doi:10.1016/j.marpol.2015.07.012.

Alt-Epping, U., Mil-Homens, M., Hebbeln, D., Abrantes, F., and Schneider, R. R. (2007). Provenance of organic matter and nutrient conditions on a river- and upwelling influenced shelf: A case study from the Portuguese Margin. *Mar. Geol.* 243, 169–179. doi:10.1016/j.margeo.2007.04.016.

American Public Health Association (1998). *Standard methods for the examination of water and wastewater*, 20th ed. , eds. L. S. Clesceri, A. E. Greenberg, and A. D. Eaton. Washington DC.

Anderson, C. R., Kudela, R. M., Kahru, M., Chao, Y., Rosenfeld, L. K., Bahr, F. L., et al. (2016). Initial skill assessment of the California Harmful Algae Risk Mapping (C-HARM) system. *Harmful Algae* 59, 1–18.

Anderson, D. M., Pitcher, G. C., and Estrada, M. (2005a). The comparative "systems" approach to HABs research. *Oceanography* 18, 148–157.

Anderson, M. R., Armstrong, S. M., Auffrey, L. M., Barbeau, M. A., Black, K., Bugden, J., et al. (2005b). E*nvironmental Effects of Marine Finfish Aquaculture*. Ed. B. Hargrave, Springer-Verlag. Berlin.

Australian and New Zealand Environment and Conservation Council, and Agriculture and Resource Management Council of Australia and New Zealand (2000). *Australian and New Zealand Guidelines for Fresh and Marine Water Quality*. Available at: http://www.dofa.gov.au/infoaccess/ [Accessed January 12, 2020].

Barnabé, G. (1991). Fish growth in intensive farming. *Bases biologiques et écologiques de l'aguaculture*, 422–451.

Barton, E. D. (2001). Canary and Portugal currents. *Encycl. Ocean Sci.* 1, 380–389. doi:10.1006/rwos.2001.0360.

Bates, S. S., Bird, C. J., and Freitas, A. S. W. (1989). Pennate diatom Nitzschia pungens as the primary source of domoic acid, a toxin in shellfish from eastern Prince Edward Island, Canada. *Can. J. Fish. Aquat. Sci.* 46, 1203–1215. doi:10.1139/f89-156.

Bendschneider, K., and Robinson, R. J. (1952). A new spectrophotometric method for the determination of nitrite in sea water. *J. Mar. Res.* 11, 87–96.

Berdalet, E., Banas, N., Bresnan, E., Burford, M., Davidson, K., Gobler, C., et al. (2017). Global Harmful Algal Blooms. *Oceanography* 30:1, 70-81.

Bhatnagar, A., Jana, S. N., Garg, S. K., Patra, B. C., Singh, G., and Barman, U. K. (2004). Water quality management in aquaculture. *Course Manual of Summerschool on Development of Sustainable*

Aquaculture Technology in Fresh Andsaline Waters, Hisar, India, 203–210.

Black, K. D. (2001). Sustainability of aquaculture. *Environmental impacts of aquaculture.* Ed. K. D. Black, Sheffield Academic Press, Sheffield.

Bouwman, L., Beusen, A., Glibert, P. M., Overbeek, C., Pawlowski, M., Herrera, J., et al. (2013). Mariculture: significant and expanding cause of coastal nutrient enrichment. *Environ. Res. Lett.* 8. doi:10.1088/1748-9326/8/4/044026.

Boyd, C. E. (1998). *Water Quality for Pond Aquaculture*. 43rd ed., International Center for Aquaculture and Aquatic Environments, Alabama Agricultural Experiment Station, Auburn University, Alabama.

Brotas, V., Couto, A. B., Sá, C., Amorim, A., Brito, A., Laanen, M., et al. (2014). Deriving Aquaculture indicators from Earth Observation in the AQUA-USERS project (AQUAculture USEr driven operational Remote Sensing information Services). Available at: www.aqua-users.eu [Accessed January 27, 2020].

Cabrita, M. T., Silva, A., Oliveira, P. B., Angélico, M. M., and Nogueira, M. (2015). Assessing eutrophication in the Portuguese continental Exclusive Economic Zone within the European Marine Strategy Framework Directive. *Ecol. Indic.* 58, 286–299. doi:10.1016/j.ecolind.2015.05.044.

Cao, L., Wang, W., Yang, Y., Yang, C., Yuan, Z., Xiong, S., et al. (2007). Environmental Impact of Aquaculture and Countermeasures to Aquaculture Pollution in China. *Env Sci Pollut Res* 14, 452–462. doi:10.1065/espr2007.05.426.

Claridge, P. N., and Potter, I. C. (1983). Movements, Abundance, Age Composition and Growth of Bass, Dicentrarchus Labrax, in the Severn Estuary and Inner Bristol Channel. *J. Mar. Biol. Assoc. United Kingdom* 63, 871–879. doi:10.1017/S0025315400071289.

Correia, A., Pinto, L., and Mateus, M. (2019). Implementation of a 3-Dimensional Hydrodynamic Model to a Fish Aquaculture Area in Sines, Portugal - A Down-Scaling Approach. *Lecture Notes in Computer Science (including subseries Lecture Notes in Artificial Intelligence and Lecture Notes in Bioinformatics)*, Springer Verlag, 265–278. doi:10.1007/978-3-030-22747-0_21.

Dalsgaard, T., and Krause-Jensen, D. (2006). Monitoring nutrient release from fish farms with macroalgal and phytoplankton bioassays. *Aquaculture* 256, 302–310. doi:10.1016/j.aquaculture.2006.02.047.

David, L. T., Pastor-Rengel, D., Talaue-McManus, L., Magdaong, E., Salalula-Aruelo, R., Bangi, H. G., et al. (2014). The saga of community learning: Mariculture and the Bolinao experience. *Aquat. Ecosyst. Heal. Manag.* 17, 196–204.

Davidson, K., Gowen, R. J., Harrison, P. J., Fleming, L. E., Hoadland, G., and Moschonas, G. (2014). Anthropogenic nutrients and harmful algae in coastal waters. *J. Environ. Manage.*, 206–216.

Dean, A., and Salim, A. (2013). Remote sensing for the sustainable development of offshore mariculture. A global assessment of offshore mariculture potential from a spatial perspective, FAO Fisheries and Aquaculgure Technical Paper 549, 123–181.

Delegrange, A., Vincent, D., Courcot, L., and Amara, R. (2015). Testing the vulnerability of juvenile sea bass (Dicentrarchus labrax) exposed to the harmful algal bloom (HAB) species Pseudo-nitzschia delicatissima. *Aquaculture* 437, 167–174. doi:10.1016/j.aquaculture.2014.11.023.

Dias, L. (2018). *Sines. Calheta, do promotório ao mar*. Projeto Avançado, Exercício de Mestrado Integrado em Arquitetura, Universidade de Évora, 35 pp.

Dülger, N., Kumlu, M., Türkmen, S., Ölçülü, A., Tufan Eroldoğan, O., Asuman Yilmaz, H., et al. (2012). Thermal tolerance of European Sea Bass (Dicentrarchus labrax) juveniles acclimated to three temperature levels. *J. Therm. Biol.* 37, 79–82. doi:10.1016/j.jtherbio.2011.11.003.

Egna, H. S. (1994). Monitoring water quality for tropical freshwater fisheries and aquaculture: a review

of aircraft and satellite imagery applications. *Fish. Manag. Ecol.* 1, 165–178. doi:10.1111/j.1365-2400.1994.tb00159.x.

Enell, M., and Loef, J. (1983). Environmental impacts of aquaculture sedimentation and nutrient loadings from fish cage culture farming. *Vatten/Water*, 364–375.

Ercan, E., Ağrah, N., and Serhan, T. A. (2015). The Effects of Salinity, Temperature and Feed Ratio on Growth Performance of European Sea Bass (Dicentrarchus labrax L., 1758) in the Water Obtained Through Reverse Osmosis System and a Natural River. *Pakistan journal of zoology* 47, 625-633.

Ertör, I., and Ortega-Cerdà, M. (2015). Political lessons from early warnings: Marine finfish aquaculture conflicts in Europe. *Mar. Policy* 51, 202–210. doi:10.1016/j.marpol.2014.07.018.

European Comission (2018). *Facts and figures on the common fisheries policy*. doi:10.1108/nfs.2012.01742daa.002.

European Commission (2015). *Fisheries and aquaculture production*. Available at: https://ec.europa.eu/fisheries/print/20008 [Accessed January 12, 2020].

Fanning, K. A., and Pilson, M. (1973). On the Spectrophotometric determination of dissolved silica in natural waters. *Anal. Chem.* 45, 136–140. doi:10.1021/ac60323a021.

FAO (2014). *The State of World Fisheries and Aquaculture*, Opportunities and challenges. Rome.

FAO (2015). Global Aquaculture Production statistics database updated to 2013: Summary information. Rome. Available at: www.fao.org/fishery/statistics/global-aquaculture- [Accessed January 4, 2020].

FAO (2018). *Fisheries and Aquaculture Statistics 2016*. Rome. doi:10.5860/CHOICE.50-5350.

FAO (2020). *Fisheries and Aquaculture.* Cultured Aquatic Species Information Programme, Dicentrarchus labrax (Linnaeus, 1758). Available at: http://www.fao.org/fishery/culturedspecies/Dicentrarchus_labrax/en [Accessed January 22, 2020].

Ferreira, A., Garrido-Amador, P., and Brito, A. C. (2019). Disentangling environmental drivers of phytoplankton biomass off Western Iberia. *Front. Mar. Sci.* 6, 1–17. doi:10.3389/fmars.2019.00044.

Ferreira, J. G., Hawkins, A. J. S., and Bricker, S. B. (2007). Management of productivity, environmental effects and profitability of shellfish aquaculture-the Farm Aquaculture Resource Management (FARM) model. *Aquaculture* 264, 160–174. doi:10.1016/j.aquaculture.2006.12.017.

Furuya, K., Gilbert, P. M., Zhou, M., and Raine, R. (2010). Global Ecology and Oceanography of Harmful Algal Blooms in Asia: A Regional Comparative Programme. GEOHAB Asia.

Garcia, S. M., and Rosenberg, A. A. (2010). Food security and marine capture fisheries: Characteristics, trends, drivers and future perspectives. *Philos. Trans. R. Soc. B Biol. Sci.* 365, 2869–2880. doi:10.1098/rstb.2010.0171.

Garrison, D. L., Conrad, S. M., Eilers, P. P., and Waldron, E. M. (1992). Confirmation of domoic acid production by Pseudonitzschia Australis (Bacillariophyceae) cultures. *J. Phycol.* 28, 604–607. doi:10.1111/j.0022-3646.1992.00604.x.

Gentry, R. R., Lester, S. E., Kappel, C. V., White, C., Bell, T. W., Stevens, J., et al. (2017). Offshore aquaculture: Spatial planning principles for sustainable development. *Ecol. Evol.* 7, 733–743. doi:10.1002/ece3.2637.

Godfray, H. C. J., Beddington, J. R., Crute, I. R., Haddad, L., Lawrence, D., Muir, J. F., et al. (2010). Food security: The challenge of feeding 9 billion people. *Science* 327, 812–818. doi:10.1126/science.1185383.

Gohin, F., Druon, J. N., and Lampert, L. (2002). A five channel chlorophyll concentration algorithm applied to SeaWiFS data processed by SeaDAS in coastal waters. *Int. J. Remote Sens.*, 1639–

1661.

Goldburg, R. J., Elliott, M. S., and Naylor, R. L. (2001). *Marine aquaculture in the United States: Environmental impacts and policy options.* Virginia. Available at: www.pewtrusts.org/uploadedFiles/ wwwpewtrustsorg/Reports/Protecting_ocean_life/ env_pew_oceans_aquaculture [Accessed January 15, 2020].

Goldburg, R., and Naylor, R. (2005). Future Seascapes, Fishing, and Fish Farming. *Frontiers in Ecology and the Environment* 3, 21-28.

Grant, M., Jackson, T., Chuprin, A., Sathyendranath, S., Zuhlke, M., Storm, T., et al. (2017). Ocean-Colour Climate Change Initiative, Climate Assessment Report D4.2, Report 2. Plymouth.

Grasshoff, K. (1977). *Methods of seawater analysis*. Ed. K. Grasshoff Weinheim, Verlag Chemie. New York. doi:10.4319/lo.1977.22.6.1103.

Grigorakis, K., and Rigos, G. (2011). Aquaculture effects on environmental and public welfare - The case of Mediterranean mariculture. *Chemosphere* 85, 899–919. doi:10.1016/j.chemosphere.2011.07.015.

Guerreiro, C., Sá, C., de Stigter, H., Oliveira, A., Cachão, M., Cros, L., et al. (2014). Influence of the Nazaré Canyon, central Portuguese margin, on late winter coccolithophore assemblages. *Deep. Res. Part II Top. Stud. Oceanogr.* 104, 335–358. doi:10.1016/j.dsr2.2013.09.011.

Harrison, W. G., Perry, T., and Li, W. K. W. (2005). Ecosystem indicators of water quality, Part I. *Plankton biomass, primary production and nutrient demand. Environmental Effects of Marine Finfish Aquaculture* in Handbook of Environmental Chemistry. Ed. Hargrave. Berlin.

Helleren, S. (2016). The diatom Chaetoceros spp. as a potential contributing factor to fish mortality events in Cockburn Sound, November 2015. Dalcon Environmental Report DE00000.R1, Department of Fisheries Western Australia. New South Wales.

Holmer, M. (2010). Environmental issues of fish farming in offshore waters: Perspectives, concerns and research needs. *Aquac. Environ. Interact.* 1, 57–70. doi:10.3354/aei00007.

Holmer, M., Argyrou, M., Dalsgaard, T., Danovaro, R., Diaz-Almela, E., Duarte, C. M., et al. (2008). Effects of fish farm waste on Posidonia oceanica meadows: Synthesis and provision of monitoring and management tools. *Mar. Pollut. Bull.* 56, 1618–1629. doi:10.1016/j.marpolbul.2008.05.020.

Hu, C., Lee, Z., and Franz, B. (2012). Chlorophyll a algorithms for oligotrophic oceans: A novel approach based on three-band reflectance difference. *J. Geophys. Res. Ocean.* 117. doi:10.1029/2011JC007395.

Huguenin, J. E., and Colt, J. (1989). *Design and Operating Guide for Aquaculture Seawater Systems*. 2nd Ed., Elsevier Science. Amsterdam.

Imsland, A. K., Foss, A., Conceicao, L. E. C., Dinis, M. T., Delbare, D., Schram, E., et al. (2003). A review of the culture potential of Solea solea and S. senegalensis. *Rev. Fish Biol. Fish.*, 379–407.

IOCCG (2008). *Why Ocean Colour? The Societal Benefits of Ocean- Colour Technology*. Eds. T. Platt, N. Hoepffner, V. Stuart, C. Brown. Reports of the International Ocean-Color Coordinating Group, Report Number 7.

IOCCG (2009). *Remote sensing in fisheries and aquaculture*. Eds. M. Forget, V. Stuart, T. Platt. Reports of the International Ocean-Color Coordinating Group, Report Number 8.

IOCCG (2014). *Phytoplankton Functional Types from Space*. Ed. S. Sathyendranath. Reports of the International Ocean-Color Coordinating Group, Report Number 15.

IOCCG (2018). *Earth Observations in Support of Global Water Quality Monitoring*. Eds. S. Greb, A. Dekker and C. Binding. Reports of the International Ocean-Color Coordinating Group, Report Number 17.

Jackson, T., Sathyendranath, S., and Mélin, F. (2017). An improved optical classification scheme for

the Ocean Colour Essential Climate Variable and its applications. *Remote Sens. Environ.* 203, 152–161. doi:10.1016/j.rse.2017.03.036.

Jansen, H. M., Reid, G. K., Bannister, R. J., Husa, V., Robinson, S. M. C., Cooper, J. A., et al. (2016). Discrete water quality sampling at open-water aquaculture sites: Limitations and strategies. *Aquac. Environ. Interact.* 8, 463–480. doi:10.3354/AEI00192.

JPL MUR MEaSUREs Project (2015). GHRSST Level 4 MUR Global Foundation Sea Surface Temperature Analysis (v4.1). Ver. 4.1. PO.DAAC, Caifornia. doi:10.5067/GHGMR-4FJ04.

Kaiser, M. J., Yu, Y., and Snyder, B. (2010). Economic feasibility of using offshore oil and gas structures in the Gulf of Mexico for platform-based aquaculture. *Mar. Policy* 34, 699–707.

Kämpf, J., and Chapman, P. (2016). *The Canary/Iberia Current Upwelling System BT - Upwelling Systems of the World: A Scientific Journey to the Most Productive Marine Ecosystems*. Eds. J. Kämpf and P. Chapman, Springer International Publishing. Switzerland. doi:10.1007/978-3-319-42524-5_6.

Karakassis, I., Hatziyanni, E., Tsapakis, M., and Plaiti, W. (1999). Benthic recovery following cessation of fish farming: A series of successes and catastrophes. *Mar. Ecol. Prog. Ser.* 184, 205–218. doi:10.3354/meps184205.

Koroleff, F. (1969). Direct determination of ammonia in natural waters as indophenol blue. *Int. Rep. Cons. Int. Explor. Mer.* 3, 19–22.

Kratzer, S., Brockmann, C., and Moore, G. (2008). Using MERIS full resolution data (300 m spatial resolution) to monitor coastal waters– a case study from Himmerfjärden, a fjord-like bay in the north-western Baltic Sea. *Remote Sens. Environ.* 112, 2284–2300.

Kroupova, H., Machova, J., and Svobodova, Z. (2005). Nitrite influence on fish: A review. *Vet. Med. (Praha).* 50, 461–471. doi:10.17221/5650-VETMED.

Kuhn, A. M., Fennel, K., and Mettern, J. P. (2015). Model investigations of the North Atlantic spring bloom initiation. *Prog. Oceanogr.*, 176–193.

Kutti, T., Hansen, P. K., Ervik, A., Høisæter, T., and Johannessen, P. (2007). Effects of organic effluents from a salmon farm on a fjord system: temporal and spatial patterns in infauna community composition. *Aquaculture* 262, 355–366. doi:10.1016/j.aquaculture.2006.10.008.

Lafferty, K. D., Harvell, C. D., Conrad, J. M., Friedman, C. S., Kent, M. L., Kuris, A. M., et al. (2015). Infectious Diseases Affect Marine Fisheries and Aquaculture Economics. *Ann. Rev. Mar. Sci.* 7, 471–496. doi:10.1146/annurev-marine-010814-015646.

Lawson, T. B. (1995). *Fundamental of Aquacultural Engineering*. Elsevier Scientific Publishers. Amsterdam.

Lefebvre, K. A., Silver, M. W., Coale, S. L., and Tjeerdema, R. S. (2002). Domoic acid in planktivorous fish in relation to toxic Pseudo-nitzschia cell densities. *Mar. Biol.* 140, 625–631. doi:10.1007/s00227-001-0713-5.

Lloyd, R. (1992). *Pollution and Freshwater Fish*. West Byfleet: Fishing News Books. Massachusetts.

Longhurst, A. (2007). *Ecological Geography of the Sea*. 2nd ed., Academic Press. doi:10.1016/B978-0-12-455521-1.X5000-1.

Loureiro, S., Newton, A., and Icely, J. D. (2005). Microplankton composition, production and upwelling dynamics in Sagres (SW Portugal) during the summer of 2001. *Sci. Mar.* 69, 323–341. doi:10.3989/scimar.2005.69n3323.

Lutterschmidt, W. I., and Hutchison, V. H. (1997). The critical thermal maximum: History and critique. *Can. J. Zool.* 75, 1561–1574. doi:10.1139/z97-783.

Martin, S. (2014). *An Introduction to Ocean Remote Sensing*. Cambridge University Press. Cambridge. doi:10.1017/CBO9781139094368.

Jerónimo Martins (2017). Relatório e Contas 2016. Apresentações e Relatórios. Available at: https://www.jeronimomartins.com/wp-content/uploads/files%20to%20download/DOCUMENTOS%20IR/RELATORIO%20E%20CONTAS/2016/PT/relatoriocontasjm2016.pdf [Accessed December 12, 2019].

Jerónimo Martins (2018). Relatório e Contas 2017. Apresentações e Relatórios. Available at: https://www.jeronimomartins.com/wp-content/uploads/files%20to%20download/DOCUMENTOS%20IR/RELATORIO%20E%20CONTAS/2017/Relatorio-Contas-Jeronimo-Martins-2017.pdf [Accessed December 14, 2019].

Masroor, W., Farcy, E., Gros, R., and Lorin-Nebel, C. (2018). Effect of combined stress (salinity and temperature) in European sea bass Dicentrarchus labrax osmoregulatory processes. *Comp. Biochem. Physiol. -Part A Mol. Integr. Physiol.* 215, 45–54. doi:10.1016/j.cbpa.2017.10.019.

Matos, J., Costa, S., Rodrigues, A., Pereira, R., and Sousa Pinto, I. (2006). Experimental integrated aquaculture of fish and red seaweeds in Northern Portugal. *Aquaculture* 252, 31–42. doi:10.1016/j.aquaculture.2005.11.047.

Maurer, J. (2002). Infrared and microwave remote sensing of sea surface temperature (SST). Remote Sensing Seminar, Department of Aerospace Engineering Sciences*, University of Hawai'i at Mānoa.* Honolulu.

Moita, M. T. (2001). Estrutura , variabilidade e dinâmica do Fitoplâncton na Costa de Portugal Continental. PhD Thesis, Faculty of Sciences of University of Lisbon, 209 pp.

Moita, M. T., and Vilarinho, M. G. (1999). Checklist of phytoplankton species off Portugal: 70 years (1929-1998) of studies. *Port. Acta Biol.* 18, 5–50.

Murphy, J., and Riley, J. P. (1962). A modified single solution method for the determination of phosphate in natural waters. *Anal. Chim. Acta* 27, 31–36. doi:10.1016/S0003-2670(00)88444-5.

Navarrete-Mier, F., Sanz-Lázaro, C., and Marín, A. (2012). Navarrete-Mier 10. Does bivalve mollusc polyculture reduce marine fin fish farming. *Aquaculture* 306, 101–107.

Njoku, E. G. (1990). Satellite remote sensing of sea surface temperature. *Surf. Waves Fluxes* 2, 311–338.

Oliveira, A., Rodrigues, A., and Jouanneau, J. M. (1999). Suspended particulate matter distribution and composition on the northern Portuguese margin. *Bol. - Inst. Esp. Oceanogr.* 15, 101–109.

Oliveira, P. B., Nolasco, R., Dubert, J., Moita, M. T., and Peliz, Á. (2009). Surface temperature, chlorophyll and advection patterns during a summer upwelling event off central Portugal. *Cont. Shelf Res.* 25, 759–774.

Ornamental Aquatic Trade Association (2008). Water Quality Criteria. Available at: www.ornamentalfish.org [Accessed January 12, 2020].

Ottinger, M., Clauss, K., and Kuenzer, C. (2016). Aquaculture: Relevance, distribution, impacts and spatial assessments – A review. *Ocean Coast. Manag.* 119, 244–266. doi:10.1016/J.OCECOAMAN.2015.10.015.

Palma, A. S. (1998). Interannual trends in the longshore distribution of Dinophysis off the Portuguese coast. *Harmful Algae*, 124–127.

PEAP (2016). Plano Estratégico para a Aquicultura Portuguesa 2014-2020. Available at: https://www.dgrm.mm.gov.pt/documents/20143/43770/Plano_Estrat%C3%A9gico_Aquicultura_2014_2020.pdf [Accessed January 12, 2020].

Pérez, Ó., Almansa, E., Riera, R., Rodriguez, M., Ramos, E., Costa, J., et al. (2014). Food and faeces settling velocities of meagre (Argyrosomus regius) and its application for modelling waste dispersion from sea cage aquaculture. *Aquaculture* 420–421, 171–179. doi: 10.1016/j.aquaculture.2013.11.001.

Philips, M., and Beveridge, M. C. M. (1986). Cages and the effect on water condition. *Fish Farmer*,

17–19.

Philminaq Project (2013). *Mitigating aquaculture impact in the Philippines*. Outputs and recommendations, Annex 2, 1–97. Available at: https://www.researchgate.net/publication/259089454_Mitigating_aquaculture_impact_in_the_Philippines_PHILMINAQ_Outputs_and_Recommendations [Accessed January 4, 2020].

Pinto, J. S., and Silva, E. S. (1956). The toxicity of Cardium edule L. and its possible relation to the dinnoflagellate Prorocentrum micans Ehr. Notas e Estudos Inst. Biol. Marít., no. 12, 21 pp.

Platt, T., Shah, P., George, G., Menon, N., Nashad, M., Trottan, M. P., et al. (2015). Use of remote sensing in the context of cage aquaculture. 5th International Symposium on Cage Aquaculture in Asia. Available at: http://eprints.cmfri.org.in/10588/1/CAA5 Souvenir_Grinson.pdf [Accessed January 24, 2019].

PODAAC (2019). Sea Surface Temperature. Available at: https://podaac.jpl.nasa.gov/SeaSurfaceTemperature [Accessed January 20, 2019].

Port of Sines Administration (2020). Porto de Sines. Available at: http://www.portodesines.pt/o-porto/características-gerais/ [Accessed January 22, 2020].

Prema, D. (2013). Site selection and water quality in mariculture. *Cust. Train. Maric. Maldivian Off. Manual.*, 35–43.

Price, C. S., and Morris, J. A. (2015). Marine cage culture and the environment: Twenty-first century science informing a sustainable industry. *Mar. Finfish Aquac. Environ.*, 1–156.

Quansah, J. E., Rochon, G. L., Quagrainie, K. K., Amisah, S., Muchiri, M., and Ngugi, C. (2007). Remote sensing applications for sustainable aquaculture in Africa. IEEE International Geoscience and Remote Sensing Symposium (IEEE), 1255–1259. doi:10.1109/IGARSS.2007.4423034.

Ramalho, A., and Dinis, M. T. (2011). Portuguese aquaculture : Current status and future perspectives. *World Aquac.* 42, 26–32.

Ramos, A. M., Pires, A. C., Sousa, P. M., and Trigo, R. M. (2013). The use of circulation weather types to predict upwelling activity along the western Iberian Peninsula coast. *Cont. Shelf Res.* 69, 38–51. doi:10.1016/j.csr.2013.08.019.

Relvas, P., Barton, E. D., Dubert, J., Oliveira, P. B., Peliz, Á., da Silva, J. C. B., et al. (2007). Physical oceanography of the western Iberia ecosystem: Latest views and challenges. *Prog. Oceanogr.* 74, 149–173. doi:10.1016/j.pocean.2007.04.021.

Relvas, P., Luís, J., and Santos, A. M. P. (2009). Importance of the mesoscale in the decadal changes observed in the northern Canary upwelling system. *Geophys. Res. Lett.* 36. doi:10.1029/2009GL040504.

Rensel, J. E., and Whyte, J. N. C. (2004). *Finfish mariculture and harmful algal blooms*. Manual on Harmful Marine Microalgae, eds. G. M. Hallegraeff, D. M. Anderson, and A. D. Cembella, UNESCO. Paris.

Robinson, I. S. (2010). *Discovering the Ocean from Space: The unique applications of satellite oceanography*. Springer. Berlin.

Rosa, T., Mirto, S., Favaloro, E., Savona, B., Sara, G., Danavaro, R., et al. (2002). Impact on the water column biogeochemistry of a Mediterranean mussel and fish farm. *Water Res.*, 713–721.

Roy, S., Llewellyn, C., Egeland, E., and Johnsen, G. (2011). *Phytoplankton Pigments: Characterization, Chemotaxonomy and Applications in Oceanography*. Cambridge University Press. Cambridge. doi: 10.1017/CBO9780511732263.

Ruiz-Villarreal, M., García-García, L. M., Cobas, M., Díaz, P. A., and Reguera, B. (2016). Modelling the hydrodynamic conditions associated with Dinophysis blooms in Galicia (NW Spain). *Harmful Algae*, 40–62.

Russel, N. R., Fish, J. D., and Wootton, R. J. (1996). Feeding and growth of juvenile sea bass: effect of ration and temperature on growth rate efficiency. *J. Fish Biol.*, 206–220.

Sá, C. (2013). Ocean Colour off the Portuguese Coast: Chlorophyll a products validation and applicability. PhD Thesis, Faculty of Sciences of University of Lisbon, 228 pp.

Sá, C., Brito, A. C., Beltrán, C., Eleveld, M. A., Dale, T., Grafoso, B. D. D., et al. (2014). Aquaculture Indicators Report. AQUA-USERS deliverable D3.5, EC FP7 grant agreement no: 607325, 50 pp.

Salgueiro, D. V, De Pablo, ; H, Neves, ; R, and Mateus, ; M (2015b). Modelling the thermal effluent of a near coast power plant (Sines, Portugal). *J. Integr. Coast. Zo. Manag.* 15, 533–544. doi:10.5894/rgci577.

Santhosh, B., and Singh, N. P. (2007). Guidelines for Water Quality Management for Fish Culture in Tripura. Indian Council of Agricultural Research, Research Complex for North Eastern Hill Region. Available at: https://www.scirp.org/(S(351jmbntvnsjt1aadkposzje))/reference/ReferencesPapers.aspx?ReferenceID=2092317 [Accessed January 22, 2020].

Santos, A. M. P., Chícharo, A., Dos Santos, A., Moita, T., Oliveira, P. B., Peliz, Á., et al. (2007). Physical-biological interactions in the life history of small pelagic fish in the Western Iberia Upwelling Ecosystem. *Prog. Oceanogr.* 74, 192–209. doi:10.1016/j.pocean.2007.04.008.

Santos, A. M. P., and Fiúza, A. F. G. (1992). Supporting the Portuguese fisheries with satellites. Proceedings of the European International Space Year Conference, Part 2, 663–668.

Sarà, G. (2007a). Aquaculture effects on some physical and chemical properties of the water column: A meta-analysis. *Chem. Ecol.* 23, 251–262. doi:10.1080/02757540701379493.

Sarà, G. (2007b). A meta-analysis on the ecological effects of aquaculture on the water column: Dissolved nutrients. *Mar. Environ. Res.* 63, 390–408. doi:10.1016/j.marenvres.2006.10.008.

Sarà, G., Lo Martire, M., Sanfilippo, M., Pulicanò, G., Cortese, G., Mazzola, A., et al. (2011). Impacts of marine aquaculture at large spatial scales: Evidences from N and P catchment loading and phytoplankton biomass. *Mar. Environ. Res.* 71, 317–324. doi:10.1016/j.marenvres.2011.02.007.

Sathyendranath, S., Subba, R. D. V, Chen, Z., Stuart, V., Platt, T., Budgen, G. L., et al. (1997). Aircraft remote sensing of toxic phytoplankton blooms: a case study from Cardigan River, Prince Edward Island. *J. Remote Sens.*, 15–23.

Sriyasak, P., Chitmanat, C., Whangchai, N., Promya, J., and Lebel, L. (2015). Effect of water de-stratification on dissolved oxygen and ammonia in tilapia ponds in Northern Thailand. *Int. Aquat. Res.* 7, 287–299. doi:10.1007/s40071-015-0113-y.

Steinmetz, F., Deschamps, P.-Y., and Ramon, D. (2011). Atmospheric correction in presence of sun glint: application to MERIS. *Opt. Express* 19, 9783. doi:10.1364/oe.19.009783.

Stone, N., and Thomforde, H. (2003). Understanding Your Fish Pond Water Analysis Report. University of Arkansas at Pine Bluff, United States Department of Agriculture. Cooperative Extension Program.

Stumpf, R. P., Culver, M. E., Tester, P. A., Tomlinson, M., Kirkpatrick, G. J., Pederson, B. A., et al. (2003). Monitoring Karenia brevis blooms in the Gulf of Mexico using satellite ocean color imagery and other data. *Harmful Algae* 2, 147–160. doi:10.1016/S1568-9883(02)00083-5.

Sugiura, S., Marchant, D., Kelsey, K., Wiggins, T., and Ferraris, R. (2006). Effluent profile of commercially used low-phosphorus fish feeds. *Environ. Pollut.* 140, 95–101. doi:10.1016/j.envpol.2005.06.020.

Talley, L. D., Pickard, G. L., Emery, W. J., and Swift, J. H. (2011). *Descriptive physical oceanography: An introductio.* 6th ed., Academic Press. Boston. doi:10.1016/C2009-0-24322-4.

Tang, D., Kawamura, H., Oh, I. S., and Baker, J. (2006). Satellite evidence of harmful algal blooms and related oceanographic features in the Bohai Sea during autumn 1998. *Adv. Sp. Res.* 37, 681–689.

doi:10.1016/J.ASR.2005.04.045.

Tovar, A., Moreno, C., Mánuel-Vez, M. P., and García-Vargas, M. (2000). Environmental impacts of intensive aquaculture in marine waters. *Water Res.* 34, 334–342. doi:10.1016/S0043-1354(99)00102-5.

Treasurer, J. W., Hannah, F., and Cox, D. (2003). Impact of a phytoplankton bloom on mortalities and feeding response of farmed Atlantic salmon, Salmo salar, in west Scotland. *Aquaculture* 218, 103–113. doi:10.1016/S0044-8486(02)00516-1.

Trindade, A., Peliz, A., Dias, J., Lamas, L., Oliveira, P. B., and Cruz, T. (2016). Cross-shore transport in a daily varying upwelling regime: A case study of barnacle larvae on the southwestern Iberian coast. *Cont. Shelf Res.* 127, 12–27. doi:10.1016/j.csr.2016.08.004.

Uiboupin, R., Laanemets, J., Sipelgas, L., Raag, L., Lips, I., and Buhhalko, N. (2012). Monitoring the effect of upwelling on the chlorophyll a distribution in the gulf of Finland (Baltic Sea) using remote sensing and in situ data. *Oceanologia* 54, 395–419. doi:10.5697/oc.54-3.395.

United Nations (2020). Oceans - United Nations Sustainable Development Goals (Goal 14). Available at: https://www.un.org/sustainabledevelopment/oceans/ [Accessed January 12, 2020].

Valdemarsen, T., Bannister, R. J., Hansen, P. K., Holmer, M., and Ervik, A. (2012). Biogeochemical malfunctioning in sediments beneath a deep-water fish farm. *Environ. Pollut.* 170, 15–25. doi:10.1016/j.envpol.2012.06.007.

Vale, P., Botelho, M. J., Rodrigues, S. M., Gomes, S. S., and Sampayo, M. A. de M. (2008). Two decades of marine biotoxin monitoring in bivalves from Portugal (1986-2006): A review of exposure assessment. *Harmful Algae* 7, 11–25. doi:10.1016/j.hal.2007.05.002.

Valente, A. S., and da Silva, J. C. B. (2009). On the observability of the fortnightly cycle of the Tagus estuary turbid plume using MODIS ocean colour images. *J. Mar. Syst.* 75, 131–137. doi:10.1016/j.jmarsys.2008.08.008.

Valente, A., Sousa, F., and Dias, J. (2019). Decadal changes in temperature and salinity of Central Waters off Western Iberia. *Deep. Res. Part I Oceanogr. Res. Pap.* 151, 103068. doi:10.1016/j.dsr.2019.103068.

Van Der Linde, D. W. (1998). Protocol for the determination of Total Suspended Matter in Oceans and coastal zones. Ispra, Italy.

Voelker, A. H. L., Bell, D., and Oliveira, P. (2014). Relatórios de Campanha. Available at: http://ipma.pt/pt/publicacoes/index.jsp [Accessed February 29, 2020].

Wronna, M., Omira, R., and Baptista, M. A. (2015). Deterministic approach for multiple-source tsunami hazard assessment for Sines, Portugal. *Nat. Hazards Earth Syst. Sci.* 15, 2557–2568. doi:10.5194/nhess-15-2557-2015.

Wu, R. S. S. (1995). The environmental impact of marine fish culture: towards a sustainable future. *Mar. Pollut. Bull.*, 4–12.

Wu, R. S. S., Lam, K. S., MacKay, D. W., Lau, T. C., and Yam, V. (1994a). Impact of marine fish farming on water quality and bottom sediment: A case study in the sub-tropical environment. *Mar. Environ. Res.* 38, 115–145. doi:10.1016/0141-1136(94)90004-3.

Wu, R. S. S., Lam, K. S., McKay, D. W., Lau, T. C., and Yam, V. (1994b). Impact of marine fish farming on water quality and bottom sediment: a case study in the sub-tropical environment. *Mar. Environ. Res.*, 115–145.

Wurts, W. A., and Durborow, R. (1992). Interactions of pH, Carbon Dioxide, Alkalinity and Hardness in Fish Ponds. *South. Reg. Aquac. Cent.,* 3363.

Yilmaz, H. A., Turkmen, S., Kumlu, M., Eroldogan, O. T., and Perker, N. (2019). Alteration of growth and temperature tolerance of european sea bass (Dicentrarchus labrax linnaeus 1758) in different temperature and salinity combinations. *Turkish J. Fish. Aquat. Sci.* 20, 331–340.

doi:10.4194/1303-2712-v20_5_01.

Yin, K., Harrison, P. J., Chen, J., Huang, W., and Qian, P. Y. (1999). Red tides during spring 1998 in Hong Kong: is El Niño responsible? *Mar. Ecol. Prog. Ser.*, 289–294.

Zapata, M., Rodríguez, F., and Garrido, J. L. (2000). Separation of chlorophylls and carotenoids from matine phytoplankton: a new HPLC method using a reverse phase C8 column and pyridina-containing mobile phases. *Mar. Ecol. Prog. Ser.*, 29–45.

A. Annexes

Table A.1 - Sampling station latitude, longitude and depth.

Sampling station	Latitude	Longitude	Depth
1	37.93272	-8.855261	14 m
2	37.92932	-8.851303	21 m
3	37.92775	-8.847949	24 m
5	37.92482	-8.843557	30 m

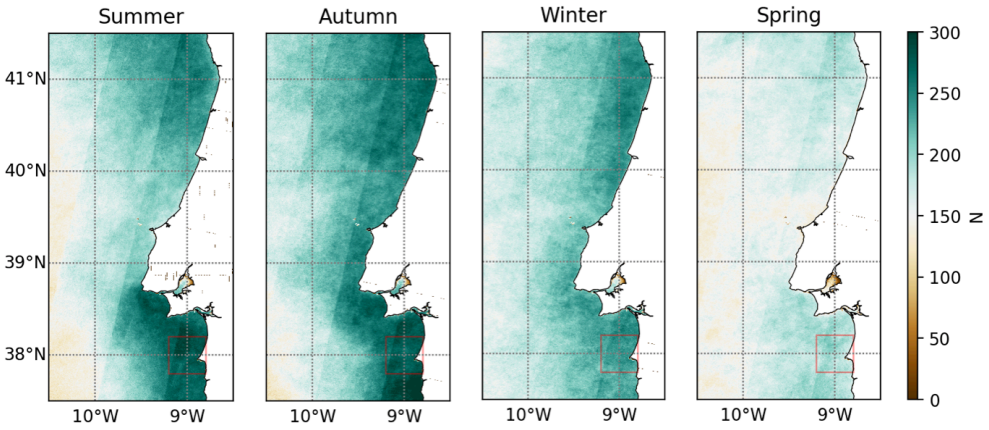

Figure A.1 - Number of observations that contributed to the Chl-*a* climatological seasonal average (MERIS).

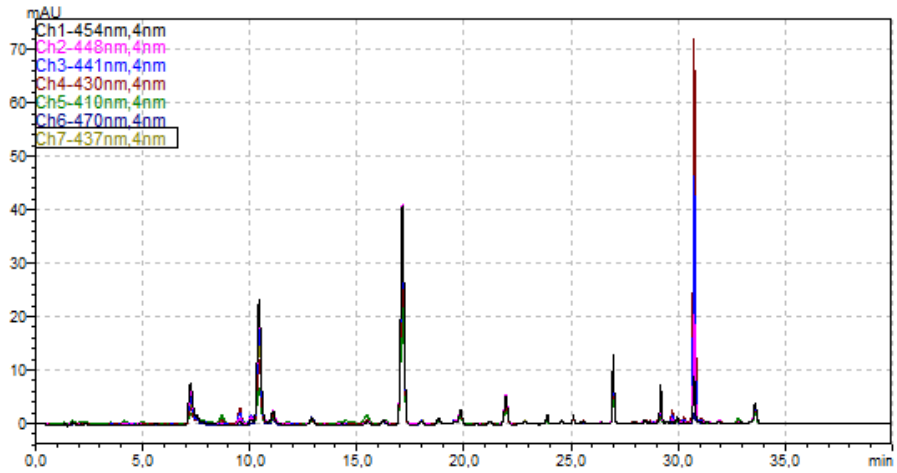

Figure A.2 – Example of chromatogram from the station 3 (surface, May 2019).

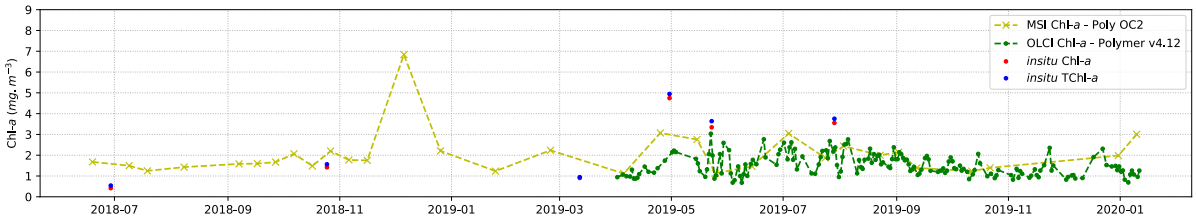

Figure A.3 – RS Chl-*a* (MSI – light green dashed line and dots; OLCI – dark green dashed line and dots) and in situ Chl-*a* (HPLC – red dots) and TChl-*a* (HPLC – blue dots) time series for all four sampling stations averaged.

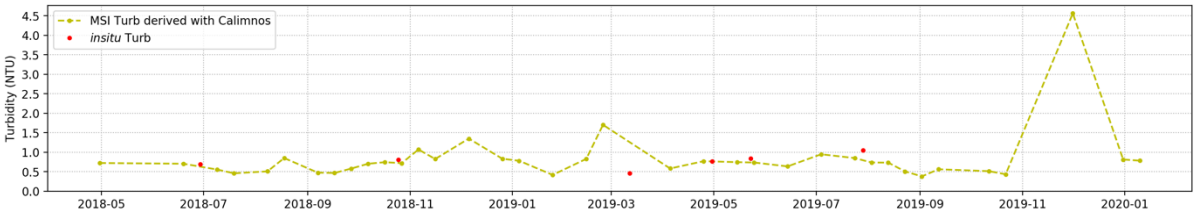

Figure A.4 – RS Turb (MSI – light green dashed line and dots) and *in situ* Turb (red dots) time series for all four sampling stations averaged.